30795

National Library of Canada | Bibliothèque nationale du Canada

CANADIAN THESES ON MICROFICHE | THÈSES CANADIENNES SUR MICROFICHE

NAME OF AUTHOR/*NOM DE L'AUTEUR* Miss Sukon Pirakitigoon.

TITLE OF THESIS/*TITRE DE LA THÈSE* Intramolecular Exchange of Some Tris(trifluoromethyl) Phosphoranes

UNIVERSITY/*UNIVERSITÉ* University of Alberta

DEGREE FOR WHICH THESIS WAS PRESENTED/ *GRADE POUR LEQUEL CETTE THÈSE FUT PRÉSENTÉE* M.Sc.

YEAR THIS DEGREE CONFERRED/*ANNÉE D'OBTENTION DE CE GRADE* 1976

NAME OF SUPERVISOR/*NOM DU DIRECTEUR DE THÈSE* Dr. R.G. Cavell

Permission is hereby granted to the NATIONAL LIBRARY OF CANADA to microfilm this thesis and to lend or sell copies of the film.

The author reserves other publication rights, and neither the thesis nor extensive extracts from it may be printed or otherwise reproduced without the author's written permission.

L'autorisation est, par la présente, accordée à la BIBLIOTHÈQUE NATIONALE DU CANADA de microfilmer cette thèse et de prêter ou de vendre des exemplaires du film.

L'auteur se réserve les autres droits de publication; ni la thèse ni de longs extraits de celle-ci ne doivent être imprimés ou autrement reproduits sans l'autorisation écrite de l'auteur.

DATED/*DATÉ* Oct 8, '76 SIGNED/*SIGNÉ* Sukon Pirakitigoon.

PERMANENT ADDRESS/*RÉSIDENCE FIXE* 64 Rotfai Road
Chiang Mai
THAILAND.

NL-91 (3-74)

INFORMATION TO USERS

THIS DISSERTATION HAS BEEN MICROFILMED EXACTLY AS RECEIVED

This copy was produced from a microfiche copy of the original document. The quality of the copy is heavily dependent upon the quality of the original thesis submitted for microfilming. Every effort has been made to ensure the highest quality of reproduction possible.

PLEASE NOTE: Some pages may have indistinct print. Filmed as received.

Canadian Theses Division
Cataloguing Branch
National Library of Canada
Ottawa, Canada K1A ON4

AVIS AUX USAGERS

LA THESE A ETE MICROFILMEE TELLE QUE NOUS L'AVONS RECUE

Cette copie a été faite à partir d'une microfiche du document original. La qualité de la copie dépend grandement de la qualité de la thèse soumise pour le microfilmage. Nous avons tout fait pour assurer une qualité supérieure de reproduction.

NOTA BENE: La qualité d'impression de certaines pages peut laisser à désirer. Microfilmee telle que nous l'avons reçue.

Division des thèses canadiennes
Direction du catalogage
Bibliothèque nationale du Canada
Ottawa, Canada K1A ON4

THE UNIVERSITY OF ALBERTA

INTRAMOLECULAR EXCHANGE OF SOME TRIS(TRIFLUOROMETHYL)-PHOSPHORANES

by

© SUKON PIRAKITIGOON

A THESIS

SUBMITTED TO THE FACULTY OF GRADUATE STUDIES

IN PARTIAL FULFULMENT OF THE REQUIREMENTS FOR THE DEGREE

OF

MASTER OF SCIENCE

DEPARTMENT OF CHEMISTRY

EDMONTON, ALBERTA

FALL 1976

THE UNIVERSITY OF ALBERTA

FACULTY OF GRADUATE STUDIES

The undersigned certify that they have read, and recommend to the Faculty of Graduate Studies for acceptance, a thesis entitled "INTRAMOLECULAR EXCHANGE OF SOME TRIS(TRIFLUOROMETHYL)PHOSPHORANES" submitted by SUKON PIRAKITIGOON in partial fulfulment of the requirements for the degree of Master of Science.

R. G. Cavell
Supervisor

W. A. G. Graham

J. S. Martin

J. Dalla Lana

Date August 23, 1976

TO MY PARENTS

ABSTRACT

$(CF_3)_3P(F)NH(CH_3)$ (I) and $(CF_3)_3P(F)NCH_3(CH_2C_6H_5)$ (II) have been obtained from the pentavalent fluoride $(CF_3)_3PF_2$ and the appropriate amine, CH_3NH_2 or $CH_3(CH_2C_6H_5)NH$. $CH_3(CF_3)_2P(F)NH(CH_3)$ (III) was prepared from $CH_3(CF_3)_2PF_2$ and CH_3NH_2. The ^{19}F and ^{31}P nmr spectra of (I) and (II) at low temperature, and of (III) at room temperature show the presence of different CF_3 environments consistent with substitution at axial or equatorial positions of the assumed trigonal bipyramidal framework. The former are characterized by relatively small $^2J_{PF}$ (and $^1J_{PC}$) and the latter by relatively large $^2J_{PF}$ (and $^1J_{PC}$) values. Ground state structures are consistent with the preferential location of fluorine in the axial position and of CH_3, $NH(CH_3)$ or $NCH_3(CH_2C_6H_5)$. groups in the equatorial positions. The CF_3 groups occupy the remaining axial and equatorial positions. $PF_4NCH_3(CH_2C_6H_5)$ (IV) was prepared by the thermal decomposition of the phosphorus pentafluoride-methylbenzylamine adduct. The four new compounds appear to be five coordinate molecular phosphoranes and not isomeric phosphonium salts. At very low temperatures, a small splitting of signals in the ^{31}P and ^{19}F spectra of (IV) may be due to the presence of nonequivalent axial fluorine atoms.

The changes in the appearance of the spectra of all of the phosphoranes studied herein upon lowering the

temperature are interpreted in terms of a reduction in the rates of (i) equilibrating permutational process and ii) the hindered rotation around the P-N bond which is coupled with inversion at nitrogen.

The temperature dependence of the ^{31}P nmr spectra of a series of compounds of the type $(CF_3)_3P(F)Y$, where $Y = NH(CH_3)$, $N(CH_3)_2$, $NCH_2(CH_2C_6H_5)$, OCH_3; $CH_3(CF_3)_2P(F)NH(CH_3)$ and $PF_4NCH_3(CH_2C_6H_5)$ has been examined. The interchange of axial and equatorial fluorines in $PF_4NCH_3(CH_2C_6H_5)$, of axial and equatorial CF_3 groups in $(CF_3)_3P(F)Y$ series and $CH_3(CF_3)_2P(F)NH(CH_3)$ occurs by a pairwise exchange mechanism. The temperature dependence of the $^{13}C - \{^{19}F\}$ spectra of one compound $(CF_3)_3P(F)NCH_3(CH_2C_6H_5)$ was also examined for comparison of the resultant activation parameters with those obtained from ^{31}P nmr spectroscopy.

Line shape analysis of ^{13}C and ^{31}P nmr spectra obtained at different temperatures (by means of the computer programs DNMR3 and EXCHSYS) yielded activation parameters for the exchange process. In $(CF_3)_3P(F)X$ series, the barriers to the averaging of CF_3 environments (deduced from $\Delta G^{\ddagger}$) are in order: $NH(CH_3) > NCH_3(CH_2C_6H_5) > N(CH_3)_2 > OCH_3$. For $(CF_3)_3P(F)NCH_3(CH_2C_6H_5)$, the activation parameters obtained from nmr of two different nuclei were in good agreement.

ACKNOWLEDGEMENTS

The author wishes to express appreciation to her research supervisor, Dr. R. G. Cavell, for his direction and assistance during the course of these studies and to Dr. K. I. The and Dr. J. A. Gibson for many helpful discussions and suggestions.

Thanks are also due to members of the Department of Chemistry technical staff, especially to Mr. T. Brisbane, Dr. T. Nakashima, and Mrs. L. Kong.

Appreciation is also extended to Mrs. J. Jorgensen for her able preparation of this manuscript and Mr. V. Ball for drafting of many diagrams which appear.

Financial assistance from the University of Alberta is gratefully acknowledged.

TABLE OF CONTENTS

	PAGE
CHAPTER 1	
INTRODUCTION	1
CHAPTER 2	
MATERIALS, APPARATUS, TECHNIQUES AND PREPARATIONS	11
High vacuum system and techniques	11
Materials	11
Instrumental techniques	12
Hydrolysis	13
Preparations	14
Preparation of $(CF_3)_3P(F)NH(CH_3)$	14
Preparation of $(CF_3)_3P(F)NCH_3(CH_2C_6H_5)$	15
Preparation of $PF_4NCH_3(CH_2C_6H_5)$	20
Preparation of $CH_3(CF_3)_2P(F)NH(CH_3)$	21
Results and Discussion	23
Synthesis and Characterization	23
Hydrolysis	25
Mass Spectra of the Phosphoranes	39
Infrared Spectra of the Phosphoranes	44
CHAPTER 3	
GROUND STATE STRUCTURE AND STEREOCHEMISTRY OF SOME PHOSPHORANES	45

PAGE

The Ground State Structures of $(CF_3)_3P(F)$-$NH(CH_3)$ and $(CF_3)_3P(F)NCH_3(CH_2C_6H_5)$ 45

The Ground State Structure of $CH_3(CF_3)_2$-$P(F)NH(CH_3)$ 65

The Ground State Structure of PF_4NCH_3-$(CH_2C_6H_5)$ 73

CHAPTER 4

PERMUTATIONAL INTERCHANGE BARRIERS OBTAINED BY DYNAMIC NMR SPECTROSCOPY 80

Analysis of the Spectra 86

Exchange Barriers 113

CHAPTER 5

SUMMARY AND CONCLUSIONS 119

REFERENCES 123

APPENDIX 133

The Exchange Matrix Method 133

K-matrices, Spin Assignments, Intensity and Frequency Tables 136

LIST OF TABLES

TABLE		PAGE
1	Hydrolysis of Some Phosphoranes	27
2	NMR Data of Phosphorus Containing Hydrolysis Products of $CH_3(CF_3)_2P(F)NH(CH_3)$.	28
3	Mass Spectra Data for $(CF_3)_3P(F)NH(CH_3)$, $(CF_3)_3P(F)NCH_3(CH_2C_6H_5)$ and $CH_3(CF_3)_3P(F)$-$NH(CH_3)$.	30
4	Mass Spectra Data for $PF_4NCH_3(CH_2C_6H_5)$.	35
5	Mass Measurement Data	37
6	Infrared Spectral Data for $(CF_3)_3P(F)NH(CH_3)$, $(CF_3)_3P(F)NCH_3(CH_2C_6H_5)$ and $CH_3(CF_3)_2P(F)$-$NH(CH_3)$.	41
7	Infrared Spectral Data for $PF_4NCH_3(CH_2C_6H_5)$.	43
8	NMR Data for Tris(trifluoromethyl)phosphoranes.	50
9	^{13}C NMR Data for $(CF_3)_3P(F)NCH_3(CH_2C_6H_5)$	62
10	NMR Data of Two New Phosphoranes, PF_4NCH_3-$(CH_2C_6H_5)$ and $CH_3(CF_3)_2P(F)NH(CH_3)$.	68
11	Values of Rates of Exchange of Magnetization at Particular Temperatures for Various Phosphoranes using K-matrix Method.	87
12	Values of Rate of Exchange of Magnetization at Particular Temperatures of $(CF_3)_3P(F)$-$NCH_3(CH_2C_6H_5)$ using DNMR3.	88
13	Activation Parameters of Some Phosphoranes.	116

TABLE		PAGE
14	Line Numbers, Spin States, Intensities, and Frequencies used for Simulation of ^{31}P Spectra of $PF_4NCH_3(CH_2C_6H_5)$.	136
15	Line Numbers, Spin States, Intensities, and Frequencies used for Simulation of ^{31}P Spectra of $CH_3(CF_3)_2P(F)NH(CH_3)$.	137
16	Line Numbers, Spin States, Intensities, and Frequencies used for Simulation of ^{31}P Spectra of $(CF_3)_3P(F)Y$.	138
17	K-matrix Describing Transfer of Magnetization Between the Lines of the Observed ^{31}P Spectrum of $PF_4NCH_3(CH_2C_6H_5)$.	141
18	K-matrix Describing Transfer of Magnetization Between the Lines of the Observed ^{31}P Spectrum of $CH_3(CF_3)_2P(F)NH(CH_3)$.	142
19	64 x 64 Matrix for $(CF_3)_3P$ Systems (2 equatorial, 1 axial).	143
20	40 x 40 Matrix for $(CF_3)_3P$ Systems (2 equatorial, 1 axial).	144

LIST OF FIGURES

FIGURE		PAGE
1	Berry Pseudorotation	7
2	Components of the Turnstile Mechanism	8
3a	Gas Phase Reactor	16
3b	Apparatus for Transferring Products of Low Volatility.	16
4	Structures of the Phosphoranes	46
5	^{19}F and ^{1}H nmr Spectra of $(CF_3)_3P(F)NH(CH_3)$.	48
6	^{19}F nmr Spectra of $(CF_3)_3P(F)NCH_3(CH_2C_6H_5)$.	49
7	Temperature Dependent ^{19}F nmr Spectra of $(CF_3)_3P(F)NCH_3(CH_2C_6H_5)$.	54
8	^{19}F nmr Spectra of $(CF_3)_3P(F)NH(CH_3)$.	55
9	Observed and Calculated ^{31}P nmr Spectra of $(CF_3)_3P(F)NH(CH_3)$.	58
10	Observed and Calculated ^{31}P nmr Spectra of $(CF_3)_3P(F)NCH_3(CH_2C_6H_5)$.	59
11	^{13}C nmr Spectra of $(CF_3)_3P(F)NCH_3(CH_2C_6H_5)$.	61
12	^{1}H nmr Spectra of $CH_3(CF_3)_2P(F)NH(CH_3)$.	66
13	^{1}H nmr Spectra of $CH_3(CF_3)_2P(F)NH(CH_3)$.	67
14	^{19}F nmr Spectra of $CH_3(CF_3)_2P(F)NH(CH_3)$.	72
15	Observed and Calculated ^{31}P nmr Spectra of $CH_3(CF_3)_2P(F)NH(CH_3)$.	74
16	^{19}F nmr Spectra of $PF_4NCH_3(CH_2C_6H_5)$.	76
17	^{31}P nmr Spectra of $PF_4NCH_3(CH_2C_6H_5)$.	77

FIGURE		PAGE
18	Two Orientations of Substituent p_π Donor Orbitals in Trigonal Bipyramid	82
19	Stepwise Interconversion by Means of P-N Bond Rotation and Inversion at Nitrogen for $PF_4NCH_3(CH_2C_6H_5)$.	84
20	Structure of $PF_4NCH_3(CH_2C_6H_5)$.	85
21	Spectral Assignments for the ^{31}P Spectrum of $PF_4NCH_3(CH_2C_6H_5)$.	89
22	Temperature Dependent ^{31}P nmr Spectra of $PF_4NCH_3(CH_2C_6H_5)$ Compared with Spectra Calculated for Appropriate Rates of Exchange.	92
23	Spectral Assignments for the ^{31}P Half-spectrum of $CH_3(CF_3)_2P(F)NH(CH_3)$.	95
24	Temperature Dependent ^{31}P nmr Spectra of $CH_3(CF_3)_2P(F)NH(CH_3)$ Compared with Spectra Calculated for Appropriate Rates of Exchange.	97
25	Spectral Assignments for the ^{31}P Half-spectrum of $(CF_3)_3P(F)Y$.	100
26	Temperature Dependent ^{31}P nmr Spectra of $(CF_3)_3P(F)NH(CH_3)$ Compared with Spectra Calculated for Appropriate Rates of Exchange.	102
27	Temperature Dependent ^{31}P nmr Spectra of $(CF_3)_3P(F)N(CH_3)_2$ Compared with Spectra Calculated for Appropriate Rates of Exchange.	104

FIGURE		PAGE
28	Temperature Dependent ^{31}P nmr Spectra of $(CF_3)_3P(F)NCH_3(CH_2C_6H_5)$ Compared with Spectra Calculated for Appropriate Rates of Exchange.	106
29	Temperature Dependent ^{31}P nmr Spectra of $(CF_3)_3P(F)OCH_3$ Compared with Spectra Calculated for Appropriate Rates of Exchange.	108
30	Temperature Dependent ^{13}C nmr Spectra of $(CF_3)_3P(F)NCH_3(CH_2C_6H_5)$ Compared with Spectra Calculated for Appropriate Rates of Exchange.	112
31	Arrhenius Plots for Phosphorane Exchange.	115

CHAPTER 1

INTRODUCTION

In recent years the chemistry of five coordinate phosphorus compounds has received increased attention, directed particularly toward an understanding of the bonding and stereochemistry[1-9] in these systems. The basic trigonal bipyramidal framework, which is now well established for these compounds,[1,4,9,29,80] provides two different ligand environments, a pair of "axial" substituents and a set of three "equatorial" substituents. The axial bond in the trigonal bipyramidal framework is longer than the equatorial bond[10]; a result which can be rationalized by considering the interactions of bond pairs with neighboring ligands following the rules of Gillespie.[17] Theoretical calculations[6,7,12,13] of varying sophistication have been also used to analyze the geometry of the five coordinate molecules. The locations of substituent groups within this structure are much less certain in cases where two or more different groups are present. Initial studies[14] suggested that axial positions were preferentially occupied by the most electronegative substituents, perhaps the result of greater ionic character of bonding in this direction or possibly a consequence of enhanced π bonding in the equatorial plane. The concept of apicophilicity[15] recognizes that the location of substituent groups is

determined by a balance of various factors such as electronegativity, π bonding and possibly also steric effects but does not imply any particular origin. Recent nmr studies[16] suggested an apicophilicity series with the order:

F	>	Cl, Br	>	CF_3	>	$OSiMe_3$, OMe, SMe, NMe_2, H, Me
0.51		0.47 0.45		0.41		? 0.26 0.19 0.05 0.0 -0.05

wherein groups separated by a comma were regarded as indistinguishable on the basis of available data. This apicophilicity order seemed to follow the substituent parameter σ_I,[17] values of which are listed under each substituent.

The presence of phosphorus, fluorine and carbon atoms, all of which have nuclear spin of 1/2, provides a variety of useful nmr probes for the study of these compounds. Although ^{19}F and ^{31}P are present in 100% natural abundance, the sensitivity of the nmr technique is ~7% for ^{31}P *vs.* ^{19}F [18] whereas nmr sensitivity of the latter nucleus is comparable to that of the proton. The low natural abundance of the ^{13}C isotope (1.1%) and its low nuclear sensitivity (~2% of that for equivalent number of fluorine nuclei under similar field) make ^{13}C resonances much more difficult to obtain than ^{19}F resonances. Additional complexities arise from extensive

and large nuclear spin splitting interactions which spread the spectrum over a large frequency range. Recently the availability of Fourier transform nmr spectroscopy[19] has allowed measurement of such spectra in high quality from small samples of these compounds. Additional flexibility and long term stability for these and similar experiments has been provided by the development of nmr instruments which can be locked on a nucleus different from the one being observed. The heteronuclear lock system has proved invaluable in measuring low temperature ^{31}P spectra since lock compounds containing phosphorus which are useful at low temperatures are not readily available. Decoupling techniques have been used in both ^{31}P and ^{13}C spectra in order to obtain simplified spectra with reduced spin splitting interaction; such techniques are essential for the latter nucleus because of its low sensitivity.

There are two main approaches[48] to the theoretical description of high resolution nmr spectra of liquids and gases: the phenomenological description in terms of Bloch equations and the quantum mechanical description in terms of a spin Hamiltonian. Time or field dependent effects in the simple nmr spectra of a molecule with a single magnetic nucleus can be described by means of the Bloch equations which include two relaxation times, T_1 and T_2, which govern the line shapes. The nmr spectra of molecules with several magnetic nuclei can be completely

analyzed in terms of resonance frequencies and intensities which are obtained from the spin Hamiltonian in order to obtain a set of parameters: the chemical shift σ_i and coupling constants J_{ij}. These parameters fully determine the energy levels of the nuclear spins in the external magnetic field, H_o, and therefore comprise the static information that can be extracted from an nmr experiment. In addition to chemical shifts and coupling constants, nmr spectra are a function of certain time dependent phenomena. The changing of the nmr signals with temperature can be related to the stereochemical changes of the molecule. The processes are characterized by lifetimes of the nuclei in distinct environments, and the magnitude of lifetimes is inversely related to the total spread (in cycles per second) of the nmr spectrum of the magnetic isotope of interest (typically 10^{-1} to 10^{5} sec^{-1}). The rate constants for the exchange process are further inversely related to the lifetimes of initial and final states of the system. If the average lifetimes of a number of species in equilibrium exceed an upper limit, the nmr spectrum will show them as individual entities. Conversely, if the lifetimes are short with respect to the nmr time scale, one will obtain a single spectrum in which the chemical shifts and, for intramolecular process, the coupling constants, are statistically weighted averages of the corresponding

values for the various forms of the exchanging species. The analysis of the characteristic phenomena that can be observed during the transition from one extreme to the other constitutes the field of "dynamic nuclear magnetic resonance spectroscopy" (DNMR)[20] and such analyses have proven to be especially valuable in the study of molecular conformational changes.

The polytopal exchange of ligands in five coordinate phosphorus compounds has been studied in greater detail than other systems, such as five coordinate metal complexes,[27,28] for many reasons. First, the five coordinate phosphorus compounds are relatively stable and are easily synthesized and purified. Second, the polytopal exchange reactions of many of these compounds occur at rates that are convenient for study by magnetic resonance techniques. Finally, the observation that magnetic spin coupling interactions (eg. ^{19}F-^{31}P) are usually preserved during these exchange reactions helps to assure their intramolecularity[28] within the constraining assumption that there are no strong solvent cage interactions which promote recombination of dissociated molecular fragments with unchanged spin states.[29] Other tests such as concentration dependence must also be performed in order to establish the molecularity of the process; in general the results[28-29] on phosphorane exchanges have supported the proposal of intramolecular

polytopal exchange.

In a classic analysis of the interchange of axial and equatorial fluorines in XPF_4[29] molecules it was shown that the permutational process involves pairwise exchange such as that described by a Berry pseudorotation[30] (BPR). Other more complex processes also are possible which provide pairwise interchanges.

Berry postulated that positional exchange in trigonal bipyramidal five coordinate compounds (PX_5) occurred by means of a symmetric deformation of the molecule which leads, through a square pyramidal intermediate, to a new configuration in which two axial and two equatorial atoms have been interchanged. One of the equatorial ligands does not participate in the positional exchange and is called the "pivot". The originally axial pair undergoes an angular bending displacement (4P5 angle changes from 180° to 120°) (Figure 1) in a plane defined by ligand 3 (the pivot) and the axial pair (4 and 5). The initially equatorial pair participates in a simultaneous bending displacement (1P2 angle changes from 120° to 180°) in the original equatorial plane. The bond distances must be adjusted to the new geometry. An intermediate C_{4v} transition state is traversed only if all bonds other than the pivot bond are identical in the transition state, otherwise the transition state symmetry is formally C_{2v}.

An alternative to Berry pseudorotation is the turnstile rotation (TR) mechanism, the details of which

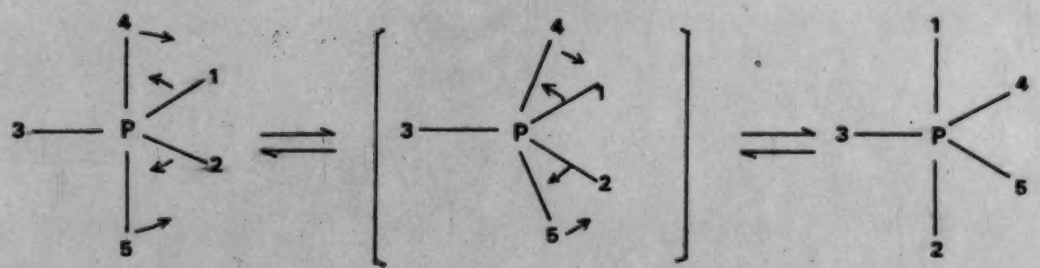

D_{3h} C_{4v} or C_{2v} D_{3h}

4P5 angle: 180° → 120°

1P2 angle: 120° → 180°

* 3 as a "pivot" ligand

Figure 1. Berry pseudorotation: A postulated exchange mechanism for positional exchange in five coordinate trigonal bipyramidal compounds.

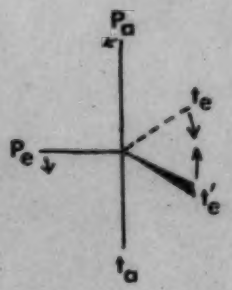

2a

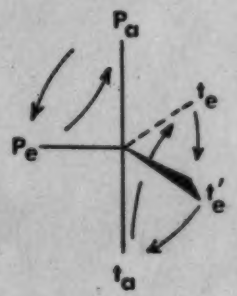

2b

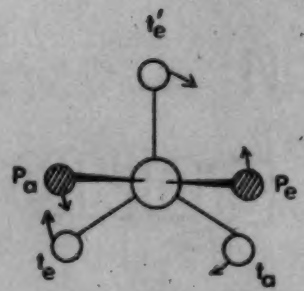

2c

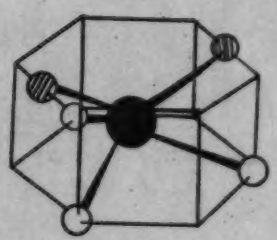

2d

Figure 2 Components of the Turnstile Mechanism[5]

are given elsewhere.[5] The unique motion of TR mechanism is illustrated by the figures 2a and 2b. A displacement of two equatorial ligands (te and te' in 2a) reducing the original 120° angle to ≈90° combined with the simultaneous bending of the axial and equatorial ligands (Pe and Pa in 2a) by approximately 9° give the structure 2b. Superimposed upon the above motions is the internal rotation of the pair (Pa and Pe) *vs.* the trio (ta, te and te') according to 2b. The combination of these three motions leads to the TR barrier situation 2c,d which is reached by a relative internal rotation of 30°; from this point a further 30° rotation leads to an intermediate which can relax by the reverse of the above bending motions to an analogous conformation of the original trigonal bipyramidal molecule.

The gradual transformation of certain lines in an nmr spectrum upon variation of the temperature indicate the presence and nature of a rate process. Such changes can be measured with standard nmr equipment and followed by line-shape analysis. The line-shape calculations of the nmr spectra employ the density matrix approach of Kaplan [31] and Alexander[32] together with the theories of Redfield[33] and Sack.[34] With the advent of the numerical techniques developed by Gordon and McGinnis,[35] Binsch,[36] and Schinmer, Noggle and Gaines[34] has it become possible to treat spin systems of considerable complexity. Details concerning the nmr line-shape calculations used herein are given elsewhere.[20,28]

The principal goal of the research described in this thesis was to understand the chemical and stereochemical properties of some five coordinate phosphorus compounds (phosphoranes). In the course of this study four new phosphoranes; $(CF_3)_3P(F)NH(CH_3)$, $(CF_3)_3P(F)NCH_3(CH_2C_6H_5)$, $CH_3(CF_3)_2P(F)NH(CH_3)$, $PF_4NCH_3(CH_2C_6H_5)$, were prepared. The preparation and characterization are described in Chapter 2. The temperature dependence of the ^{19}F and ^{31}P spectra of the new compounds (which are fluxional) plus some related known compounds were examined to gain an understanding of the energetics of polytopal exchange of the ligands and to determine the ground state geometry in the trigonal bipyramidal framework. One compound $(CF_3)_3P(F)NCH_3(CH_2C_6H_5)$, was examined by means of both ^{31}P and ^{13}C - $\{^{19}F\}$ temperature dependent nmr spectra to compare activation parameters for positional exchange obtained by different methods. The ground state structures of these compounds and the exchange mechanism are discussed in Chapters 3 and 4. Energetics of the processes were derived by means of line-shape analysis of the ^{13}C and ^{31}P nmr spectra obtained at different temperatures by means of existing computer programs (DNMR3[38] and EXCHSYS[88]) in order to obtain rate values for the process which were then used to prepare an Arrhenius plot from which the activation parameters (E_a, the Activation energy; A, the frequency factor and $\Delta H^{\ddagger}$, enthalpy; $\Delta S^{\ddagger}$, entropy $\Delta G^{\ddagger}$, free energy of activation) were obtained.

CHAPTER 2

MATERIALS, APPARATUS, TECHNIQUES AND PREPARATIONS

High Vacuum Apparatus and Techniques

Due to the air and moisture sensitivity of many of the reactants and reaction products all reactions were done in sealed tubes using standard high vacuum techniques.[39] An ultimate pressure of less than 10 microns of mercury was attainable by use of a mercury diffusion pump separated from the main vacuum system by a cold trap held at -196°C and backed by a rotary oil pump. The vacuum system was constructed with Pyrex glass and the stopcocks lubricated with Apiezon N grease. Separation of volatile compounds was usually achieved by passing them through a series of U-traps cooled with slush baths[40] to various temperatures. Pressure measurements were made using mercury manometers. Nonvolatile materials which remained in the reaction vessel following vacuum fractionation were handled in a nitrogen or an argon atmosphere while aqueous solutions were handled in the air since it had been found by experience that such products were invariably air stable.[46]

Materials

$(CF_3)_2PI$,[45] $(CF_3)_2PCl$,[43] $(CF_3)_2PCl_3$,[44] $(CF_3)_2PF_3$,[42] $(CF_3)_2CH_3PF_2$,[45] $(CF_3)_3P$,[41] $(CF_3)_3PF_2$[42] were prepared according to published methods. Reagent grade commercially

available materials generally were fractionated before use to remove impurities, or, if this was not possible, were pumped on to remove entrained air.

Instrumental Techniques

The starting material and new compounds were checked for purity by infrared or nuclear magnetic resonance spectroscopy. Infrared spectra were recorded with a Perkin-Elmer 457 spectrometer in a 9 cm gas cell with potassium bromide windows or in potassium bromide plates for liquid samples. All nmr spectra were recorded with either a Varian A56/60, a Varian HA 100 or Bruker HFX-90 spectrometers. Proton spectra were recorded at 60.0 MHz and fluorine spectra at 56.4 MHz using the A56/60 instrument. Higher resolution spectra were obtained on a Varian HA 100 instrument, equipped with a V6040 temperature controller, which was capable of attaining temperatures as low as about -120°C. This spectrometer operates at 100 MHz for protons, 94.1 MHz for fluorine and 40.5 MHz for phosphorus nuclei. Since the Varian system was unsatisfactory for recording ^{31}P spectra at low temperatures due to the difficulty in finding a good low temperature lock compound, the Bruker HFX-90 system with Fourier transform capability and heteronuclear lock was used for low temperature studies of this nucleus as well as ^{13}C. This system operates at 90 MHz for protons,

84.6 MHz for fluorine, 36.4 MHz for phosphorus and 22.6 MHz for carbon nuclei. Phosphorus spectra were run in Fourier transform mode and either 2000, 2500 or 5000 Hz sweep widths were collected in 2K data points on the Nicolet-1085 20K memory computer associated with the system. The temperature controller is reproducible to ± 1°. Samples of volatile products for nmr measurements were prepared under vacuum in 5 mm o.d. medium wall sample tubes consisting of about 30% by volume of the compound in $CFCl_3$ or a mixture of $CFCl_3$ and CF_2Cl_2 depending on the temperature requirements. Involatile products were investigated as solutions in CD_3CN, CD_2Cl_2 or H_2O. Fluorine chemical shifts were measured relative to internal $CFCl_3$ solvent or to an external (capillary) of $CFCl_3$ if other solvents were used. Proton and phosphorus chemical shifts were measured relative to internal tetramethylsilane or an external capillary of P_4O_6(neat)[47] respectively.

Mass spectra were obtained on the AEI M59 mass spectrometer, operating at an ionizing voltage of 70 eV, and were introduced as gases using a heated inlet system.

Hydrolysis

The three new compounds $(CF_3)_3P(F)NH(CH_3)$, $(CF_3)_3P(F)NCH_3(CH_2C_6H_5)$, and $CH_3(CF_3)_2P(F)NH(CH_3)$ were hydrolysed in saturated NaOH solution at room temperature for 48 hours and the yields of fluoroform, characterized by infrared spectroscopy, are quoted in Table 1. Anions remaining in solution were characterized by ^{19}F nmr.[46] The results

of neutral hydrolyses are also given in Table 1.

Preparations

Preparation of tris(trifluoromethyl)fluoromethylaminophosphorane.

Gaseous methylamine (0.168 gm, 5.15 mmole) was slowly admitted to a sample of gaseous $(CF_3)_3PF_2$ (1.018 g, 3.69 mmoles) contained in a 1 ℓ gas phase reactor[50] at room temperature. A white solid formed immediately upon contact of the two vapours. After 1/2 hour at room temperature, separation of the volatile products in vacuum gave tris(trifluoromethyl)fluoromethylaminophosphorane $(CF_3)_3P(F)NH(CH_3)$ (0.353 g, 1.23 mmoles) trapped at -45° and a mixture of unreacted $(CF_3)_3PF_2$ and methylamine (0.0380 gm), trapped at -196°. The compound $(CF_3)_3P(F)$-$NH(CH_3)$ was characterized by its spectroscopic properties (ir, Table 6; nmr, Table 8) mass spectral data, Tables 3 and 5, and hydrolysis (Table 1).

The ^{19}F nmr spectrum of a deuterated methylene chloride solution of the remaining white solid showed three multiplets, centered at (ϕ) 68.8, 88.1, and 103.3 (J_{PF} = 854 Hz) ppm which were consistent with those reported[49] for $(CF_3)_3PF_3^-$. The other signals from the same sample at 64.0 and 49.0 ppm were assigned to a small amount of $(CF_3)_3P(F)NH(CH_3)$ which had been trapped in the solid.

In a second preparation, white solid and liquid were left in the reaction vessel (C) and (A) of Figure 3a respectively after removal of the desired product. The ^{19}F nmr spectra of a solution of the solid in (C) were the same as those obtained above. The ^{1}H nmr spectrum of this solution showed two singlets of equal relative intensity at τ = 7.52 and 4.42, assigned to CH_3 and NH_3 protons of $CH_3NH_3^+$. The ^{1}H nmr spectra of the liquid which remained in (A) showed a singlet at τ = 4.70 and a doublet with coupling constant of 9 Hz at τ = 7.47 there was no ^{19}F signal from this sample and its identity was not established. The yield of $(CF_3)_3P(F)$-$NH(CH_3)$ was calculated based on the amount of the product in -45° trap related to the initial weight of $(CF_3)_3PF_2$.

Preparation of tris(trifluoromethyl)fluoro(N-methyl-benzylamino)phosphorane.

N-methylbenzylamine, $CH_3(CH_2C_6H_5)NH$, (0.541 g, 4.48 mmoles) was weighed under nitrogen by difference into a reaction tube in the drybox and the tube was removed to the vacuum line and evacuated. At -196° 0.323 g of diethyl ether was condensed into the reaction tube and allowed to mix with the N-methylbenzylamine, then (1.128 g, 4.09 mmoles) of $(CF_3)_3PF_2$ was condensed into the reaction tube and the tube was sealed. Upon slow warming from -196° to room temperature a white solid was first formed,

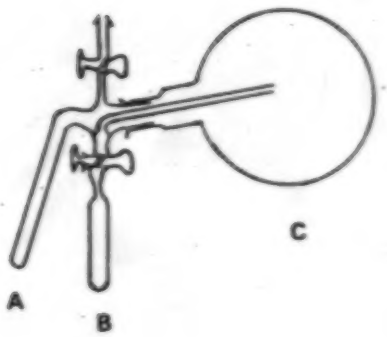

Figure 3a Gas Phase Reactor

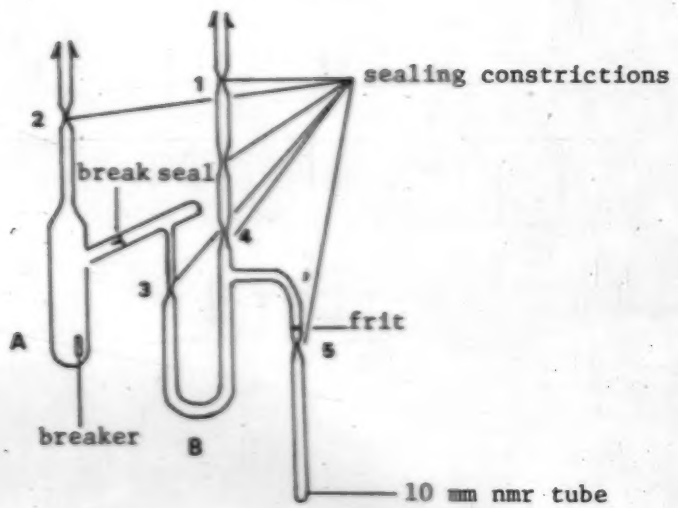

Figure 3b

Apparatus for Transferring Products of Low Volatility

which dissolved to form a yellow, oily liquid. Separation of the volatile products gave $(CF_3)_3P(F)NCH_3(CH_2C_6H_5)$, tris(trifluoromethyl)fluoro(N-methylbenzylamino)phosphorane, (0.593 g, 1.57 mmoles) trapped at -45°, unreacted $(CF_3)_3PF_2$ (0.013 g, 0.05 mmole) trapped at -116° and diethyl ether (0.323 g) trapped at -196°. $(CF_3)_3P(F)$-$NCH_3(CH_2C_6H_5)$ was characterized by its spectroscopic properties (ir, Table 6; nmr, Tables 8 and 9), by mass spectral data, Tables 3 and 5, and hydrolysis (Table 1).

The ^{19}F nmr spectrum of the yellow, oily liquid in deuterated methylene chloride showed 3 multiplets, centered at 67.2, 88.0 and 103.2 (J_{PF}, 859 Hz) ppm, were consistent with those reported[49] for $(CF_3)_3PF_3^-$. The other signals, a doublet and a broad singlet belong to CF_3 region of $(CF_3)_3P(F)NCH_3(CH_2C_6H_5)$ centered at 60.5 ppm and doublet of multiplets centered at 30.4 ppm due to the fluorine of the portion of the volatile product which had been trapped in the solid residues.

Convenient preparation of the ^{13}C nmr sample which required transfer of large amounts of relatively nonvolatile phosphorane was effected by means of the special apparatus illustrated in Figure 3b. The system was evacuated and sealed off at (1). Synthesis was accomplished in (A) as follows: (0.976 g, 7.80 mmoles) of N-methylbenzylamine $CH_3(CH_2C_6H_5)NH$ was loaded into the reaction tube (A) under nitrogen through the ground

glass joint. The system was connected to the vacuum line and evacuated. Diethyl ether (0.683 g) was condensed into the reaction tube (A), warmed to mix and then cooled again to -196° in order to condense $(CF_3)_3PF_2$ (0.933 g, 8.04 mmole) into (A). The reaction vessel was sealed at (2) and the sealed tube was slowly warmed up to room temperature whereupon a white solid was formed, which dissolved upon subsequent shaking of the reaction mixture for 3 hours at room temperature to form, finally, an apparently homogeneous oily liquid. The connection between reaction tube (A) and the U-tube (B) was opened by means of a breaker, and the system was connected to the vacuum line by means of the sealing constriction (1). The desired compound, $(CF_3)_3P(F)NCH_3(CH_2C_6H_5)$ was distilled from (A) and trapped in the U-tube (B), which was cooled to -45°. Diethyl ether (0.683 g) and unreacted $(CF_3)_3PF_2$ (0.134 g 0.49 mmole) were separated in the main vacuum system. Reaction tube (A) was then removed by sealing off at (3). Approximately 1.5 ml of deuterated methylene chloride was condensed into the U-tube (B) from the vacuum system, and the apparatus was sealed at (4). After warming and mixing, the solution was filtered through the frit into the nmr tube, which was immersed in a 5°C ice-water bath. The solution in the nmr tube was frozen and the tube was sealed with a torch at (5).

In order to obtain a sample suitable for measurement of high temperature nmr spectra, the above procedure was repeated using instead deuterated methyl cyclohexane as the solvent.

For ^{31}P and ^{19}F nmr spectra the above procedure was repeated using arbitrary mixtures of $CFCl_3$ and CF_2Cl_2 as the solvent. $(CF_3)_3P(F)NCH_3(CH_2C_6H_5)$ was prepared by analogous technique as above except that a 5 mm nmr tube was used and filtration of the sample omitted.

The yellow oily liquid remaining in the reaction tube (A) consisted of $(CF_3)_3P(F)NCH_3(CH_2C_6H_5)$ and $CH_3(CH_2C_6H_5)NH_2^+ \cdot (CF_3)_3PF_3^-$. The ^1H nmr spectrum of a solution of the remaining yellow, oily liquid showed two doublets at τ = 7.45 and 6.08, two singlets at τ = 4.1 and 2.82 with the intensity ratio of 3:2:2:5 which were respectively assigned to methyl (CH_3), methylene (CH_2) protons (2H) and phenyl (C_6H_5) signals of $CH_3(CH_2C_6H_5)$-NH_2^+. The other signals in the same sample, a singlet at τ = 2.87, two doublets centered at τ = 5.78 and 735, were assigned to phenyl (C_6H_5), methylene (CH_2) and methyl (CH_3) signals of $(CF_3)_3P(F)NCH_3(CH_2C_6H_5)$ in agreement with the signals shown by a pure sample (nmr Table 5). The relative molar ratio of $(CF_3)_3P(F)NCH_3$-$(CH_2C_6H_5)$ to $CH_3(CH_2C_6H_5)NH_2^+ \cdot (CF_3)_3PF_3^-$ in the residues, 1 to 5.1, obtained from the relative total intensities of

the phenyl group peaks in the nmr spectrum was combined with the total weight of the residue in (A) to compute the total yield of phosphate salt, 89% (eq 2), which is presumed to equal the yield of $(CF_3)_3P(F)NCH_3(CH_2C_6H_5)$.

The Preparation of N-methylbenzylaminofluorophosphorane by the Thermal Decomposition of N-methylbenzylamine - Phosphorus Pentafluoride Adduct.

Using the same apparatus as described above (Figure 3b), except for a pretreatment with PF_5 to remove water, phosphorus pentafluoride (0.466 g, 3.70 mmoles) was condensed on to a solution of N-methylbenzylamine (0.380 g, 3.13 mmoles) in toluene (1.0459 g) in (A) at -196°. The pale yellow solid N-methylbenzylamine-phosphorus pentafluoride adduct was formed upon warming the mixture to room temperature. After 2 hours at room temperature the system was connected to the vacuum line and the volatile products were removed by pumping for several hours. The reaction vessel was then heated to 75° and the evolved N-methylbenzylaminotetrafluorophosphorane $[PF_4NCH_3(CH_2C_6H_5)]$ was trapped in the U-tube (B) at -78°C; some excess phosphorus pentafluoride and toluene were trapped in the vacuum system at -196°. Reaction tube (A) was removed. Approximately 0.25 ml of $CFCl_3$ was condensed into the U-tube (B), the apparatus was sealed and removed from the vacuum line. The solution was transferred into a 5 mm nmr tube at -196° without filtration as described above.

Upon heating the remaining adduct in the reaction tube (A) which was connected to the vacuum system by means of the sealing constriction, an additional quantity of $PF_4NCH_3(CH_2C_6H_5)$ was trapped at -78°, which was used for characterization. $PF_4NCH_3(CH_2C_6H_5)$ was characterized by its spectroscopic properties (ir, Table 7; nmr, Table 10) and by mass spectral data (Tables 4 and 5).

Preparation of methylbis(trifluoromethyl)fluoromethyl-aminophosphorane.

$CH_3(CF_3)_2PF_2$ (0.244 g, 1.23 mmoles) and CH_3NH_2 (0.042 g, 1.35 mmoles) were allowed to react in the gas phase in a reactor described elsewhere.[50] An immediate reaction took place upon contact of the reagents with formation of a white solid material. After 1 hour at room temperature, separation of volatile products in vacuum gave methylbis(trifluoromethyl)fluoro(methylamino)-phosphorane $CH_3(CF_3)_2P(F)NH(CH_3)$ (0.140 g, 0.603 mmole) trapped at both -45° and -78° and unreacted $CH_3(CF_3)_2PF_2$ and CH_3NH_2 (0.011 g) at -196°. The compound $CH_3(CF_3)_2P(F)NH(CH_3)$ was characterized by its spectroscopic properties (ir, Table 6; nmr, Table 10) mass spectral data (Tables 3 and 5) and hydrolysis (Table 1). $CFCl_3$ was used as a solvent for ^1H, ^{19}F and ^{31}P nmr at normal (+31°) temperature. For high temperature nmr spectra, the above procedure was repeated using d_8-toluene as the

solvent and the nmr tube was sealed under 1 atm of Ar gas to prevent refluxing of the solvent.

The ^{19}F nmr spectrum of a solution of the remaining white solid in deuterated acetonitrile showed 2 multiplets centered at 67.2 and 69.1 ppm, two doublets at 78.3 and 80.5 ppm with $^{2}J_{PF}$; 86.5 and 79.5 Hz respectively, which were assigned to ^{19}F signals of $CH_3(CF_3)_2PF_3^-$.

The ^{1}H nmr spectrum of the same sample showed two singlets of equal intensity ratio at τ = 7.85 and 3.56 which were assigned to protons of $CH_3NH_3^+$. The other signals in the same sample were due to the CH_3 group directly bound to phosphorus atom in $CH_3(CF_3)_2PF_3^-$, centered at τ = 9.17. The yield of $CH_3(CF_3)_2P(F)NH(CH_3)$ (50%) was calculated based on the amount of the product in -45° and -78° traps relative to the starting weight of $CH_3(CF_3)_2PF_2$.

Results and Discussion

Synthesis and Characterization

Controlled aminolysis of the difluorophosphorane $(CF_3)_3PF_2$ in the gas phase at room temperature gave the monofluoroaminophosphorane, $(CF_3)_3P(F)NH(CH_3)$, in about 35% recovered yield according to the equation (1):

$$2(CF_3)_3PF_2 + 2CH_3NH_2 \longrightarrow (CF_3)_3P(F)NH(CH_3) + CH_3NH_3^+(CF_3)_3PF_3^- \quad (1)$$

Nmr spectroscopy of the solid residues in (C) of Figure 3a indicated the presence of the substituted fluorophosphate salt $CH_3NH_3^+(CF_3)_3PF_3^-$ and another unidentified compound in (A) of Figure 3a which contained no fluorine nucleus showed ^1H nmr spectrum as a sharp singlet at $\tau = 4.70$ and a doublet with $J = 9.0$ Hz at $\tau = 7.47$.

The reaction of $(CF_3)_3PF_2$ with $CH_3(CH_2C_6H_5)NH$ gave tris(trifluoromethyl)fluoro(N-methylbenzylamino)phosphorane, $(CF_3)_3P(F)N(CH_3)CH_2C_6H_5)$, in estimated 89% yield according to the equation (2):

$$2(CF_3)_3PF_2 + 2CH_3(CH_2C_6H_5)NH \longrightarrow (CF_3)_3P(F)NCH_3(CH_2C_6H_5) + CH_3(CH_2C_6H_5)NH_2^+(CF_3)_3PF_3^- \quad (2)$$

The involatile salt $CH_3(CH_2C_6H_5)NH_2^+(CF_3)_3PF_3^-$ was the only other product found along with ~20% of $(CF_3)_3P(F)NCH_3(CH_2C_6H_5)$ in the reaction vessel.

The reaction of $CH_3(CF_3)_2PF_2$ with CH_3NH_2 in gas phase gave methylbis(trifluoromethyl)fluoromethylaminophosphorane $CH_3(CF_3)_2P(F)NH(CH_3)$, in 50 % yield according to the equation (3):

$$2CH_3(CF_3)_2PF_2 + 2CH_3NH_2 \longrightarrow CH_3(CF_3)_2P(F)NH(CH_3) + CH_3NH_3^+CH_3(CF_3)_2PF_3^- \quad (3)$$

The only other product was identified as the salt $CH_3NH_3^+CH_3(CF_3)_2PF_3^-$, a white solid.

Phosphorus pentafluoride formed a 1:1 adduct with N-methylbenzylamine typical of analogous adducts previously reported.[55] When heated at 75° the solid melts and evolves N-methylbenzylaminofluorophosphorane, $PF_4N(CH_3)$-$CH_2C_6H_5$ leaving behind a salt, $CH_3(CH_2C_6H_5)NH_2^+PF_6^-$.

$$2PF_5 \cdot N(CH_3)(CH_2C_6H_5)H \xrightarrow{\Delta} PF_4NCH_3(CH_2C_6H_5) + CH_3(CH_2C_6H_5)NH_2^+ \cdot PF_6^- \quad (4)$$

Hydrolysis

Alkaline hydrolysis of the two new phosphoranes $(CF_3)_3P(F)NH(CH_3)$ (I) and $(CF_3)_3P(F)NCH_3(CH_2C_6H_5)$ (II) gave two molar equivalents of fluoroform, leaving the $CF_3PO_3^=$ anion[46] in the solution (equation 5). Neutral hydrolysis yielded one molar equivalent of fluoroform, leaving the $(CF_3)_2PO_2^-$ anion[46] in the solution (equation 6).

$$(CF_3)_3P(F)NR_1R_2 + 3H_2O \xrightarrow{OH^-} CF_3PO_3^= + 2CF_3H + R_1R_2NH_2^+ + F^- + 2H^+ \quad (5)$$

$$(CF_3)_3P(F)NR_1R_2 + 2H_2O \longrightarrow (CF_3)_2PO_2^- + CF_3H + R_1R_2NH_2^+ + F^- + H^+ \quad (6)$$

$R_1 = H, CH_3$

$R_2 = CH_3, CH_2C_6H_5$

Alkaline hydrolysis of $CH_3(CF_3)_2P(F)NH(CH_3)$ gave two molar equivalents of fluoroform, leaving the $CH_3PO_3^=$ ion and an anion tentatively identified as $CH_3PO_2NH(CH_3)^-$ in the solution (equation 7). The ^{19}F nmr spectrum of the

$$2CH_3(CF_3)_2P(F)NH(CH_3) + 5H_2O \xrightarrow{OH^-} CH_3PO_2NH(CH_3)^- + CH_3PO_3^= + 2F^- + 4CF_3H + CH_3NH_3^+ + 4H^+ \quad (7)$$

hydrolysate showed only one signal at 120.6 ppm due to F^- anion, therefore no CF_3 or F remains attached to phosphorus. The ^1H nmr spectrum showed three doublets at τ = 8.87,

8.70, and 7.51. The more intense doublet at τ = 8.87, due to the coupling of CH_3 protons with phosphorus, ($^2J_{PH}$ = 15.8 Hz), was assigned to known proton resonances[54] of $CH_3PO_3^=$. The other two doublets of equal relative intensity were assigned to the two CH_3 groups in $CH_3PO_2NH(CH_3)^-$. The doublets of the CH_3 group attached to the nitrogen and the CH_3 group directly bound to the phosphorus ($^3J_{PH}$, 12.7 Hz and $^2J_{PH}$, 15.6 Hz respectively) arise from coupling with the phosphorus atom. The assignment of the CH_3 group attached to nitrogen atom (τ = 7.51) was made by analogy to $(CH_3)_2N(F)PO_2^-$ [76] ($\tau[(CH_3)_2N]$ = 7.40). No further splittings were observed upon expansion of the spectral signals. The parameters are given in Table 2.

Neutral hydrolysis of $CH_3(CF_3)_2P(F)NH(CH_3)$ yielded one molar equivalent of fluoroform, leaving the $CH_3(CF_3)PO_2^-$ ion in the solution (equation 8).

$$CH_3(CF_3)_2P(F)NH(CH_3) + H_2O \longrightarrow CH_3(CF_3)PO_2^- + CF_3H + CH_3NH_3^+ + F^- \quad (8)$$

Table 1

Hydrolysis of Phosphoranes

	Conditions	Quantity of Compound		Yield of CF_3H		Ions (or Compounds) Remaining in Hydrolysate[a]
		wt(gm)	(mmole)	wt(gm)	(mmole)	
$(CF_3)_3P(F)NH(CH_3)$	neutral	0.082	0.29	0.021	0.30	$(CF_3)_2PO_2^-$
	alkaline	0.174	0.61	0.82	1.16	$CF_3PO_3^=$
$(CF_3)_3P(F)NCH_3(CH_2C_6H_5)$	neutral	0.076	0.20	0.015	0.21	$(CF_3)_2PO_2^-$
	alkaline	0.166	0.44	0.061	0.87	$CF_3PO_3^=$
$CH_3(CF_3)_2P(F)NH(CH_3)$	neutral	0.066	0.28	0.017	0.24	$[CH_3(CF_3)PO_2^-]$
	alkaline	0.074	0.32	0.045	0.64	$[CH_3PO_2NH(CH_3^-)]+$ $CH_3PO_3^=$

(a) species in [] brackets have been tentatively identified by nmr spectroscopy.

TABLE 2

NMR Data of Phosphorus Containing Hydrolysis Products of $CH_3(CF_3)_2P(F)NH(CH_3)$

Compound	τ[a]	ϕ_F[b]	ϕ_{CF_3}[b]	$^2J_{PF}$	$^2J_{PH}$	$^3J_{PH}$	$^3J_{FH}$	$^4J_{FH}$	$^5J_{FH}$
$CH_3PO_3^=$	8.87[e]	120.6			15.8				
$CH_3PO_2NH(CH_3)^-$	7.51[c,e]					12.7			
	8.7[b,e]				15.6				
$CH_3(CF_3)PO_2^-$	7.4[c,f]		77.1[g]	91.0				0.7	6.0
	8.54[d,g]				15.25		0.8		

Footnotes for Table 2

[a] τ relative to internal Tetramethylsilane, τ = 10.0.

[b] ϕ relative to internal (solvent) $CFCl_3$ standard with positive values indicating resonance to high field of standard.

[c] CH_3 group attached to nitrogen

[d] CH_3 group attached to phosphorus

[e] doublet

[f] quartet

[g] doublet of quartets.

TABLE 3

Mass Spectra Data for $(CF_3)_3P(F)NH(CH_3)$, $(CF_3)_3P(F)NCH_3(CH_2C_6H_5)$ and $CH_3(CF_3)_2P(F)NH(CH_3)$

m/e	Intensity[a] $(CF_3)_3P(F)NH(CH_3)$	Intensity[a] $(CF_3)_3P(F)NCH_3(CH_2C_6H_5)$	Intensity[a] $CH_3(CF_3)_2P(F)NH(CH_3)$	Assignment[b]
308		0.21		$(CF_3)_2P(F)N(CH_3)CH_2C_6H_5$
286	0.075			$(CF_3)_3PFNCH_3$
268	0.94	0.54		$(CF_3)_3PNCH_4$
257	1.09	3.26		$(CF_3)_3PF$
230	0.30			$(CF_2)_2CF_3PNCH_4$
219	13.52			$(CF_3)_2PCF_2$
218		7.14	0.50	$(CF_3)_2P(F)NCH_4$
214			1.54	$CH_3(CF_3)_2PNCH_4$
213			0.66	$CH_3(CF_3)_2PNCH_3$
208		0.44		$C_8H_{10}F_3PN$

TABLE 3 (continued)

207	1.32	18.35		C_3F_9
203			2.55	$CH_3(CF_3)_2PF$
198	0.84	0.58		$(CF_3)_2PNCH_3$
179	0.74			$(CF_3)CF_2PNCH_3$
169	0.44	0.37		$(CF_3)_2P$
168	9.20	4.62	1.99	$(CF_3)PF_2NCH_4$
165			0.50	$CH_3(CF_3)PFNCH_5$
164			13.53	$CH_3(CF_3)PFNCH_4$
157	0.94	14.95	0.64	CF_3PF_3
153			6.37	CF_5HNP
148	0.33			CF_3PFNCH_3
144			2.20	$C_3H_8F_3PN$
134			0.34	CHF_4PN
130	1.96			$C_2H_4F_3PN$
129	1.23			$C_2H_3F_3PN$
119	0.63	1.84		CF_4P; C_8H_9N

TABLE 3 (continued)

118	14.18	3.23	2.28	CH_4PF_3PN
115			0.50	CHF_3PN
114			16.98	CF_3PN
112		0.37	0.50	C_2F_3P, $C_2H_5F_2PN$
107		1.09		C_7H_9N
105			0.98	F_3PNH_3
103			6.63	FPNH
101			8.89	
100	0.60	0.92		CH_5F_2PN; CF_3P
98	0.51		0.37	CH_3F_2PN
94		0.71	2.54	C_2H_6FPN
88		0.88		F_3P
86	0.44	1.16		F_2PNH_3
84			0.56	F_2PNH
81	0.30			C_2F_3
80	6.79	2.00	2.57	CH_4FPN

TABLE 3 (continued)

79	0.54		0.69	CH_3FPN
78	1.48	0.51	0.58	CH_2FPN
76			0.37	FPNC
73			0.82	H_2PF_2
69	17.04	27.19	8.22	CF_3, F_2P
66			1.01	CF_2H_2N
65			2.57	CHF_2N
64			0.34	CF_2N
62		0.44		CH_5PN
60	3.39	0.58	1.41	CH_3PN
59	0.33			CH_2PN
57	2.40			CFN
56	2.41			CH_3F
55	0.48			F_2H_3N
53		0.44		FPH_3
52			2.20	H_2PF; H_2CF_2

TABLE 3 (continued)

51	2.63	1.73		CF_2H, PHF
50	1.49	1.49	0.77	CF_2; FP
47		0.82	0.53	$HPCH_3$; HPNH
46	1.29		0.56	HNCF
45			1.17	NCF
44			1.25	C_2H_6N
43	1.89			C_2F
42	1.15		0.61	C_2H_4N
41	2.41			$CNCH_3$
39	.75			HF_2
37			0.34	NH_4F
36			0.45	NH_3F
32	.82	1.97	0.37	CFH, CH_3NH, PH
31	2.07	2.04	2.07	CF, P

TABLE 4

Mass Spectra Data For $PF_4NCH_3(CH_2C_6H_5)$

m/e	Intensity[a]	Assignment[b]
137	6.32	PF_4NHCH_3
136	2.71	PF_4NCH_3
131	1.04	$PF_3NC_2H_5$
128	0.90	$PF_3NC_2H_2$
119	0.84	PF_3NCH_5, $NCH_3CH_2C_6H_5$
118	9.03	PF_3NCH_4
117	0.52	PF_3NCH_3
116	1.76	PF_3NCH_2
115	3.39	PF_3NCH, POF_2NCH_4
114	3.39	PF_3NC
112	1.67	$PF_2NC_2H_5$
107	21.67	PF_4
105	1.11	$NCH_2C_6H_5$
104	2.71	$NCHC_6H_5$, PF_3NH_2
103	1.56	PF_3NH
101	0.45	PF_3CH
96	0.65	PF_2NCH
94	1.02	PF_3C
91	1.15	$CH_2C_6H_5$
88	7.45	PF_3
87	1.56	C_7H_3

TABLE 4 (continued)

86	0.95	PF_2NH_3
85	2.71	POF_2
84	0.77	PF_2NH
81	1.29	$PFNCH_5$
78	0.56	$PFNCH_2$
77	0.61	PFNCH
69	8.58	PF_2
67	0.97	NH_3CF_2
66	0.65	NH_2CF_2
65	2.56	$NHCF_2$, PFNH
63	0.70	PFHC
57	0.54	PNC
55	0.49	NH_3F_2
51	0.97	PFH
50	0.97	CF_2,PF
47	1.17	H_2NCF, PO
44	1.24	C_2H_6N
43	0.54	C_2F
42	0.45	C_2H_4N
41	0.84	C_2H_3N
39	0.61	CFH_6
32	1.24	PH, HCF

[a] Intensity is expressed as % total ionization based on the sum of the intensities of ions with m/e greater than 30.

[b] Assignments of some ions are given in terms of the structural formula for ease of recognition only.

TABLE 5

Mass Measurement Data

Compound	Ion[a]	Calculated m/e	Found m/e
$(CF_3)_3P(F)NH(CH_3)$	$(CF_3)_3P(F)NCH_3^+$	285.9844	285.9855
	$(CF_3)_3PNHCH_3^+$	267.9938	267.9928
	$(CF_3)_3PF^+$	256.9578	256.9588
$(CF_3)_3P(F)N(CH_3)(CH_2C_6H_5)$	$(CF_3)_2P(F)N(CH_3)(CH_2C_6H_5)^+$	308.0439	308.0444
	$(CF_3)_3PF^+$	256.9578	256.9585
	CF_3^+	68.9706	68.9707
$CH_3(CF_3)_2P(F)NH(CH_3)$	$CH_3(CF_3)_2PNH(CH_3)^+$	214.0221	214.0223
	$CH_3(CF_3)_2PF^+$	202.9861	202.9862
	$CH_3(CF_3)P(F)NH(CH_3)^+$	164.0253	164.0252

TABLE 5 (continued)

$PF_4NCH_3(CH_2C_6H_5)$	$PF_4NH(CH_3)^+$	137.0018	137.0016
	PF_4^+	106.9674	106.9673
	PF_3^+	87.9690	87.9690

[a] A reasonable structural formula rather than the molecular formula is given for each fragment ion for convenience only.

Mass Spectra of the Phosphoranes

In common with other pentacoordinate phosphorus compounds,[51] the mass spectra (Tables 3 and 4) of all of the phosphoranes presented herein showed no parent ions. The characteristic fragments corresponding to $(CF_3)_3PF^+$ and $(CF_3)_2P(F)NCH_3(CH_2C_6H_5)^+$ from $(CF_3)_3P(F)NCH_3(CH_2C_6H_5)$, $(CF_3)_3PF^+$ and $(CF_3)_3P(F)N(CH_3)^+$ from $(CF_3)_3P(F)NH(CH_3)$, $CH_3(CF_3)P(F)NH(CH_3)^+$ and $CH_3(CF_3)_2PF^+$ from $CH_3(CF_3)_2$-$P(F)NH(CH_3)$, PF_4^+ from $PF_4NCH_3(CH_2C_6H_5)$ (Table 5) strongly suggested their derivation from the indicated parent molecule by loss of one of the substituents.

In $(CF_3)_3P(F)NH(CH_3)$ and $(CF_3)_3P(F)NCH_3(CH_2C_6H_5)$, the most intense peak was observed at m/e 69 which was principally CF_3^+ ion but also contained small proportions of PF_2^+ ion.[52] In $CH_3(CF_3)_2P(F)NH(CH_3)$ and PF_4NCH_3-$(CH_2C_6H_5)$, CF_3PN^+ (m/e 114, 16.98%) and PF_4^+ (m/e 107, 21.67%) were found as the most intense peaks respectively. The remaining features of the mass spectra of phosphoranes were characterized by loss of substituent groups and/or CF_2 elimination. The more stable phosphorane, $CH_3(CF_3)_2$-$P(F)NH(CH_3)$, gave a significant proportion of the ion $CH_3(CF_3)P(F)NH(CH_3)^+$ (m/e 164, 13.55%) by means of CF_2 elimination.[52] The ions $CF_3PF_3^+$ (m/e 157, 14.95%) from $(CF_3)_3P(F)NCH_3(CH_2C_6H_5)$ and $CF_3PF_2NH(CH_3)^+$ (m/e 168, 9.2%) from $(CF_3)_3P(F)NH(CH_3)$ can also arise from a CF_2

elimination process. In $PF_4NCH_3(CH_2C_6H_5)$ the abundant fragments; $PF_4NH(CH_3)^+$ (m/e 137, 6.32%), PF_4^+ (m/e 107, 21.67%), PF_3^+ (m/e 88, 7.45%) and PF_2^+ (m/e 69, 8.58%) arise from the loss of $NCH_3(CH_2C_6H_5)$ group and/or F elimination.

TABLE 6

Infrared Spectral Data[a]

$(CF_3)_3P(F)NH(CH_3)$	$(CF_3)_3P(F)NCH_3(CH_2C_6H_5)$[b]	$CH_3(CF_3)_2P(F)NHCH_3$	
3454w	3270w	3500s	ν_{C-H}
2952sh	3080wsh	3000sh	
2832w	3040w	2980m	
-	2970wsh	2920sh	
-	-	2850w	
1572w	1500w	-	$\sigma_{as}\ CH_3$
1463vw	1460m	1470m	
1442vw	-	1438sh	
1362vw	1370m	1380w	$\sigma_{sym}\ CH_3$
-	1340vw	1320w	
1282vw	1300m	-	
-	1210vw	1220s	ν_{C-F}
1192s	1190vs	1190vs	
1162vs	1150vs	1170vs	
1140s	1120s	1160vs	
1105vs	-	1120s	
1074vs	-		
1044m	1000m	1090s	ν_{PNC_2}
-	960w	970m	
872vw	-	895s	ν_{P-F}
840w	-	850s	
782s	780m	765m	$\sigma_{sym}CF_3$(?)
742s	750s	760m	

TABLE 6 (continued)

-	720m	730m	ν_{PN}(?)
690vs	690m	680s	ν_{PF}
631w	630m	-	
604s	590s	600sh	$\sigma_{as}CF_3$(?)
583m	-	550m	ν_{PCF_3}
542sh	-	530sh	
522vw	-	-	
510vw	-	490w	
460w	480wsh	455m	
-	-	430sh	

[a] gas phase spectra all values in cm^{-1}. S = strong, m = medium, w = weak, v = very, sh = shoulder, ν = stretching, σ = deformation, sym = symmetric, as = asymmetric, ? = a very tentative assignment.

[b] liquid film spectrum.

TABLE 7

Infrared Spectral Data[a]

$PF_4NCH_3(CH_2C_6H_5)$	$PF_4N(CH_3)_2$[b]	
3080sh	2960	ν_{C-H}
3040s	2900	
2940m	2860	
1610w	-	
1500m	-	
1450s	1464	$\sigma_{as}CH_3$
1420m	-	$\sigma_{sym}CH_3$
-	1368	
-	1300	σ_{CH_3}
1175s	1211	CH_3 rock
1028m	1042	$\nu_{as}NC_2$
962vs	950	ν_{P-F}
874vs	882 (doublet)	
762s	-	ν_{P-N}(?)
700s	701	
580m	-	
540w	-	
510w	-	
480w	-	
470w	-	

[a] gas phase spectra all values in cm^{-1}. s = strong, m = medium, w = weak, v = very, sh = shoulder, ν = stretching, σ = deformation; sym = symmetric, as = asymmetric, ? = a very tentative assignment.

[b] Ref. 55. No relative band intensities were given.

Infrared Spectra of the Phosphoranes

The infrared spectral data are summarized in Table 7. Bands associated with C-H stretching frequencies and with P-CF_3 and P-CH_3 structure units are readily observed in the expected regions. The assignments given in Table 6, based on qualitative group shift arguments derived from related molecules,[53,54] must be regarded as very tentative. The bands at 1044 cm^{-1} in the spectrum of $(CF_3)_3P(F)NH(CH_3)$, at 1000 cm^{-1} in the spectrum of $(CF_3)_3P(F)NCH_3(CH_2C_6H_5)$, and at 1090 cm^{-1} in the spectrum of $CH_3(CF_3)_2P(F)NH(CH_3)$ are undoubtedly due to the PNC_2 (or PNC) structural unit in the molecule. The band at 690 cm^{-1} in the spectra of $(CF_3)_3P(F)NH(CH_3)$ and $(CF_3)_3P(F)NCH_3(CH_2C_6H_5)$, and at 680 cm^{-1} in the spectrum of $CH_3(CF_3)_2P(F)NH(CH_3)$ can be assigned to P-F stretching vibrations.[53]

The assignment of the ir spectrum of $PF_4NCH_3(CH_2C_6H_5)$ was made by analogy to $PF_4(CH_3)_2$ [55] (Table 7), the corresponding bands at 962, 874, and 700 cm^{-1} are identified as originating from P-F modes, and a band at 762 cm^{-1} as the P-N stretch. The peaks at 3040 and 2940 cm^{-1} are in the range which is characteristic of the N-CH_3 group.[56] A band at 1028 cm^{-1} was assigned to the antisymmetric stretching mode of a N-C_2 group.[57]

CHAPTER 3

GROUND STATE STRUCTURE AND STEREOCHEMISTRY OF SOME PHOSPHORANES.

The ground state structures of the present series of phosphoranes can be deduced from the limiting low-temperature nmr spectra. It is reasonable to assume that the basic structure of these molecules is a trigonal bipyramid in keeping with the few examples[10,58] of this structure in analogous molecules and in agreement with the extensive nmr[14,23] and vibrational[59] spectroscopic studies of closely related molecules.

The Ground State Structures of $(CF_3)_3P(F)NH(CH_3)$ and $(CF_3)_3P(F)NCH_3(CH_2C_6H_5)$

The two new tris(trifluoromethyl)phosphoranes, $(CF_3)_3P(F)NR_1R_2$ (I); $R_1 = H$, $R_2 = CH_3$, (II); $R_1 = CH_3$, $R_2 = CH_2C_6H_5$ possess structure B (Fig. 4) analogous to that of tris(trifluoromethyl)difluorophosphorane[42] (structure A, Fig. 4), according to the low temperature nmr spectral data. Methylbis(trifluoromethyl)fluoro(methylamino)phosphorane and N-methylbenzylaminofluorophosphorane have structures D and E respectively analogous to the molecular structures of their respective parent molecules $CH_3(CF_3)_2PF_2$ (C, Fig. 4) and PF_5, again according to nmr spectroscopy. The ground state structures of the phosphoranes are those predicted by application of the rule that the most electronegative substituents preferentially occupy the axial positions in the trigonal bipyramid as first

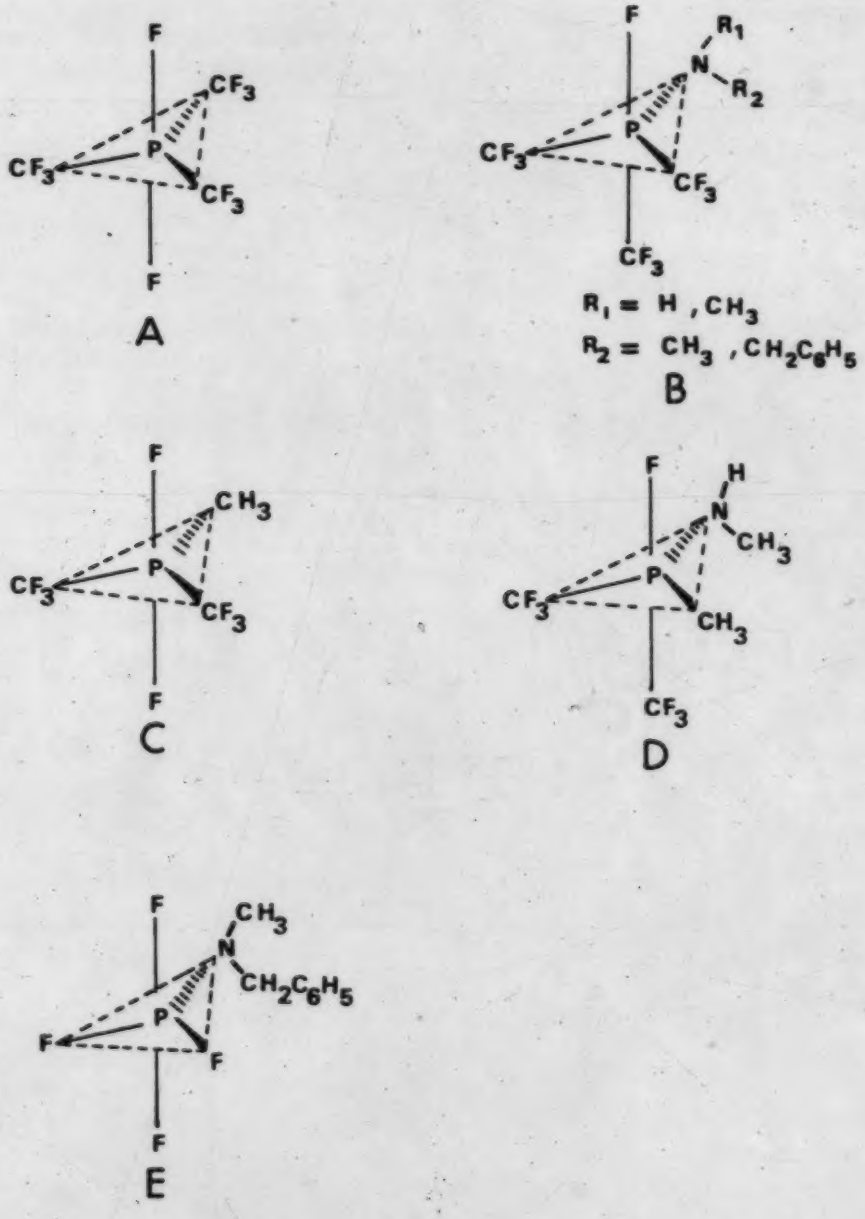

Figure 4 Structures of the Phosphoranes

proposed by Muetterties *et. al.*[14]. Thus fluorine preferentially occupies the axial position whereas CH_3, $NH(CH_3)$, $NCH_3(CH_2C_6H_5)$ prefer equatorial positions, either as a result of their low inductive character (i.e., σ_I is relatively small) or as a result of stronger π interactions between these substituents and phosphorus in the equatorial plane.[6,7,24] CF_3 groups, which appear to possess no strong preference for either position, occupy the remaining positions in the five-coordinate molecular framework. In all cases the ground state structure can be deduced from low temperature ^{19}F and ^{31}P nmr spectroscopy [and from the ^{13}C spectrum in the case of $(CF_3)_3P(F)N(CH_3)(CH_2C_6H_5)$].

The normal (+31°) temperature ^1H spectra of $(CF_3)_3P(F)NH(CH_3)$ (I) (Fig. 5) consists of a doublet with $^3J_{PH}$ = 11.5 Hz, due to coupling of protons with phosphorus. The spectra of $(CF_3)_3P(F)NCH_3(CH_2C_6H_5)$ (II) (Fig. 6) under the same conditions shows three chemically shifted regions in a 5:3:2 intensity ratio arising respectively from phenyl (C_6H_5), methyl (CH_3), and methylene (CH_2) groups attached to nitrogen. The phenyl region shows a sharp singlet at τ = 2.76 ppm and the CH_3 and CH_2 regions consist of a doublet of doublets and a doublet, respectively. The major doublet is due to $^3J_{PH}$, coupling of the CH_3 and CH_2 protons with phosphorus atom; the CH_3 protons are further split into doublets due to the coupling with the single fluorine ($^4J_{FH}$) directly bound to the phosphorus atom. In the CH_3 region, the fine structure of doublet

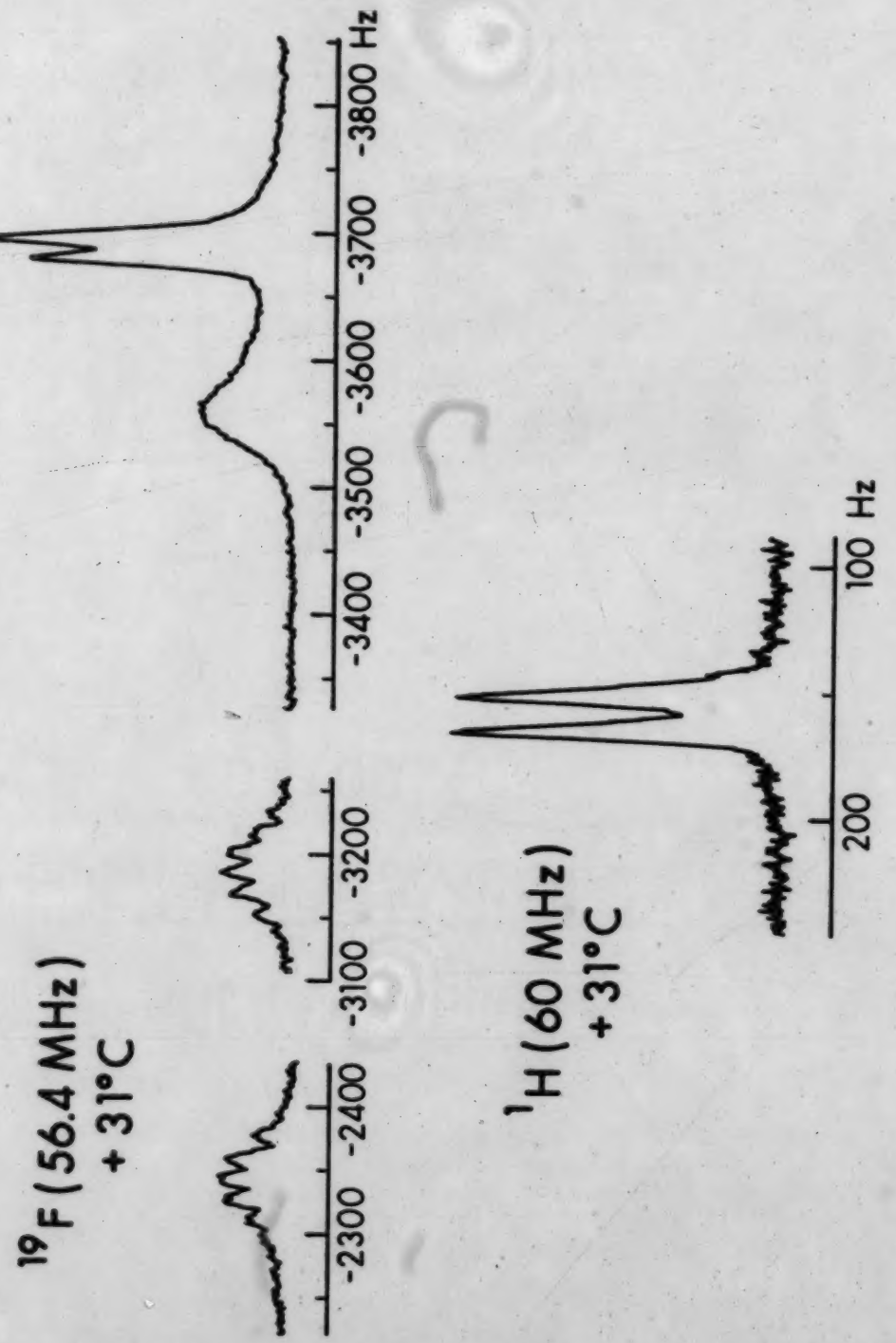

Figure 5 NMR spectra of $(CF_3)_3P(F)NH(CH_3)$ at +31° obtained in a solution of $CFCl_3$. Scale values refer to shifts (in Hz) from $CFCl_3$ and TMS respectively.

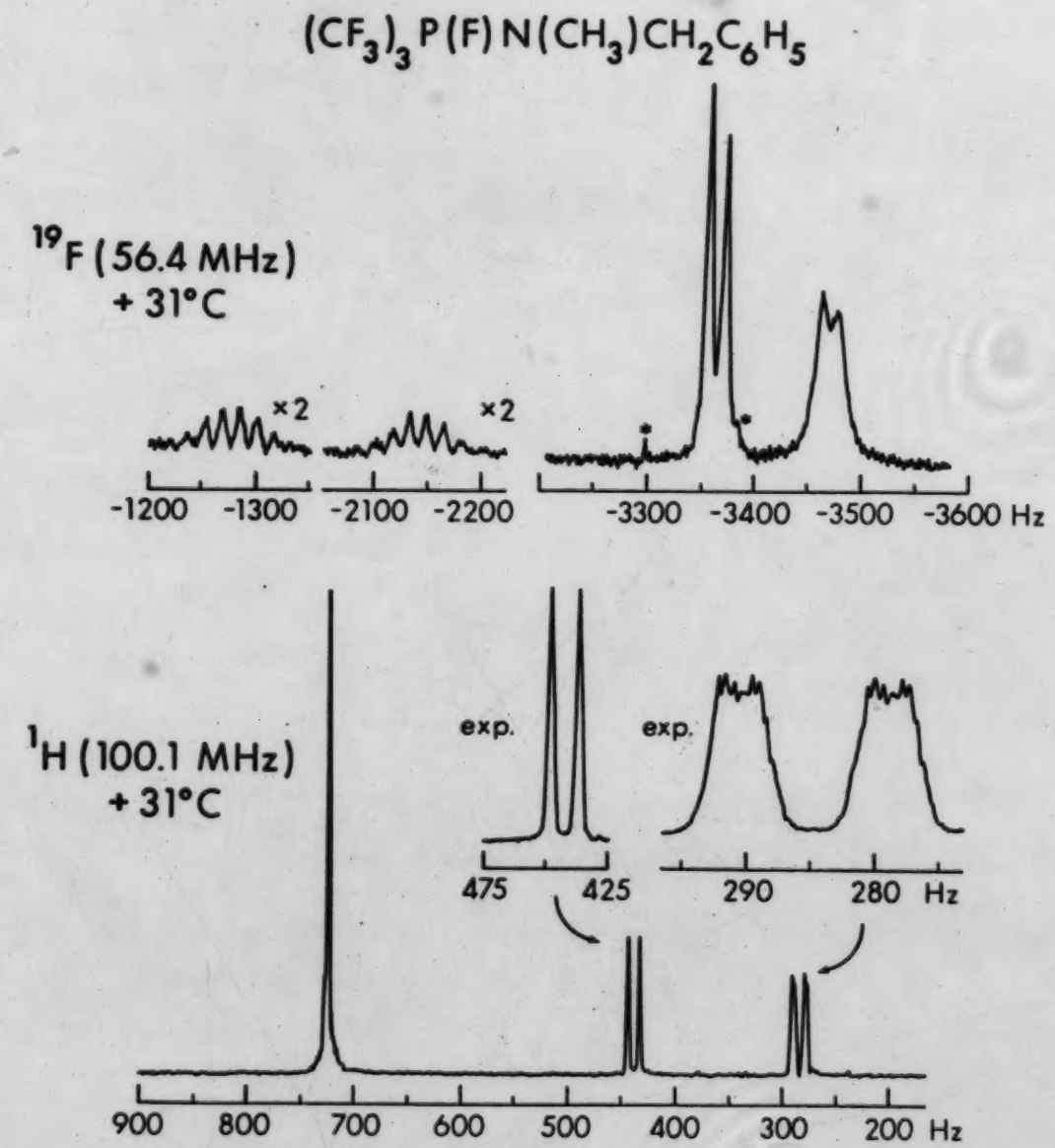

Figure 6 NMR spectra of $(CF_3)_3P(F)NCH_3(CH_2C_6H_5)$ at +31° obtained in a solution of $CFCl_3/CF_2Cl_2$. Scale values refer to shifts (in Hz) from $CFCl_3$ and TMS respectively. Impurity lines are marked by an asterisk.

TABLE 8

NMR Data of Tristrifluoromethylphosphoranes

	Temp	τ[a]	ϕ_P[b]	ϕ_{CF_3}[b]	σ_{31_P}[c]	$^1J_{PF}$	$^2J_{PF}$	$^3J_{PH}$	$^4J_{FH}$	$(^5J_{FH})$	$^3J_{FF}$	$^4J_{FF}$
$(CF_3)_3P(F)NCH_3(CH_2C_6H_5)$	+30°	7.15[d]	30.4[h]	60.6[i]	180.8[p,u]	866	108	11.4	2.0	(0.5[g])		
		5.56[e]					106[u,r]	11.4				
		2.76[f]										
	-40°		31.8[k]	59.0(1)[j,m,n]	180.1[q,u]	858	53.7[m,u]		2.0		v	v
				61.5(2)[j,l,o]			130.6[l,u]				17.6	15.0
$(CF_3)_3P(F)NH(CH_3)$	+30°	7.16	29.2[p]	64.1[i]	186[p,r,u]	843	102[p,u]	11.5				
						844[r,u]						
	-40°		49.6[s]	65.2(1)[j,m,t]	185.7[q,u]	834	49.6[m,u]				v	v
				63.7(2)[j,l,o]			133.1[l,u]				16.1	12.3

Footnotes for Table 8

[a] τ relative to internal Tetramethylsilane, τ = 10.0.

[b] ϕ relative to internal (solvent) CCl_3F standard with positive values indicating resonance to high field of standard.

[c] ppm *vs* P_4O_6 as external standard (capillary), positive values indicating resonance to high field of standard.

[d] CH_3 region, doublet

[e] CH_2 region, doublet

[f] C_6H_5 region, sharp singlet

[g] doublet of decets obtained from expansion of CH_3 region

[h] doublet of quartets of decets

[i] broad doublet

[j] relative intensity in arbitrary units

[k] doublet of multiplets

[l] CF_3 equatorial

[m] CF_3 axial

[n] two overlapped septets

[o] doublet of two overlapped quartets

[p] doublet of decets

[q] doublet of septets of quartets

[r] obtained at 55°C

[s] doublet of broad multiplets

[t] broad multiplets

[u] obtained from $^{31}P - \{^1H\}$ nmr spectra

[v] axial signal is broad and unresolved therefore the coupling constant cannot be obtained from the ^{19}F spectra.

of decets is caused by the coupling of the protons with nine equivalent fluorine nuclei of the three CF_3 groups, thus confirming the presence of three CF_3 groups in the molecules. The low temperature ^1H spectrum of (I) showed no signal from the NH group. At -40°, the CH_3 region of (II) showed a broad doublet. As the temperature was further decreased, the doublets of both the CH_3 and the CH_2 regions became broader, suggesting onset of inequivalencies arising from frozen molecular conformations. All nmr data are summarized in Table 8.

The ^{19}F nmr spectra of (I) and (II) at normal instrument temperature (+31°) showed only two distinct fluorine atom environments due to the three equivalent CF_3 groups and the single fluorine respectively. The latter signal comprises a doublet of multiplets (doublet of quartets of decets in (II), doublet of decets in (I)) (Fig. 7 and 8 .), characterized by a large coupling constant (~859 Hz) due to $^1J_{PF}$. The magnitude of $^1J_{PF}$ clearly indicates that the fluorine is directly bound to phosphorus[23] even in the solution state at ordinary temperatures and confirms the phosphorane[60] formulation. Small couplings within each component of the doublet arise from coupling of this single fluorine to the fluorine atoms of equivalent CF_3 groups ($^3J_{FF}$) and to the protons ($^4J_{FH}$) of the fifth substituent. The spectra obtained at 56.4 MHz showed the ^{19}F signal of the CF_3 region of (II) to be a doublet of doublets (Figure 6).

Figure 7 ^{19}F (94.1 MHz) nmr spectra of $(CF_3)_3P(F)NCH_3$-$(CH_2C_6H_5)$ at various temperatures obtained in a solution of $CFCl_3/CF_2Cl_2$. Scale values refer to shifts from $CFCl_3$ in Hz. Impurity lines are marked by asterisks.

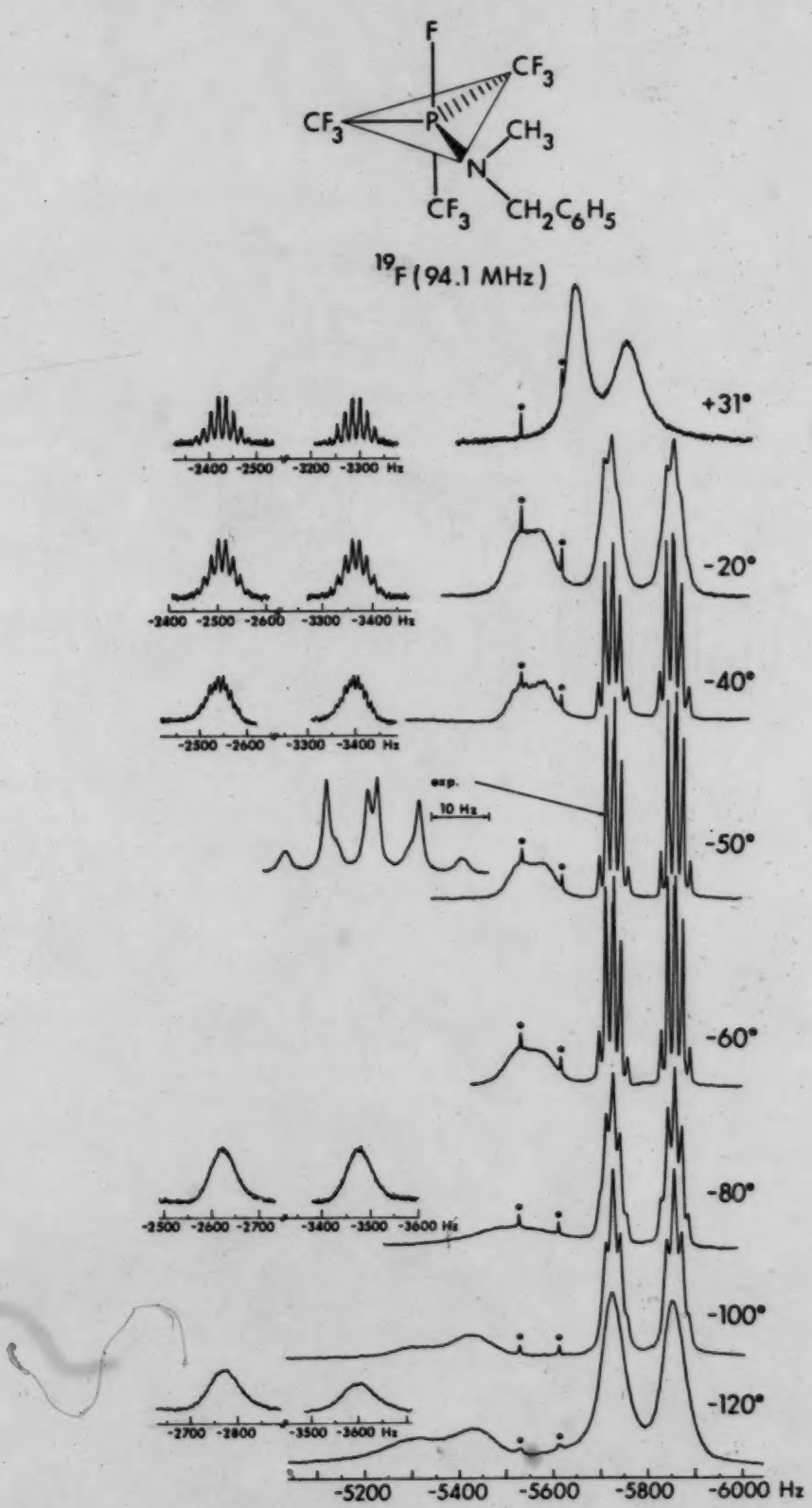
F
CF3
CF3
P
CH3
N
CF3
CH2C6H5
19F (94.1 MHz)
+31°
-20°
-40°
-50°
-60°
-80°
-100°
-120°
exp.
10 Hz
-2400 -2500 -3200 -3300 Hz
-2400 -2500 -2600 -3300 -3400 Hz
-2500 -2600 -3300 -3400 Hz
-2500 -2600 -2700 -3400 -3500 -3600 Hz
-2700 -2800 -3500 -3600 Hz
-5200 -5400 -5600 -5800 -6000 Hz

Figure 7

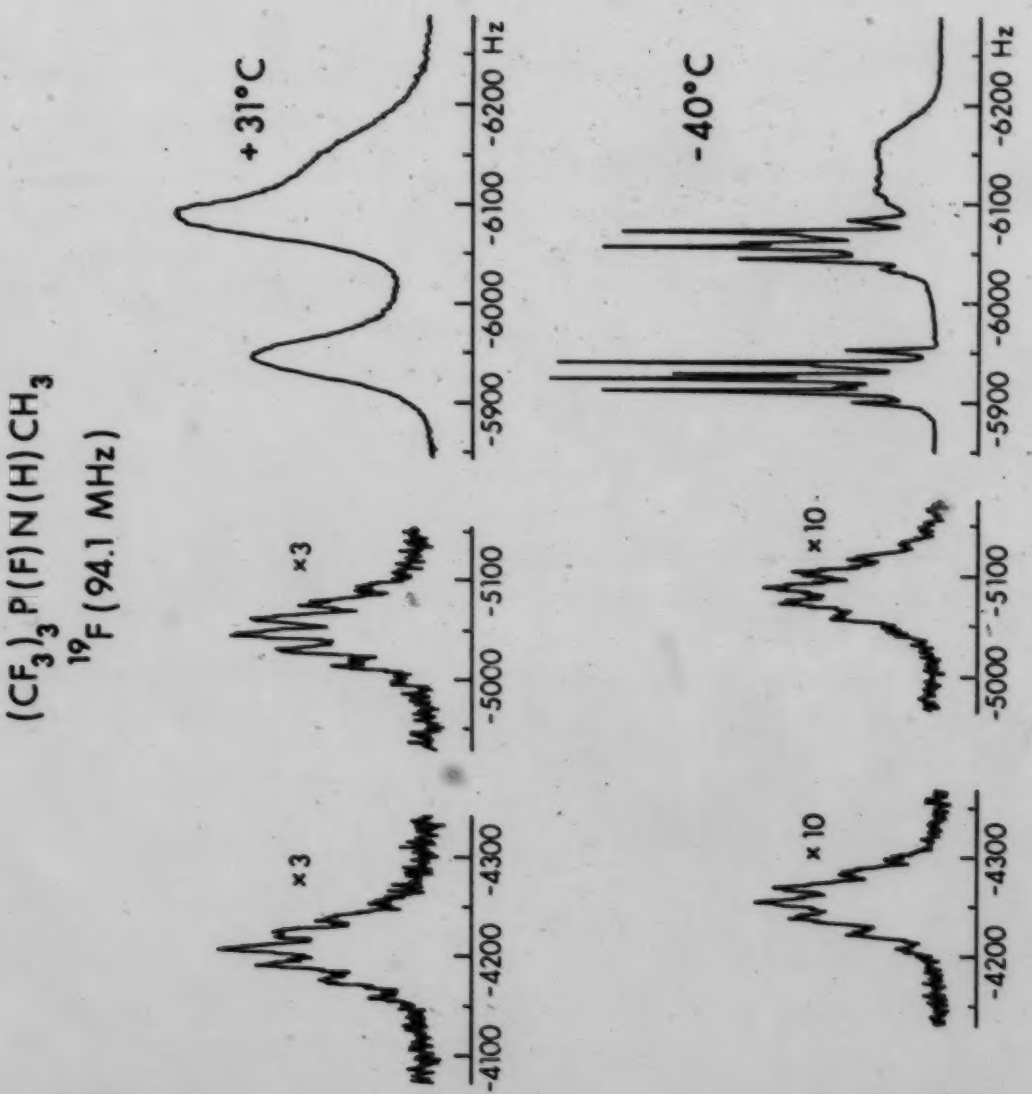

Figure 8 Fluorine nmr spectra of $(CF_3)_3P(F)NH(CH_3)$ at +31°, and -40° obtained on a solution of the compound in $CFCl_3$. The frequency scale gives shifts (in Hz) from the $CFCl_3$ reference.

The major doublet is due to $^2J_{PF}$ (~106 Hz), the average value of the coupling with phosphorus. The smaller doublet within each component is due to coupling with the single fluorine ($^3J_{FF}$) directly attached to the phosphorus atom. The signals obtained at 94.1 MHz showed an overlapping of two broad singlets in (II) (Fig. 7) with an average coupling constant $^2J_{PF}$ of 108 Hz, a broad singlet and an intermediate collapsed doublet in (I) (Fig. 8).

Fluorine nmr spectroscopy of (I) and (II) at progressively lower temperatures showed that the signal due to the single fluorine atom was essentially unaffected except for loss of the multiplet fine structure within each component of the major doublet, most probably as a result of increased multiplicity and some broadening due to solvent effects. The signal due to CF_3 resonances resolved at -40° in both compound (Fig. 7 and 8) into two chemically shifted regions with 2:1 relative intensity. In both of the above spectra the more intense signal appears as a doublet of two overlapped quartets due to $^4J_{FF}$ (12 Hz in (I), 15 Hz in (II)) coupling to the axial CF_3 group and $^3J_{FF}$ (16 Hz in (I), 18 Hz in (II)) coupling to the single fluorine. The relatively large value of $^2J_{PP}$(eq) is clearly shown by the major doublet structure in the stronger signal. The weaker signal, comprised of overlapped septets in II and a multiplet in (I), is due to the relatively smaller value of $^2J_{PP}$(ax).

Although not clearly resolved in the ^{19}F spectrum, this value can be unambiguously obtained from the low temperature $^{31}P - \{^{1}H\}$ spectrum.

At high temperatures the $^{31}P - \{^{1}H\}$ spectrum. (55° in (I), 34° in (II)) became a doublet of decets (the outermost unit intensity lines were not observed) due to coupling of phosphorus with nine equivalent fluorine nuclei of the three CF_3 groups. The signals collapsed and resolved into a doublet of septets of quartets at -30° in (I) (Fig.9) and -60° in (II)(Fig. 10). The major doublet is due to $^{1}J_{PF}$, coupling with the single fluorine. Each of the doublets is coupled with six fluorine nuclei of the two equatorial CF_3 groups $[^{2}J_{PF}(eq)]$ to give the major septet and with three fluorine nuclei of the axial CF_3 group to give the minor quartet observed.

In $(CF_3)_3P(F)NCH_3(CH_2C_6H_5)$, additional effects are observed in the ^{19}F and ^{31}P spectra upon cooling the sample below those required to clearly distinguish the CF_3 environments. The ^{19}F spectrum at temperatures below -40° (Fig. 7) showed the broadening of the lines and loss of coupling constant structure in both portions of the spectrum assigned to axial and equatorial CF_3 groups. The ^{19}F spectrum at -120° showed a doublet in the equatorial region and broad bands (rel. int. 1:2) in the axial region. It seems reasonable to suggest that cessation of additional averaging processes such as P-N bond rotation or nitrogen

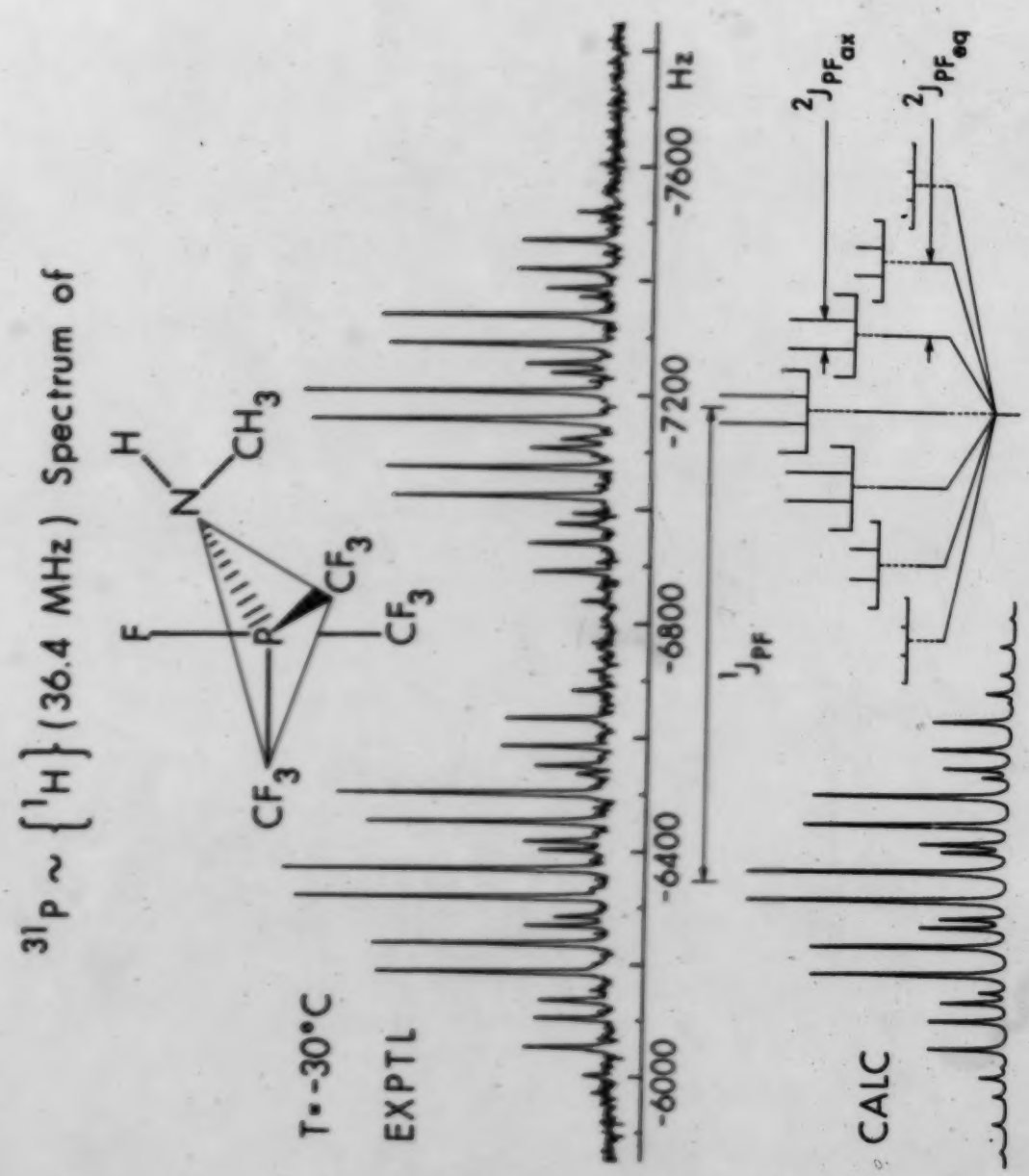

Figure 9 Observed and calculated phosphorus nmr spectra of $(CF_3)_3P(F)NH(CH_3)$ at -30°. The frequency scale gives chemical shift values relative to P_4O_6. The stick diagram shows the origin of the pattern which is a doublet of septets of quartets due to two axial CF_3 groups ($^2J_{PF}$, 49.6 Hz) and one equatorial CF_3 group ($^2J_{PF}$, 133.1 Hz) attached to phosphorus.

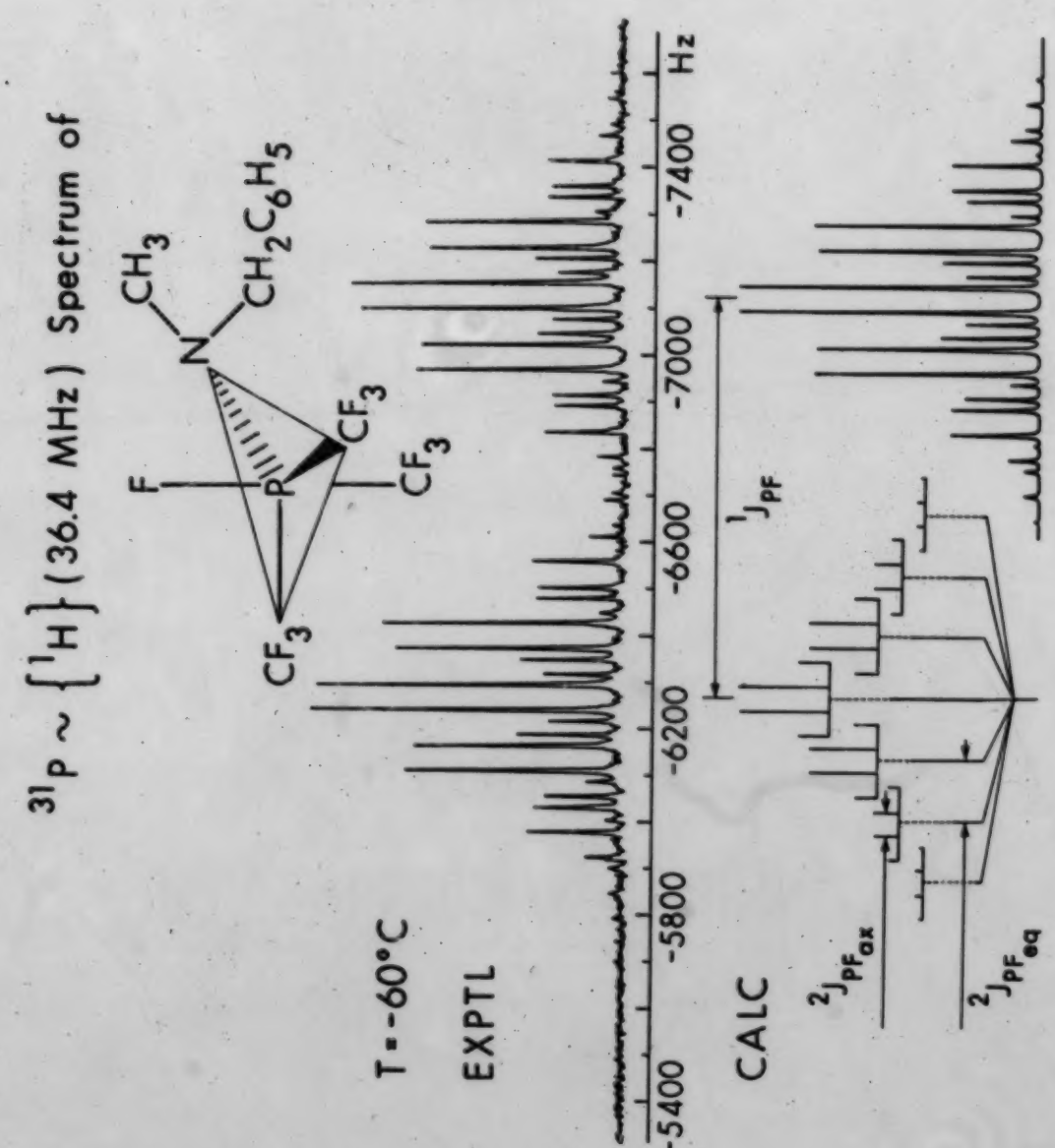

Figure 10 Observed and calculated phosphorus nmr spectra of $(CF_3)_3P(F)NCH_3(CH_2C_6H_5)$ at -60°. The frequency scale gives chemical shift values relative to P_4O_6. The stick diagram illustrates the formation of the pattern of a doublet of septets of quartets due to two axial CF_3 groups ($^2J_{PF}$, 53.7 Hz) and one equatorial group ($^2J_{PF}$, 130.6 Hz) attached to phosphorus.

inversion at these very low temperatures or possible cessation of free rotation of the axial CF_3 group creates inequivalent F atom environments within the CF_3 group and thus the complex spectra observed. We might expect to observe an A_2B pattern from the axial CF_3 group considering the projection below:

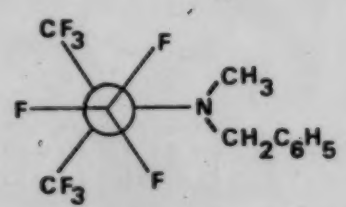

however the spectra are not clearly resolved in the present case. The ^{31}P spectrum also showed increasing complexity beyond that ascribed to the resolution of distinct axial and equatorial environments for the CF_3 groups below temperatures of the order of -80°. Unfortunately, the spectra are not fully resolved and therefore are not assignable and solidification of the sample prevented additional cooling. The dynamic nmr study of CF_3 permutational interchange in $(CF_3)_3P(F)NCH_3(CH_2C_6H_5)$ along with that of $(CF_3)_3P(F)NH(CH_3)$ are discussed below.

The ^{13}C - $\{^1H\}$ nmr spectrum of (II) (Fig. 11) in the aromatic region showed the four signals expected for a monosubstituted benzene derivative (Table 9). Assignment of the carbon signals was done by recognizing that

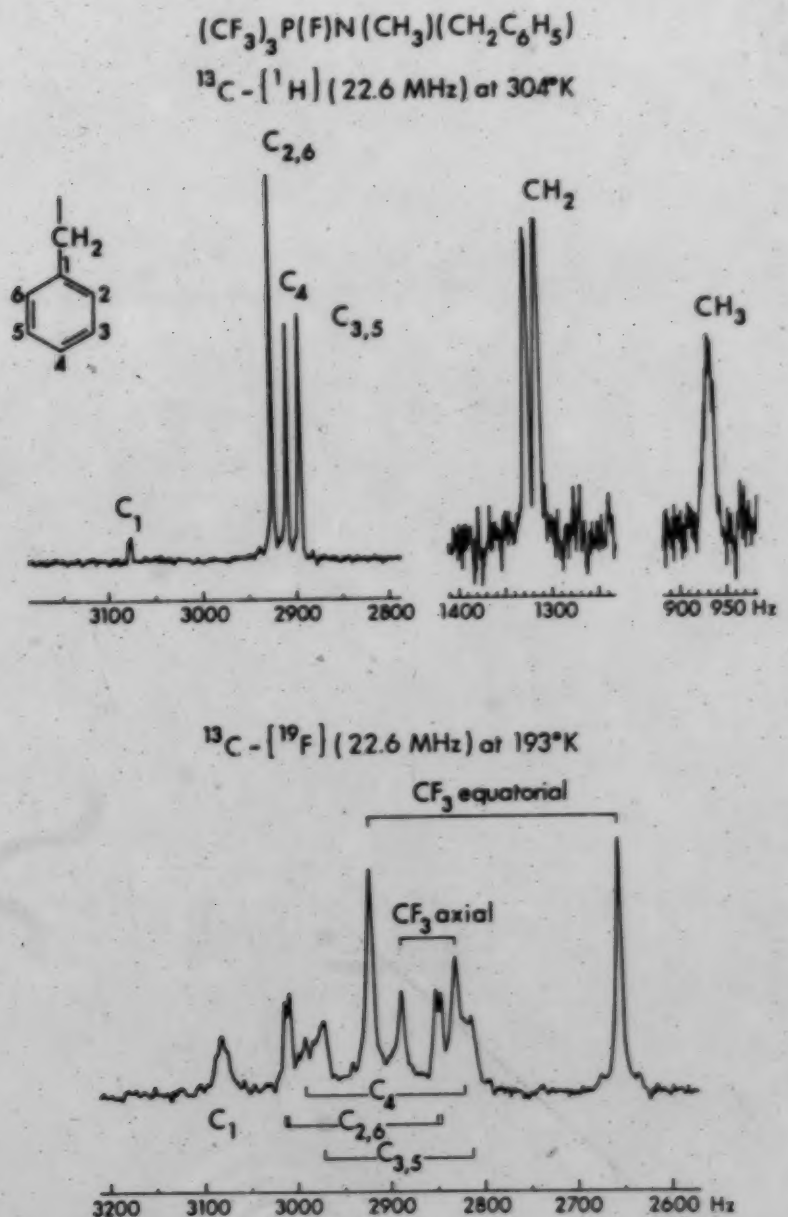

Figure 11 The upper portion of the figure shows the $^{13}C-\{^1H\}$ nmr spectrum of $(CF_3)_3P(F)NCH_3(CH_2C_6H_5)$ at +31° (304°K) obtained in a solution of CD_2Cl_2. The lower portion shows the $^{13}C-\{^{19}F\}$ spectrum of the same compound at -80°C (193°K) also in CD_2Cl_2. The frequency scales give chemical shift values from $(^{13}CH_3)_4Si$ (in Hz) both cases.

TABLE 9

^{13}C NMR Data of $(CF_3)_3P(F)NCH_3(CH_2$ 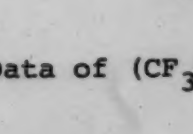)

Temp	Region	$\delta(^{13}C)$ [a]	J_{PC} (Hz)	$^1J_{CH}$ (Hz)
+31°	CH_3	38.4[b,i]	-	56.0[d,f]
	CH_2	58.4[b,e]	12.2	68.0[d,g]
	C_1	136.3[b,e]	2.0	-
	$C_{2,6}$	129.4[b,i]	6.0	162.0[e,h]
	$C_{3,5}$	128.1[b,i]	-	158.0[e,e]
	C_4	128.7[b,i]	-	uncertain
+45°	CF_3	124.9[c,e]	200[av][j]	-
+60°	CF_3	125.1[e,e]	198[av][j,k]	-
-80°	CF_3(eq)	123.4[e,e]	263[2][l,m]	-
	CF_3(ax)	126.5[e,e]	59[1][l,n]	

[a] measured values (*vs.* CD_2Cl_2; σ = 53.6 ppm) have been converted to $(^{13}CH_3)_4Si$ reference scale. Positive values indicate resonance downfield of standard.

[b] obtained from $^{13}C - \{^1H\}$ spectra.

[c] obtained from $^{13}C - \{^{19}F\}$ spectra.

[d] obtained from off-resonance decoupling technique

Footnotes for Table 9 (continued)

[e] doublet

[f] quartet overlapped with the signals from $CD_3C_6D_{11}$

[g] triplet of doublets

[h] doublet of doublets

[i] singlet

[j] the weighted average of the axial and equatorial $^1J_{PC}$ values

[k] using d_{14} methylcyclohexane as the solvent for high temperature measurement

[l] relative intensity in arbitrary units

[m] CF_3 equatorial

[n] CF_3 axial

the lack of an attached proton prevents C_1 from experiencing a nuclear Overhauser effect thus, the C_1 resonance was readily assigned to the weakest signal. The doubling of the C_1 signal may be due to $^3J_{PC}$ coupling with the P atom. Next the C_4 signal was distinguished from the $C_{2,6}$ and $C_{3,5}$ signals on the basis of relative peak intensities. Distinction between the $C_{2,6}$ and $C_{3,5}$ resonances was facilitated by a consideration of the fluorine-decoupled ^{13}C nmr spectrum (Fig. 11). The doublet structure of $C_{2,6}$ and $C_{3,5}$ signals is due to the coupling from proton directly attached to carbon. Each member of the $C_{2,6}$ doublet showed another doublet fine structure of about 6 Hz arising from $^3J_{PC}$. The assignments of $C_{2,6}$ and $C_{3,5}$ signals are also consistent with ^{13}C nmr data on phenyl containing compounds[61-63] which invariably show the $C_{2,6}$ resonance at lower field than that due to $C_{3,5}$.

The other signals at higher field, a doublet and a singlet, were assigned to methylene (CH_2) and methyl (CH_3) carbons respectively (Table 9). The assignment was assured by off-resonance decoupling technique[64] which allowed multiplicity due to H-C coupling to be observed. Under these conditions the methylene signals comprise a triplet of doublets due to two directly attached hydrogens. Each component of the triplet showed a doublet due to the coupling with the phosphorus atom. The methyl signals were overlapping with the signals from deuterated methyl

cyclohexane which was used as a solvent, therefore the $^1J_{CH}$ value in the methyl group was only approximate.

At 153°K, the $^{13}C - \{^{19}F\}$ spectrum of (II) consisted of a pair of doublets with a relative intensity ratio of 2:1. The more intense doublet with the larger coupling constant ($^1J_{PC}$; 263 Hz) can be assigned to two equatorial CF_3 groups and the doublet of lesser intensity with the smaller coupling constant ($^1J_{PC}$; 59 Hz) to the single axial CF_3 group since the $^1J_{PC}$ values appear to correlate linearly with $^2J_{PF}$ values.[65] At 333°K, the distinction between axial and equatorial environment is lost and the resultant average value of the coupling constant ($^1J_{PC}$; 198 Hz) is in good agreement with the weighted average of the above axial and equatorial $^1J_{PC}$ values.

The Ground State Structure of $CH_3(CF_3)_2P(F)NH(CH_3)$

The ^1H nmr spectrum of $CH_3(CF_3)_2P(F)NH(CH_3)$ (III) (Fig. 12 and 13) at normal temperature (+31°) shows two chemically shifted regions in a 1:1 intensity ratio arising from the CH_3 group attached to nitrogen and the CH_3 group directly bound to phosphorus. The former region consists of a doublet of doublets due to $^3J_{PH}$ coupling with phosphorus and $^3J_{HH}$ coupling from H attached to nitrogen. The latter comprises a doublet of doublets of multiplets. The major doublet is due to $^2J_{PH}$ and the minor doublet arises from $^3J_{HF}$, coupling of the CH_3 protons with the directly bound F atom, and the remaining multiplet fine structure arises from $^4J_{HF}$ coupling of the protons with the six

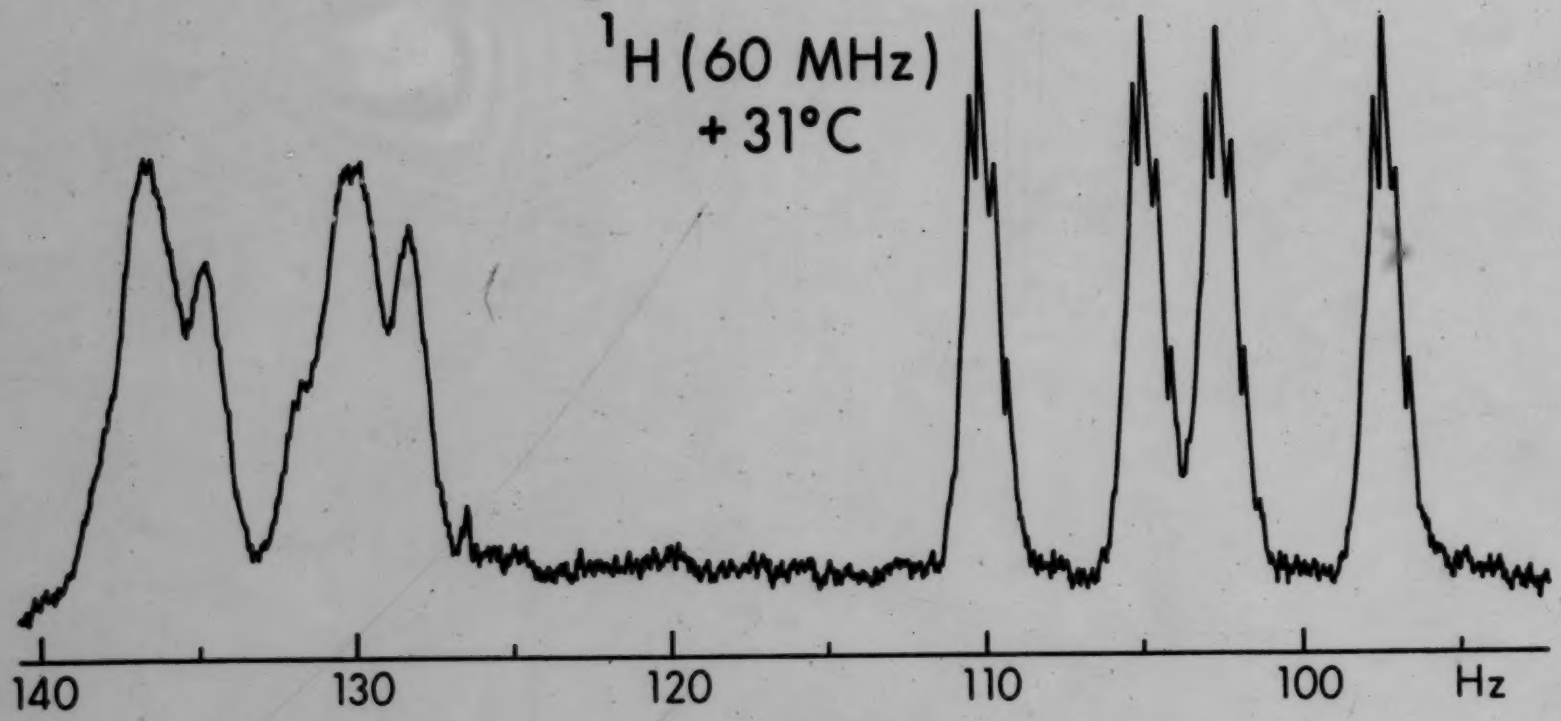

Figure 12 ^1H nmr spectra of $CH_3(CF_3)_2P(F)NH(CH_3)$ at +31° obtained in a solution of $CFCl_3$ containing a capillary of TMS in $CFCl_3$. Scale values refer to shifts from TMS in Hz.

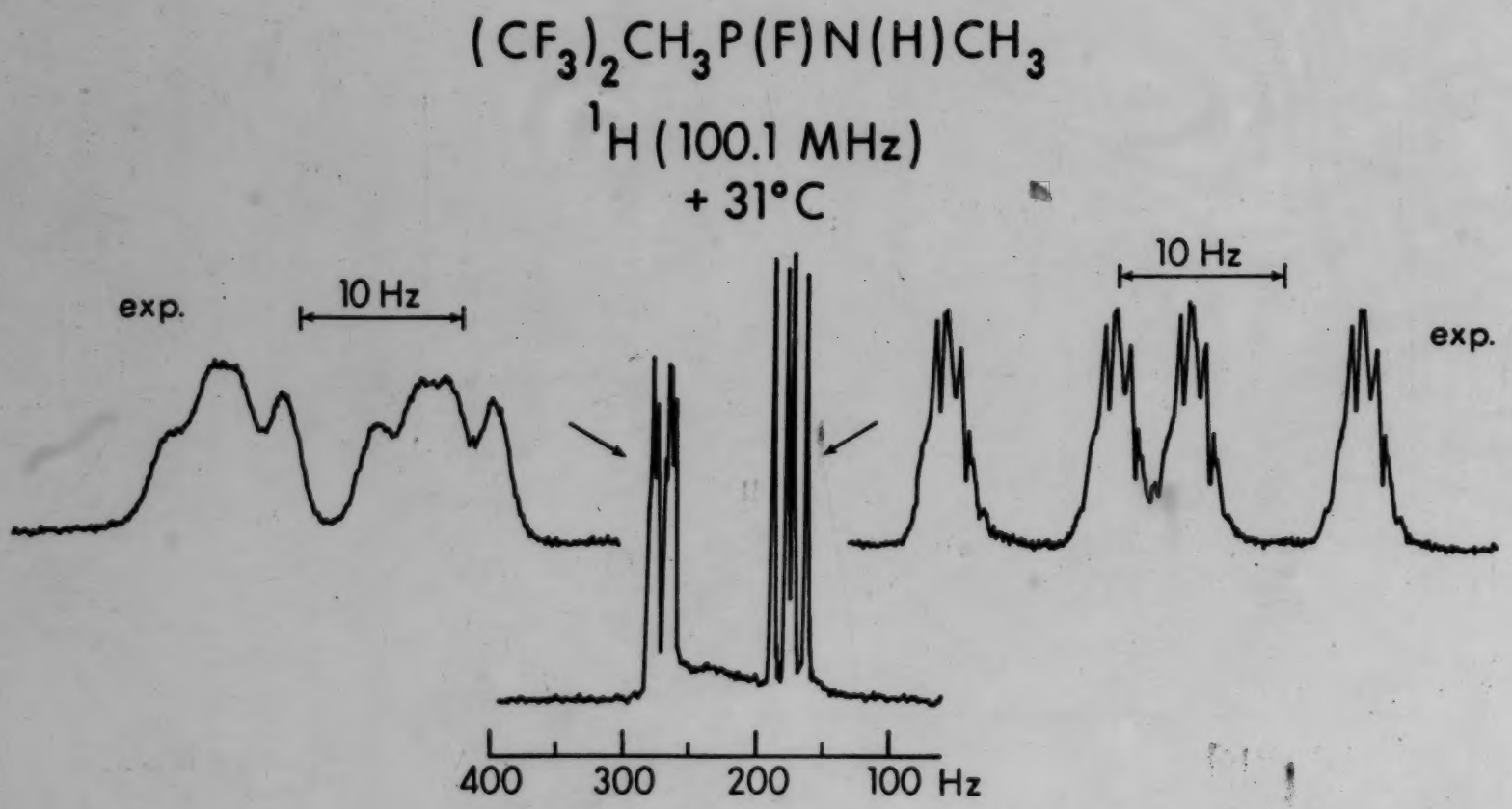

Figure 13 ^1H nmr spectra of $CH_3(CF_3)_2P(F)NH(CH_3)$ at +31° obtained in a solution of $CFCl_3$ containing a capillary of TMS in $CFCl_3$. Scale values refer to shifts from TMS in Hz.

TABLE 10

NMR Data For Two New Phosphoranes, $PF_4NCH_3(CH_2C_6H_5)$ and $CH_3(CF_3)_2P(F)NH(CH_3)$

	Temp	τ[a]	ϕ_F[b]	ϕ_{CF_3}[b]	σ_{31_P}[c]	$^1J_{PF}$	$^2J_{PF}$	$^3J_{PH}$	$^4J_{FH}$	$^2J_{FF}$	$^3J_{FF}$	$^4J_{FF}$
$PF_4NCH_3(CH_2C_6H_5)$	+31°	7.43[d]	65.9[g]		182.4[h,i,j]	855		11.6	2.25			
		5.94[e]						14.5				
		2.88[f]										
	-100°		73.2[k,l]			920				74.0		
			59.1[k,m]			780				74.0		
			56.7[k,n]			786				74.0		
	-90°				182.4[o,i,l,x]	920						
						784[m]						
$CH_3(CF_3)_2P(F)\underline{NH}(CH_3)$	+31°	7.32[p,r]	30.1[t]	67.2[u,v]	177.1[x,y]	754	125.3[u,v]	6.5			15.0	12.5
		8.27[q,s]				756[x]	124.6[x]					
				71.3[u,w]			35.0[u,w]				15.75	12.5
							35.4[x]					

Footnotes for Table 10

[a] τ relative to internal Tetramethylsilane, $\tau = 10.0$

[b] ϕ relative to internal (solvent) $CFCl_3$ standard with positive values indicating resonance to high field of standard

[c] ppm *vs* P_4O_6 as external standard (capillary), positive values indicating resonance to high field of standard

[d] CH_3 region, doublet of quintets

[e] CH_2 region, doublet

[f] C_6H_5 region, sharp singlet

[g] doublet

[h] quintet

[i] obtained from $^{31}P - \{^1H\}$ spectra

[j] at 233°K

[k] doublet of triplets

[l] F equatorial

[m] F axial

[n] F' axial

[o] triplet of triplets

[p] CH_3 group attached to nitrogen

[q] CH_3 group directly bound to phosphorus

[r] doublet of doublets

[s] doublet of doublets of multiplets

[t] broad doublet

[u] doublet of doublet of overlapped quartets

[v] CF_3 equatorial

[w] CF_3 axial

[x] obtained from $^{31}P - \{^1H\}$ nmr spectra

[y] doublet of quartets of quartets

fluorine nuclei of the two CF_3 groups. All nmr data is summarised in Table 10.

The normal (+31°) temperature ^{19}F nmr spectrum of the CF_3 region of (III) (Fig. 14) shows two chemically shifted equal intensity CF_3 signals which consist of a well spaced doublet of doublets of quartets with a large value of $^2J_{PF}$ and a doublet of doublets of overlapped quartets which indicate a smaller relative value of $^2J_{PF}$. The major doublet is due to the coupling of fluorine in CF_3 group with phosphorus. The minor doublet arises from $^3J_{FF}$ coupling with the single fluorine directly bound to phosphorus, each component of which was further split due to $^4J_{FF}$ coupling from three fluorine atoms of the second CF_3 group. These spectra are best understood in terms of the ground state structure D (Fig. 4) in which one CF_3 occupies an axial position (characterized by a small $^2J_{PF}$ value) and the other CF_3 group occupies an equatorial position (characterized by a relatively large $^2J_{PF}$ value[66]) in a trigonal bipyramid. It is also notable that the equatorial and axial CF_3 group, *cis* and *trans* to the axial fluorine respectively exhibit the same $^3J_{FF}$ coupling (~15 Hz). The signal due to the single fluorine atom directly bound to phosphorus consists of a broad doublet which shows no fine structure within each component of the major doublet, most probably because the large number of lines leads to a non-resolvable multiplet.

Figure 14 ^{19}F (94.1 MHz) nmr spectra of $CH_3(CF_3)_2P(F)$-$NH(CH_3)$ at +31° obtained in a solution of $CFCl_3$ containing a capillary of TMS in $CFCl_3$. Scale values refer to shifts from $CFCl_3$ (cap) in Hz.

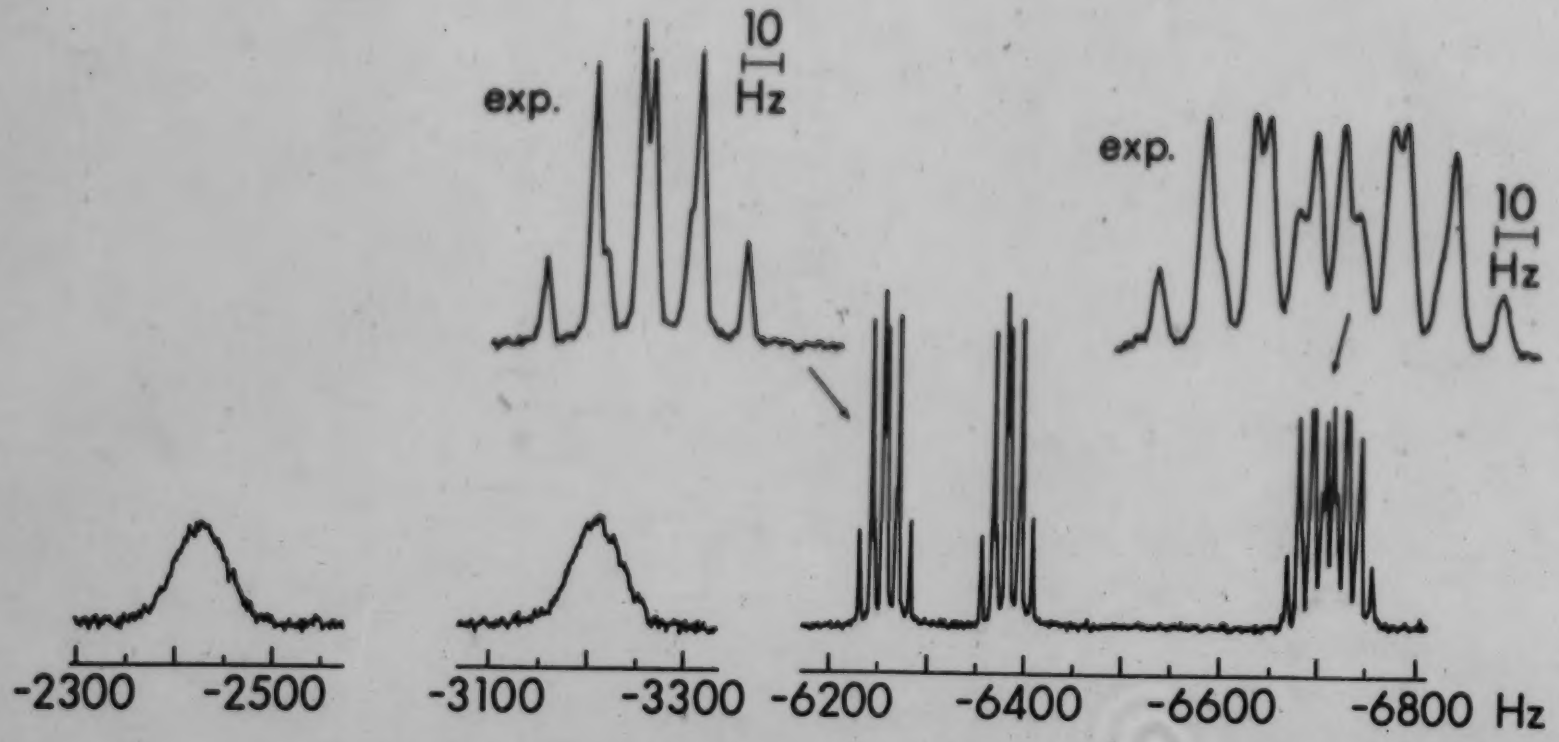
$(CF_3)_2CH_3P(F)N(H)CH_3$
^{19}F (94.1 MHz)
+31° C
exp.
10 Hz
exp.
10 Hz
-2300
-2500
-3100
-3300
-6200
-6400
-6600
-6800 Hz

Figure 14

The $^{31}P - \{^1H\}$ spectra at normal temperature (Fig. 15) consisting of a doublet of quartets of quartets also confirmed the ground state structure D (Fig. 4). The major doublet is due to the coupling of phosphorus with a single fluorine directly bound to phosphorus. The additional fine structure arises from $^2J_{PF}$(eq) and $^2J_{PF}$(ax), coupling of phosphorus with the three fluorine nuclei of each CF_3 group in the equatorial and axial positions respectively.

At elevated temperatures the $^{31}P - \{^1H\}$ spectrum was transformed into a doublet of septets due to the exchange permutation which rendered the CF_3 groups equivalent. The free energy of activation for the equilibrating process is $\Delta G^{\ddagger} = 17.5 \pm 1.4$ kcal/mole at 25°. The details of the exchange process are discussed in Chapter 4.

The Ground State Structure of $PF_4NCH_3(CH_2C_6H_5)$

The ^1H nmr spectrum of $PF_4NCH_3(CH_2C_6H_5)$ (IV) at normal instrument temperature (+31°) consists of three chemically shifted regions arising from phenyl (C_6H_5), methyl (CH_3), and methylene (CH_2) protons in 5:3:2 intensity ratio. The phenyl proton signal was a sharp singlet. The doublet in the methylene region arises from $^3J_{PH}$ coupling of proton with phosphorus atom. The methyl region shows a doublet of quintets due to $^3J_{PH}$ coupling from phosphorus and $^4J_{FH}$ coupling from four equivalent fluorine nuclei. The chemical shifts of the three different types of proton are consistent with

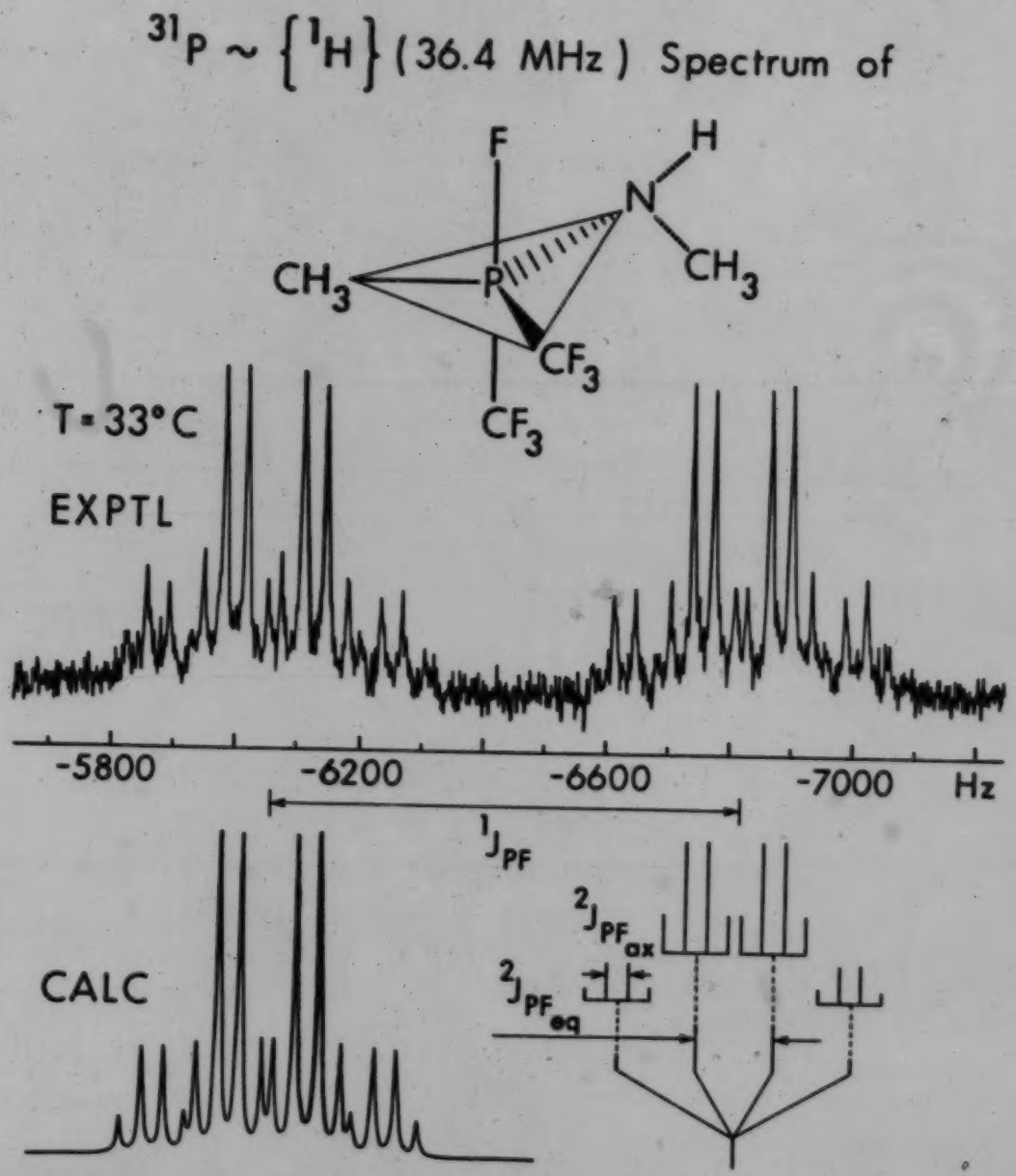

Figure 15 Observed and calculated ($^{31}P \sim \{^{1}H\}$, 36.4 MHz) nmr spectra of $CH_3(CF_3)_2P(F)NH(CH_3)$ at +33°. The frequency scale gives chemical shift values relative to P_4O_6. The stick diagram illustrates the formation of the pattern of a doublet of quartets of quartets due to one axial CF_3 group ($^{2}J_{PF}$, 35.4 Hz) and one equatorial group ($^{2}J_{PF}$, 124.6 Hz) attached to phosphorus.

those shown by $(CF_3)_3P(F)NCH_3(CH_2C_6H_5)$.

The ^{19}F nmr spectrum of (IV) at normal temperature (Fig. 16) showed only one fluorine environment. The spectrum obtained at 56.4 MHz comprised a doublet of triplets of multiplets. The major doublet is due to $^1J_{PF}$, the coupling of four equivalent fluorine nuclei with the phosphorus atom. Small couplings within each component of the doublet arise from coupling of the fluorine nuclei with protons of the methylene ($^4J_{FH}(CH_2)$ = 2.25 Hz) and the methyl groups. The spectrum obtained at 94.1 MHz at similar temperatures showed only the major doublet. At progressively lower temperature fluorine nmr spectroscopy showed that the fluorine nuclei were not equivalent. The signal coalesced at -30°C and resolved into three doublets of triplets at -100° (Fig. 16). The major doublet is due to the coupling of fluorine with phosphorus. The triplet of each component is due to $^2J_{FF}$ coupling of two axial fluorine nuclei with two equatorial fluorine nuclei and *vice versa*.

If the equatorial ^{19}F resonances appear at higher field *vs.* the axial ^{19}F resonances as is usually found,[70] this spectrum is consistent with the ground state structure in which the equatorial fluorines are equivalent but the axial fluorines have been rendered chemical shift nonequivalent due to the orientation of methyl and benzyl groups attached to nitrogen, thus the P-N bond rotation

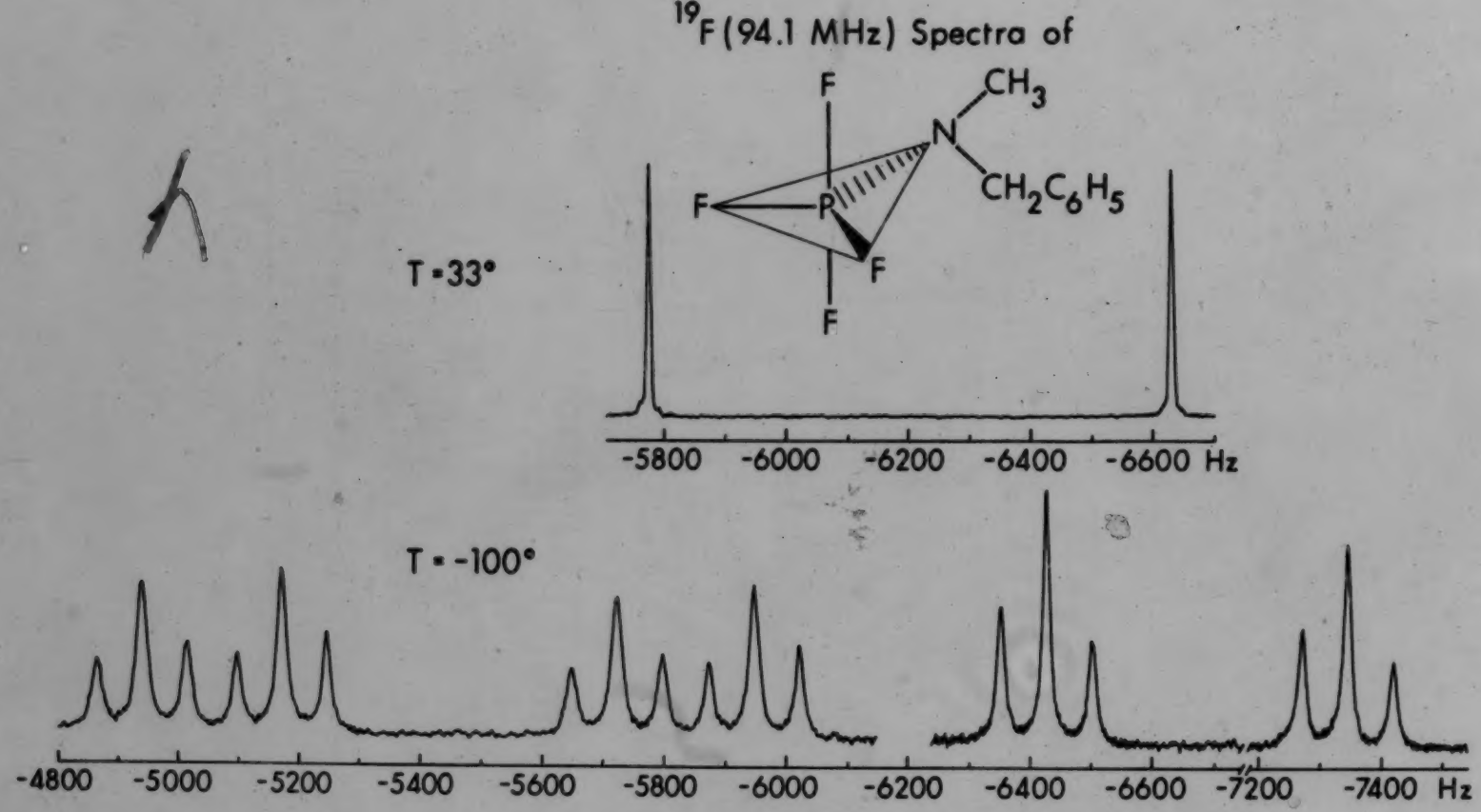

Figure 16 ^{19}F nmr spectra of $PF_4NCH_3(CH_2C_6H_5)$ at +33° and -100° obtained in a solution of $CFCl_3$. Scale values refer to shifts from $CFCl_3$ in Hz.

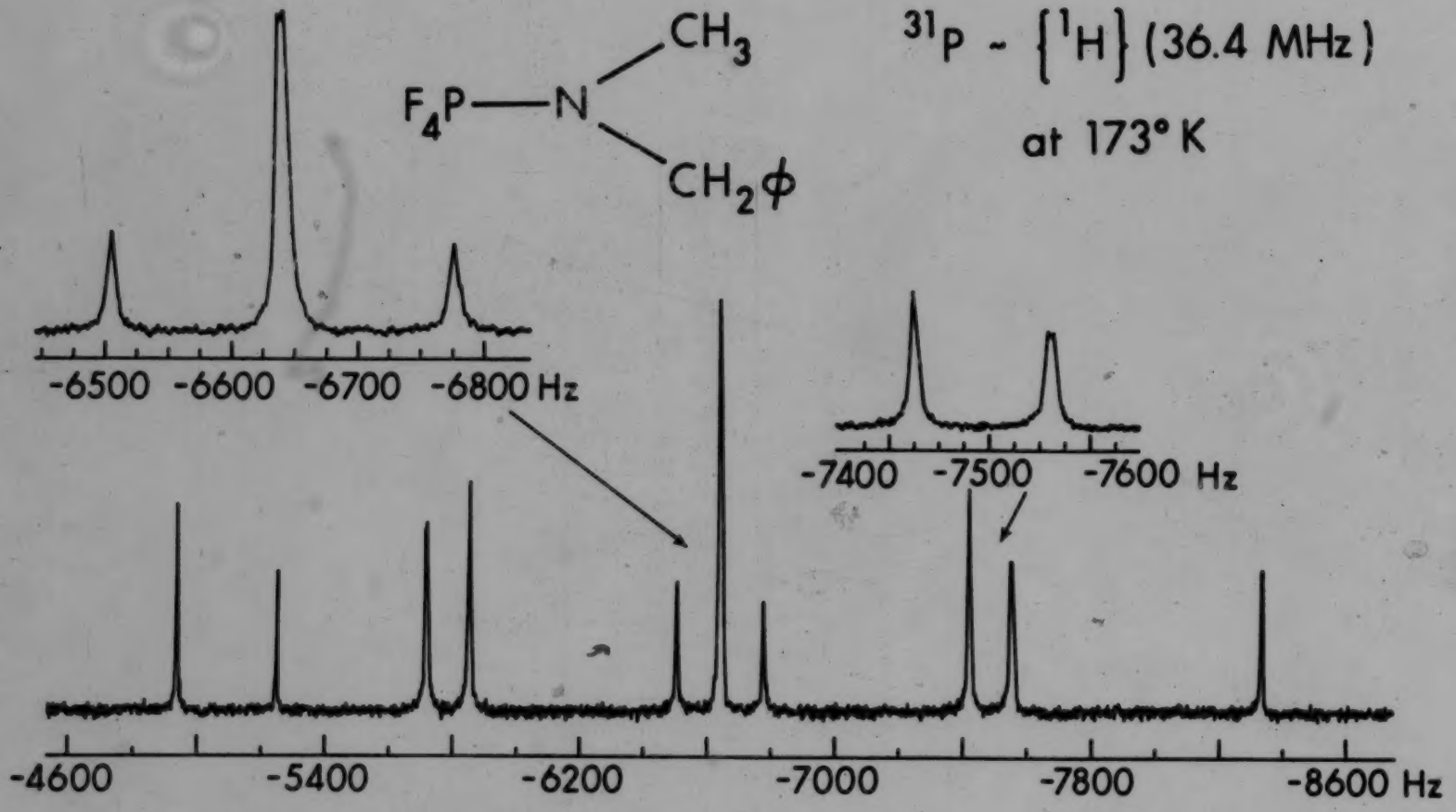

Figure 17 Phosphorus nmr spectra of $PF_4NCH_3(CH_2C_6H_5)$ at -100° (173°K). The frequency scale gives chemical shift values relative to P_4O_6.

has ceased. The spectrum is characterized by the parameters, given in Table 10. Note that the $^1J_{PF}$ for each of the individual axial F atoms are similar ($^1J_{PF_a}$, 780; $^1J_{PF_a}$', 786 Hz) and the signals are well separated ($\Delta\phi$, 2.4 ppm).

The low temperature ^{31}P spectra also proved to be informative. On cooling from -30° to -90°, the ^{31}P spectrum of (IV) changes from quintet (Figure 22) to a triplet of triplets (Figure 17) as a result of the transformation of equivalent fluorine environment for all four fluorines at -30°, presumably arising from an intramolecular exchange process, into two distinct environments (axial and equatorial); with a pair of axial fluorine nuclei and a pair of equatorial fluorine nuclei at the lower temperature characterized by the coupling constants J_{PF_e} = 920, J_{PF_a}(avg) = 784 Hz. Upon further cooling to -100° the ^{31}P spectrum showed possible non-equivalencies of axial fluorines expected as a result of the asymmetry of the nitrogen ligands in additional unresolved splitting of the lines 2,5, and 8 of approximately 8 Hz, as sketched below, however detailed assignment of this spectrum in terms of the assymmetry at nitrogen was not possible.

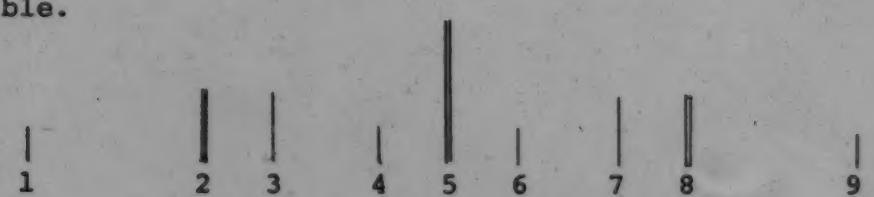

The compounds (I) and (II) show two CF_3 environments with a relative intensity ratio of 1:2 and compound (III) similarly shows two CF_3 environments with relative intensity of 1:1 at appropriate temperatures as expected for structures B or D (Fig 4). The signal characterized by a relatively small value of $^2J_{PF}$ arises from the axial CF_3 group and the signal characterized by the larger value of $^2J_{PF}$ is associated with the equatorial CF_3 substituents.

Other interpretations of the foregoing data were considered and rejected. For example, the possibility of the coexistence of different isomers of (I), (II), (III) and (IV) is eliminated by the fact that there is only one ^{31}P resonance. The possibility of a square pyramidal ground state structure[79] seems unlikely because the chemical shift and coupling constant values are in close agreement with the data for numerous trigonal bipyramidal phosphoranes.[9,80,81] It is worth noting that to the present time, characteristic nmr parameters have not been established for the square pyramidal phosphorane geometry.

CHAPTER 4

PERMUTATIONAL INTERCHANGE BARRIERS OBTAINED BY DYNAMIC NMR SPECTROSCOPY.

Like related molecules,[45,53,66-69] the compounds $(CF_3)_3P(F)NH(CH_3)$ (I), $(CF_3)_3P(F)NCH_3(CH_2C_6H_5)$ (II), $CH_3(CF_3)_2P(F)NH(CH_3)$ (III), and $PF_4NCH_3(CH_2C_6H_5)$ (IV) are fluxional. At ordinary temperature, the CF_3 environments of (I) and (II) are equivalent and axial and equatorial environments are detected at -40° (I) and -60° (II). These environments are visible in the ordinary temperature (+31°) nmr spectra of (III). The trend suggests that the barrier to positional interchange of CF_3 groups in these three phosphoranes follows the order (III) > (I) > (II). Above -30° all four fluorines in $PF_4NCH_3(CH_2C_6H_5)$ are equivalent. At temperatures between -85° and -100°, ^{19}F and ^{31}P nmr spectra showed distinct axial and equatorial fluorine environments. Further splitting of the signals which may be due to nonequivalent axial fluorines has been observed at very low temperatures in both ^{19}F and ^{31}P nmr spectra.

Nonequivalent axial fluorine atoms have previously been observed in the nmr spectra of some di- and trifluorophosphoranes containing alkylamino substituents[72], in the room-temperature ^{19}F nmr spectrum of $2,6\text{-}(C_2H_5)_2\text{-}C_6H_3\text{-}NHPF_4$[73], and in the low temperature spectra of $[(CH_3)_2CH]_2NPF_4$[74].

The characteristic changes in the nmr spectra accompanying variation of the temperature were compared to calculated shapes for various rates; fitting the calculated spectrum to the experimental spectrum gave rate constants for the process at a specific temperature. An Arrhenius plot was prepared using these rate values in order to obtain the activation parameters (E_a, the Activation energy; A, the frequency factor and $\Delta H^{\ddagger}$, enthalpy; $\Delta S^{\ddagger}$, entropy and $\Delta G^{\ddagger}$, free energy of activation). The values of $\Delta G^{\ddagger}$ are taken as the estimate of the barriers of positional interchange processes in these phosphoranes and related known phosphoranes.

The changes in the appearance of the ^{19}F and ^{31}P nmr spectra of the phosphoranes (I-IV) with reduced lowering temperatures arise from a combination of two effects similar to those postulated to occur in $RSPF_4$[71] derivatives and in $F_3P(NH_2)_2$[75], (i) a slowing down of the equilibrating permutational process and (ii) the onset of hindered rotation around the P-N bond which may be coupled with nitrogen inversion.

Muetterties, *et. al.*[75], suggested that, "the difference in rearrangement rates for the amino and alkylthiotetrafluorophosphoranes is due to P-N multiple bonding, with the P-N bond rotation and a Berry rearrangement inextricably coupled". Since they have estimated the P-N rotational barrier as 11.1 kcal/mole, they

suggested that "the resistance to P-N bond rotation makes a major contribution to the Berry rearrangment barrier in R_2NPF_4 molecules". The rotational barriers in PF_4X compounds, with X a substituent bearing a single π system, have been discussed by Hoffmann,[7] *et. al*, with the conclusion that an equatorial acceptor will prefer to have its acceptor orbital perpendicular to the equatorial plane, as in 18a, while an equatorial donor will prefer to have its donor orbital in the equatorial plane as in 18b, mostly as the result of donor-framework π bonding effects.

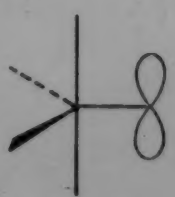

18a

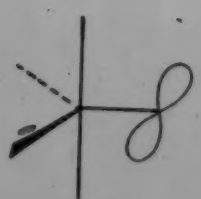

18b

Strich and Veillard[13] have computed the energy difference between the two conformations 18a and 18b in PF_4NH_2 using extended Hückel calculations. Conformation 18b with the nitrogen lone pair in the equatorial plane was found more stable than conformation 18a by 6 kcal/mole when d orbitals were not included in the basis set and by 17 kcal/mole when d orbitals were included. The nmr spectra of some S-substituted thiotetrafluorophosphoranes[71,77] show nonequivalence of the axial fluorines, hence supporting conformation 18b as the most stable According to Strich and Veillard, "the aminophosphorane

molecule PF_4NH_2 is predicted to have a planar nitrogen in its most stable conformation 18b and a pyramidal nitrogen in the less stable conformation 18a, so that the rotation process around the P-N bond appears coupled to the inversion at the N atom."

The principal factors which contribute to the rotational barrier about the P-N bond appear to be steric effects and the possibility of nitrogen-phosphorus $p_\pi - d_\pi$ bonding. The rotational barrier in alkyl and arylamino phosphines increases with increasing size of the groups attached to nitrogen.[78] Since the groups were in general electronically similar, the principal contribution to the barriers was attributed to steric effects due presumably to crowding in the transition state. Additional contributions were thought to arise from $p_\pi - d_\pi$ contributions to the rotational barrier which are possibly enhanced in the unsymmetrical compounds by an asymmetry induced in the P(3d) orbitals by virtue of the differing substituents on phosphorus.[78] The barrier to inversion at nitrogen,[87] is decreased by bulky substituents because the presence of bulky substituents on nitrogen leads to appreciable nonbonded repulsions which are stronger in the pyramidal than in the planar state. As a consequence the pyramidal state is destabilized with respect to the planar transition state and a lower barrier results.

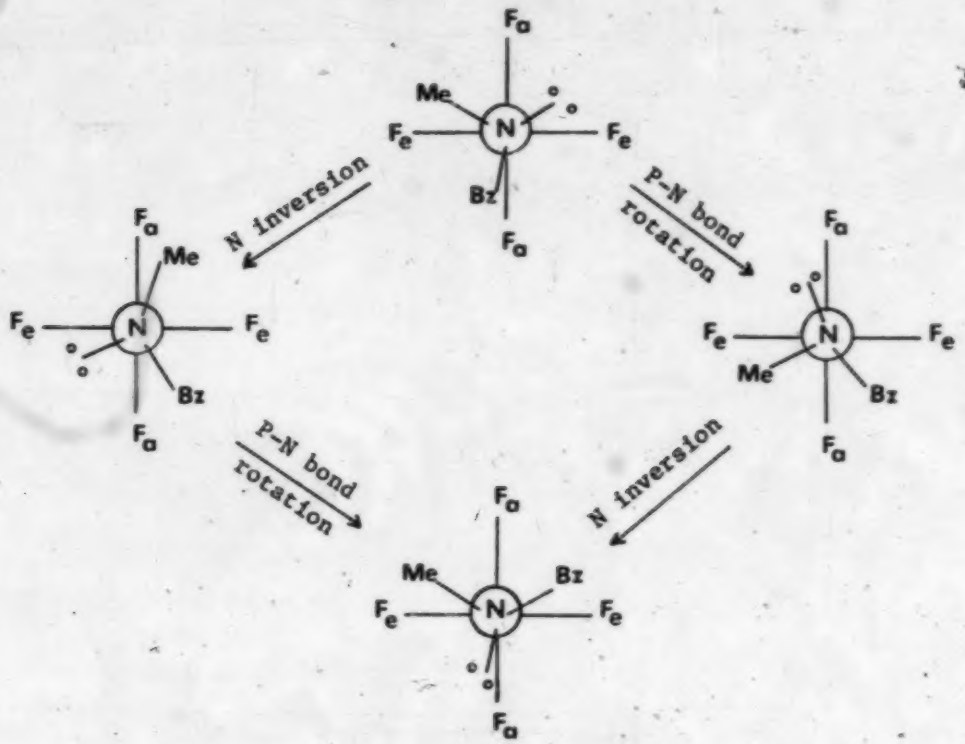

Figure 19 Stepwise Interconversion by Means of P-N Bond Rotation and Inversion at Nitrogen for $PF_4NCH_3(CH_2C_6H_5)$.

The projection formulae of the substituted amino-phosphorane, $PF_4NCH_3(CH_2C_6H_5)$ in Figure 19 indicate, within the context of the nmr time scale, that both rapid nitrogen inversion and P-N bond rotation are necessary along with the equilibrating permutation process in order to preserve the equivalence of the four fluorine atoms. If the splitting of signals observed in $PF_4NCH_3(CH_2C_6H_5)$ at very low temperature (< -100°) is indicative of non-equivalent axial fluorine atoms then the rotation around the P-N bond which appears coupled to the inversion process at the N atom has ceased and the methyl and benzyl groups on nitrogen exist in a fixed position relative to the axial fluorine atoms.

Analogous arguments account for the changes in the appearance of ^{19}F and ^{31}P nmr spectra with temperatures of the other phosphoranes.

Analysis of the temperature dependence of the ^{31}P nmr spectrum of $PF_4NCH_3(CH_2C_6H_5)$ (IV) shows that the conversion 20a $\rightleftharpoons$ 20b, occurs with pairwise exchange of axial with equatorial fluorine environments, in parallel to that established for $(CH_3)_2NPF_4$,[29] indicating that a Berry or equivalent process is involved.

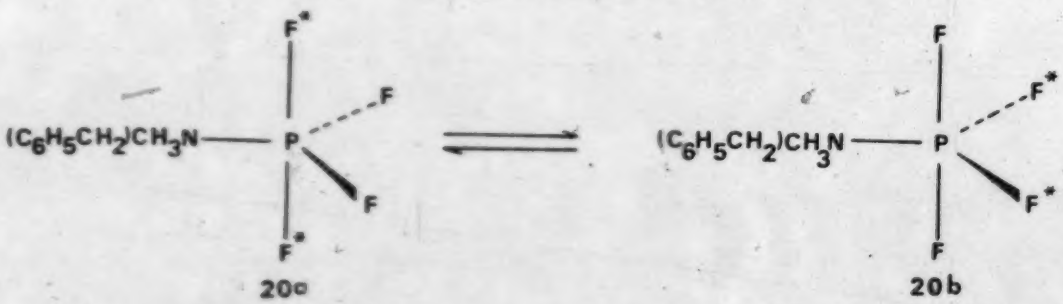

20a 20b

At low temperatures (between -85° and -100°) structure 20 is frozen; the methylbenzylamino group and two of the fluorines occupy equatorial positions, and two fluorines occupy axial positions. Above -30° all four fluorines become completely equivalent.

The calculated spectra included in Figures 22,24,26, 27,28,29, were all obtained using the computer program EXCHSYS[88] with 9 x 9, 16 x 16 and 40 x 40 "K" matrices for $PF_4NCH_3(CH_2C_6H_5)$, $CH_3(CF_3)_2P(F)NH(CH_3)$ and $(CF_3)_3P(F)Y$, respectively. The K matrix, the line numbers, spin states, intensities and frequencies for each system are given in Tables 14 to 20 of the Appendix.

The rates of exchange of magnetization were determined by varying the rates used in the calculation until the best visual fit was obtained between calculated and observed spectra. The rates of the exchange process along with the temperatures for all compounds studied herein are summarized in Tables 11 and 12.

Analysis of the Spectra

The slow-exchange ^{31}P spectrum of (IV) between -30° and -85° consists of 9 lines corresponding to 9 states of spins in axial and equatorial fluorines. The spectral assignments for the ^{31}P spectrum of (IV) are shown in Figure 21 in terms of the simple spin product functions for each state. These function are convenient to use but not strictly accurate. Ideally one should use symmetrized spin states

TABLE 11

Values of Rates of Exchange of Magnetization at Particular Temperatures for Various Phosphoranes Using the K-matrix Method.

$(CF_3)_3P(F)NHCH_3$		$(CF_3)_3P(F)N(CH_3)_2$		$(CF_3)_3P(F)NCH_3(CH_2C_6H_5)$		$(CF_3)_3P(F)OCH_3$		$CH_3(CF_3)_3P(F)NH(CH_3)$		$PF_4NCH_3(CH_2C_6H_5)$	
Temp (°C)	$k(sec^{-1})$	Temp (°C)	$k(sec^{-1})$	Temp (°C)	$k(sec^{-1})$	Temp (°C)	$k(sec^{-1})$	Temp (°C)	$k(sec^{-1})$	Temp (°C)	$k(sec^{-1})$
5	18	-40	18	-35	12.5	-50	300				
5	18	-40	18	-35	12.5	-45	455	45	5.6	-85	50
10	33	-25	145	-30	20	-40	670	50	8.3	-80	125
15	50	-20	160	-25	36	-35	1000	55	13.7	-75	250
20	80	-10	435	-20	56	-30	1890	60	20 30	-70	500
25	140	0	1000	-15	85	-25	2220	65	42	-65	1000
35	360	10	2500	-10	125	-20	3000	70		-60	2000
45	830	20	5000	0	265	-15	5000			-50	10000
55	2000			10	715					-40	20000
				20	1500						
				30	2860						

TABLE 12

Values of Rate of Exchange of Magnetization at Particular Temperatures of $(CF_3)_3P(F)NCH_3(CH_2C_6H_5)$ Obtained Using DNMR3

Temp (°C)	k (sec^{-1})	
	CD_2Cl_2	d_{14} methyl-cyclohexane
-20	15	
-15	25	
-10	40	
-5	70	
0	90	
5	155	
10	190	
15	290	
20	390	
25	650	
30	1100	1200
35	1600	1600
40	2000	2200
45	2700	2700
50		3700
55		5500
60		7000
65		9000

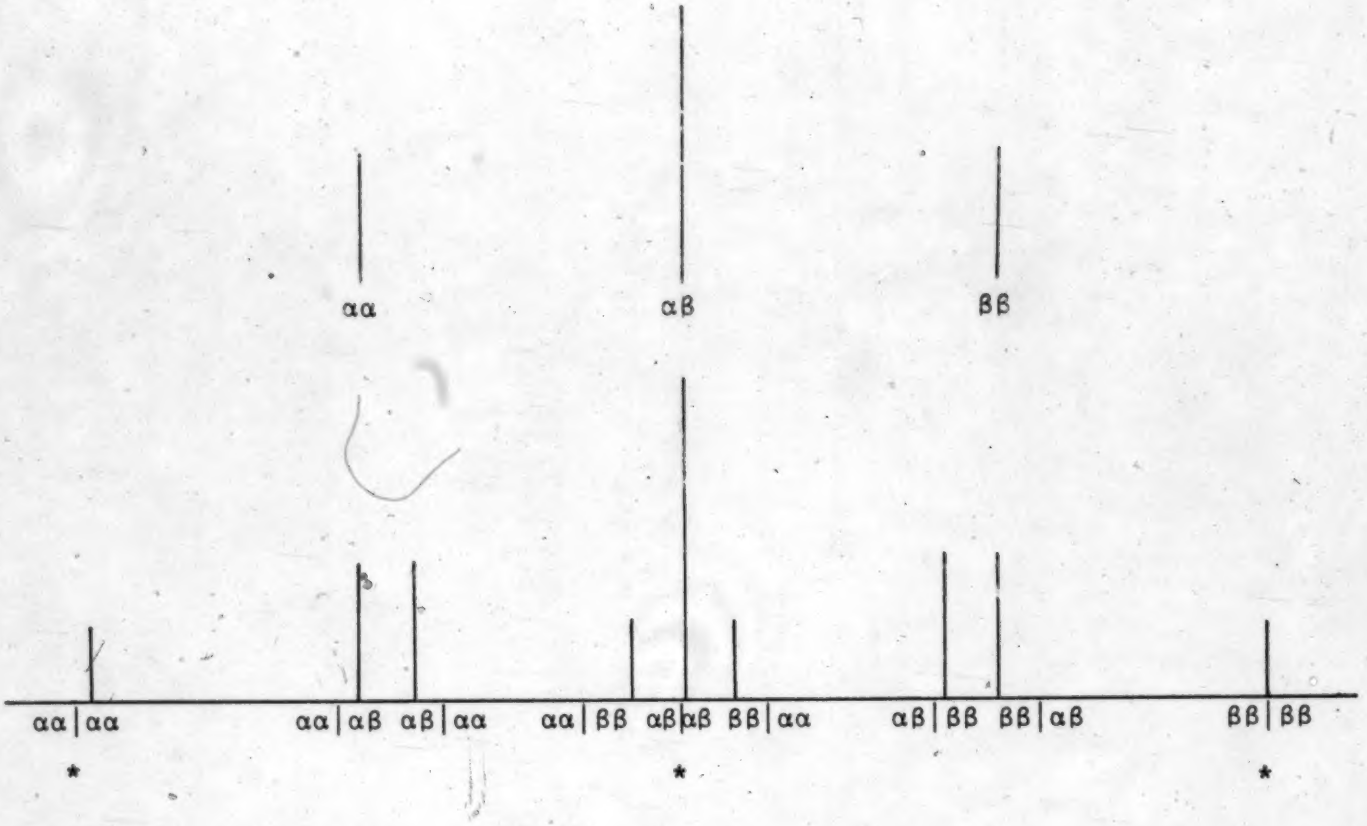

*unchanged by exchange

Figure 21 Spectral Assignments for the ^{31}P Spectrum of $PF_4NCH_3(CH_2C_6H_5)$.

but this does not affect the analysis. Furthermore, it has been shown[29] that proper calculation of the transformation matrix from the complete Hamiltonian introduces only subtle differences in the analysis which cannot be detected experimentally. The ^{31}P spectral behaviour of (IV) in the region of intermediate pseudorotation rates can be described as the transfer of magnetization between certain of the 9 lines according to the mode selected. If a pairwise exchange mechanism is chosen, three lines remain unchanged throughout the whole temperature range corresponding to the spin states of $\alpha\alpha|\alpha\alpha$, $\alpha\beta|\alpha\beta$, and $\beta\beta|\beta\beta$, since no exchange of magnetization can occur in these lines under pairwise exchange modes. Pairwise permutation clearly interchanges $\alpha\alpha|\underline{\alpha\beta}$ and $\alpha\beta|\alpha\alpha$, $\alpha\alpha|\beta\beta$ and $\beta\beta|\alpha\alpha$, $\alpha\beta|\beta\beta$ and $\beta\beta|\alpha\beta$ magnetic environments around the phosphorus nucleus and results in transfer of magnetization between lines 2 and 3, 4 and 6, 7 and 8 respectively, therefore these six lines are broadened and coalesced in the intermediate exchange region. The computer simulation of spectral line shapes based on a pairwise mode fits the observed behaviour well at temperatures ranging from -40° to -85°, (Figure 22).

In the case of $CH_3(CF_3)_2P(F)NH(CH_3)$, axial and equatorial CF_3 groups are distinguishable at ordinary temperature (+30°). The ^{31}P spectrum is doublet of quartets of quartets expected for a static trigonal-bipyramidal

Figure 22 Experimental and calculated ($^{31}P - \{^{1}H\}$, 36.4 MHz) nmr spectra at particular temperatures and appropriate rates of exchange of magnetization for $PF_4NCH_3(CH_2C_6H_5)$. The experimental spectra were obtained in a solution of $CFCl_3$, the calculated spectra were obtained using a K-matrix constructed for a pairwise (i.e., Berry etc.) exchange mechanism. The frequency scale gives chemical shift values relative to P_4O_6 but was measured by heteronuclear lock techniques relative to ^{2}D of CD_2Cl_2 (in Hz).

$^{31}P \sim \{^{1}H\}$ (36.4 MHz) Spectra of

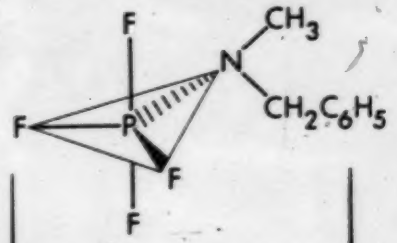

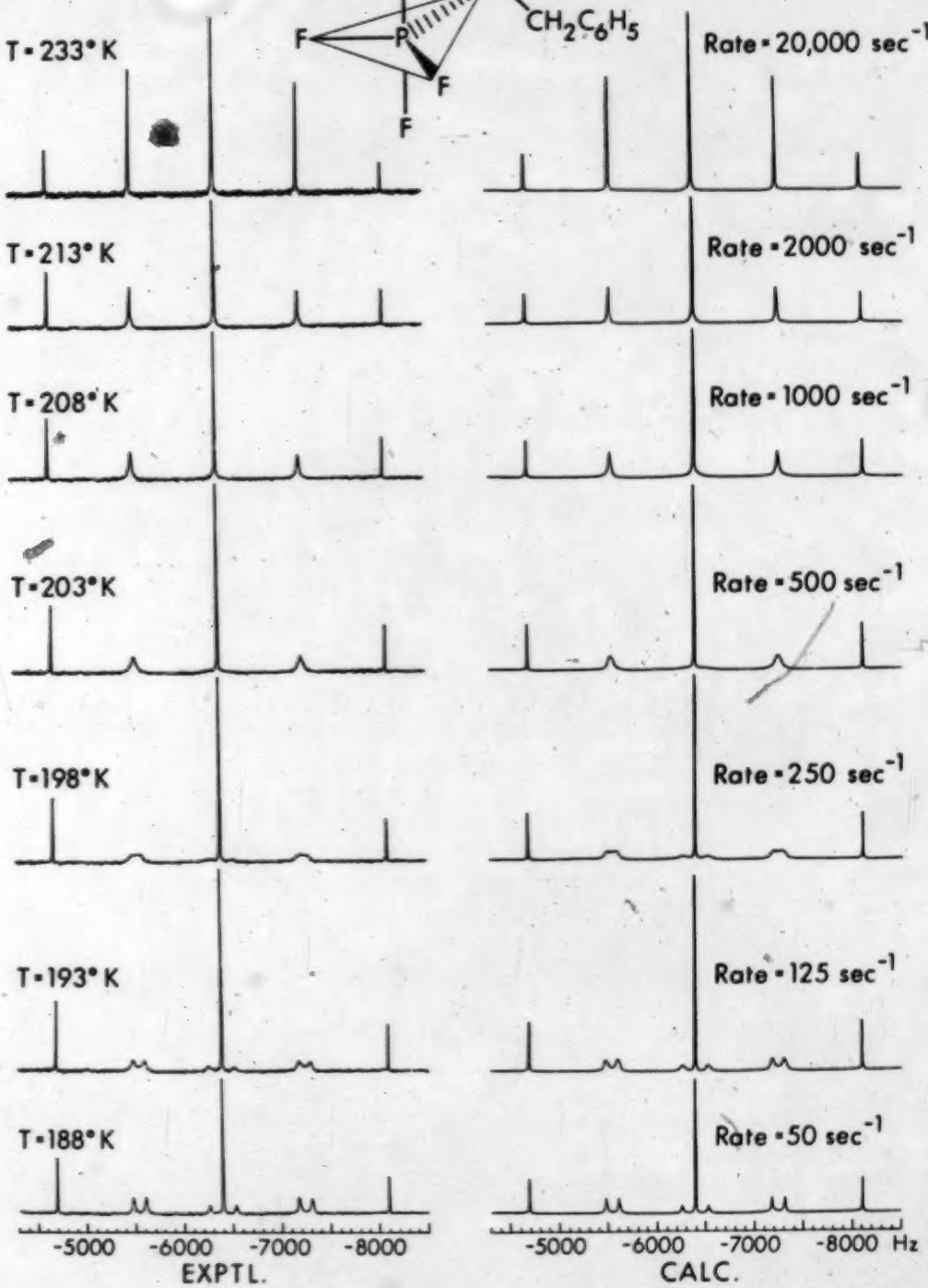

Figure 22

structure having one CF_3, the methyl, and the methylamino groups in the equatorial positions, one CF_3 group and the single F in the axial positions. The ^{31}P spectrum at +30° can be regarded as a slow exchange limit or stopped spectrum. The fast exchange should be a doublet of septets arising from the coupling of phosphorus and six equivalent fluorine nuclei of axial and equatorial CF_3 groups. However the highest accessible temperature (+70°), limited by solvent and possible decomposition problems, was not sufficient to observe the equivalency of axial and equatorial CF_3 groups. All the observed spectra were characteristic of intermediate exchange regions and could be fitted to determine the rate.

In $CH_3(CF_3)_2P(F)NH(CH_3)$ and the $(CF_3)_3P(F)Y$ system (where $Y = NH(CH_3)$, $N(CH_3)_2$, $N(CH_3)CH_2C_6H_5$, and OCH_3), the influence of pseudorotation on the ^{31}P resonances is determined by the extent to which the magnetic environment "seen" by the phosphorus is changed when the CF_3 groups interchange. If pseudorotation results in isomerization of CF_3 groups to a final configuration which is magnetically indistinguishable from the starting configuration, no change in the ^{31}P spectrum will be observed. If on the other hand, pseudorotation converts the starting configuration to a different configuration, the two (or more) slow-exchange phosphorus

lines coupled by the exchange will broaden and coalesce as the pseudorotation rate increases.

Figure 23 shows the spectral assignments for the ^{31}P half-spectrum of $CH_3(CF_3)_2P(F)NH(CH_3)$, omitting only the doubling of the spectrum arising from $^1J_{PF}$. Under the pairwise exchange process which is shown below:

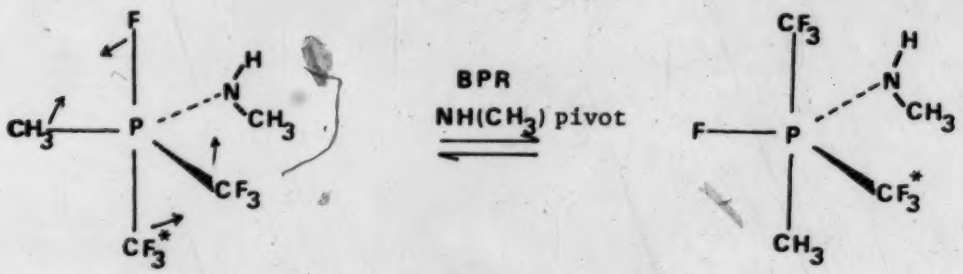

four lines remain unchanged as temperature is increased from 45° to 70° corresponding to the spin states of ααα|ααα, βαα|ααβ, ββα|αββ and βββ|βββ indicating no exchanging of magnetization in these lines (Figure 24). The transition labeled 2 in Figure 23 can be considered to be due to a phosphorus nucleus in the characteristic magnetic field provided by three fluorines of the axial CF_3 group and two fluorines of the equatorial CF_3 group in α-spin states and one fluorine of the equatorial CF_3 group in a β-spin state. The other transitions can be interpreted similarly. The symbols obey the following order: the first three spin state symbols refer to fluorines of the axial CF_3 group and the latter symbols refer to fluorines of the equatorial CF_3 group.

As the temperature increases the exchange process results in transfer of magnetization between transition

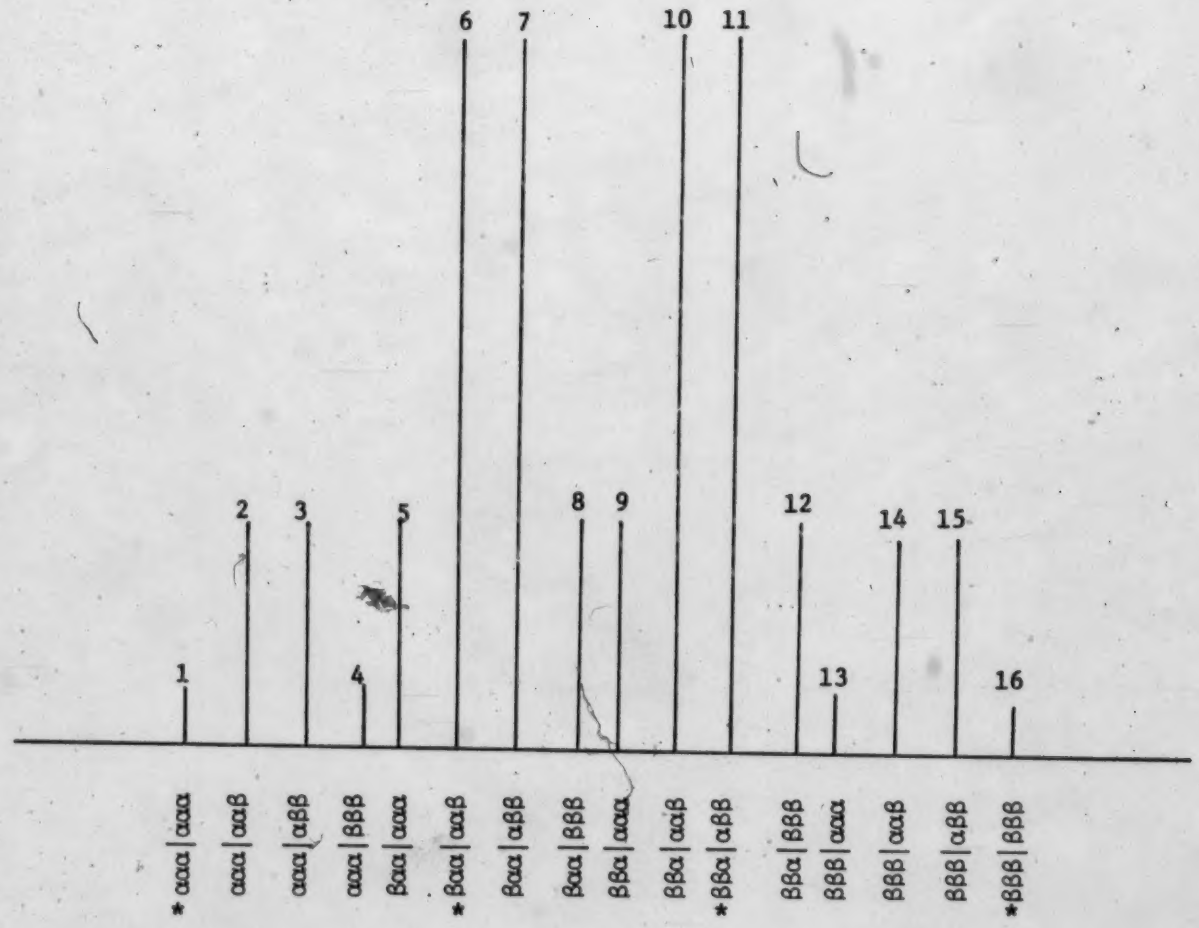

*unchanged by exchange

Figure 23 Spectral Assignments for the ^{31}P Half-spectrum of $CH_3(CF_3)_2P(F)NH(CH_3)$.

Figure 24 Experimental and calculate ($^{31}P - \{^{1}H\}$, 36.4 MHz) nmr spectra at particular temperatures and appropriate rates of exchange of magnetization for $CH_3(CF_3)_2P(F)NH(CH_3)$. The experimental spectra were obtained in a solution of d_8-toluene, the calculated spectra were obtained using a K-matrix constructed for a pairwise (i.e. Berry, etc.) exchange mechanism. The frequency scale gives chemical shift values relative to P_4O_6 but was measured by heteronuclear lock techniques relative to ^{2}D of CD_2Cl_2 (in Hz).

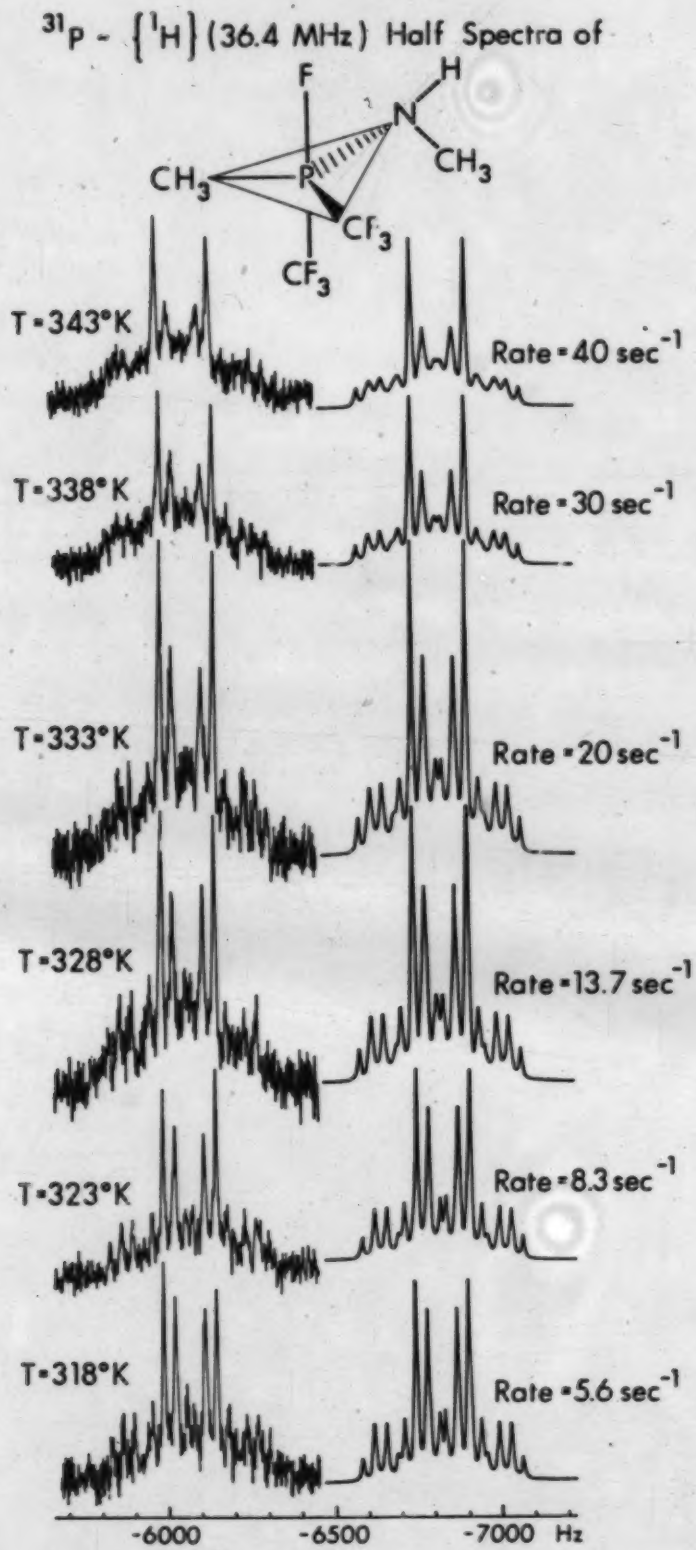
^{31}P - $\{^1H\}$ (36.4 MHz) Half Spectra of
F
H
N
CH_3
P
CH_3
CF_3
CF_3
T=343°K
Rate=40 sec^{-1}
T=338°K
Rate=30 sec^{-1}
T=333°K
Rate=20 sec^{-1}
T=328°K
Rate=13.7 sec^{-1}
T=323°K
Rate=8.3 sec^{-1}
T=318°K
Rate=5.6 sec^{-1}
-6000
-6500
-7000 Hz

Figure 24

2 and 5, 3 and 9, 4 and 13, 7 and 10, 8 and 14, 12 and 15. Within the temperature range from 45° to 70° the only significant observation was that peaks arising from transition 7 and 10 were reduced in height. The ^{31}P half-spectrum of $CH_3(CF_3)_2P(F)NH(CH_3)$ was not taken completely to the fast exchange septet because the necessary high temperatures could have caused the decomposition of the compound. Other difficulties such as increased pressure inside the sealed tube and the reflux of the solvent at elevated temperatures also precluded the study of increased temperature spectra.

In the case of $(CF_3)_3P(F)Y$ compounds, the ^{31}P spectrum at the slow exchange limit is a doublet of quartets of septets, thus in the ground state structure, F and one CF_3 group occupy the axial positions, the Y group (N, NR_1R_2, or OCH_3) and two CF_3 groups occupy the equatorial positions. At high temperature [> 30° for $(CF_3)_3P(F)NCH_3(CH_2C_6H_5)$ and $(CF_3)_3P(F)N(CH_3)_2$; and > 55° for $(CF_3)P(F)NH(CH_3)$], all nine fluorines in three CF_3 groups become completely equivalent, and the ^{31}P spectrum becomes a doublet of decets in this fast exchange limiting spectrum. In the intermediate temperature range exchange of magnetization occurs between the three CF_3 groups. Visualizing the process in terms of Berry pseudorotation we consider an equatorial CF_3 (1) as a pivot, the axial pair (CF_3* and F) becomes the equatorial pair, the remaining equatorial CF_3 (2) and Y groups becomes the axial pair in one

concerted motion:

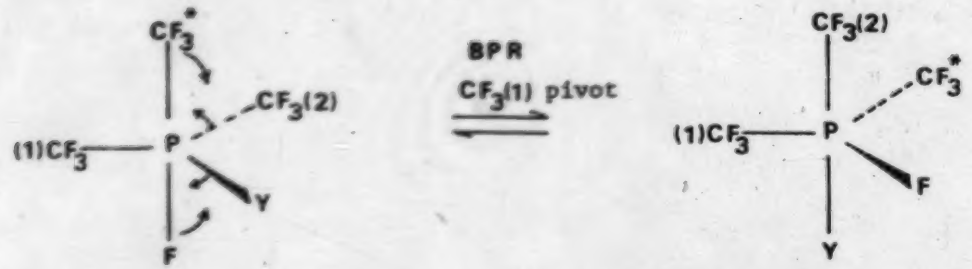

An alternative pathway in which the exchanging process can avoid the possible high energy barrier arising from the placement of Y in the axial position and F in the equatorial position, (because such locations are in opposition to the apicophilicity rule,[15,16]) is achieved by performing the transformation in two steps using first Y as the pivot, followed by CF_3*:

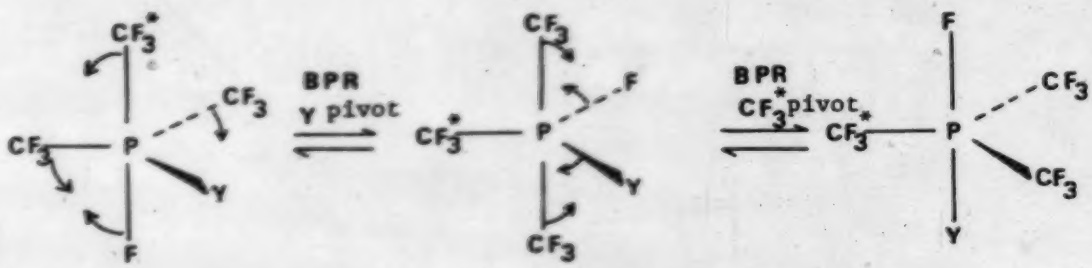

The slow-exchange ^{31}P half-spectrum of $(CF_3)_3P(F)Y$ consists of 28 lines, the spectral assignments of which are shown in Figure 25. Each transition labeled from 1 to 28 can be considered to be due to a phosphorus nucleus in the characteristic magnetic field provided by the spin states of nine fluorine atoms, six of which belong to two degenerate equatorial CF_3 groups and three

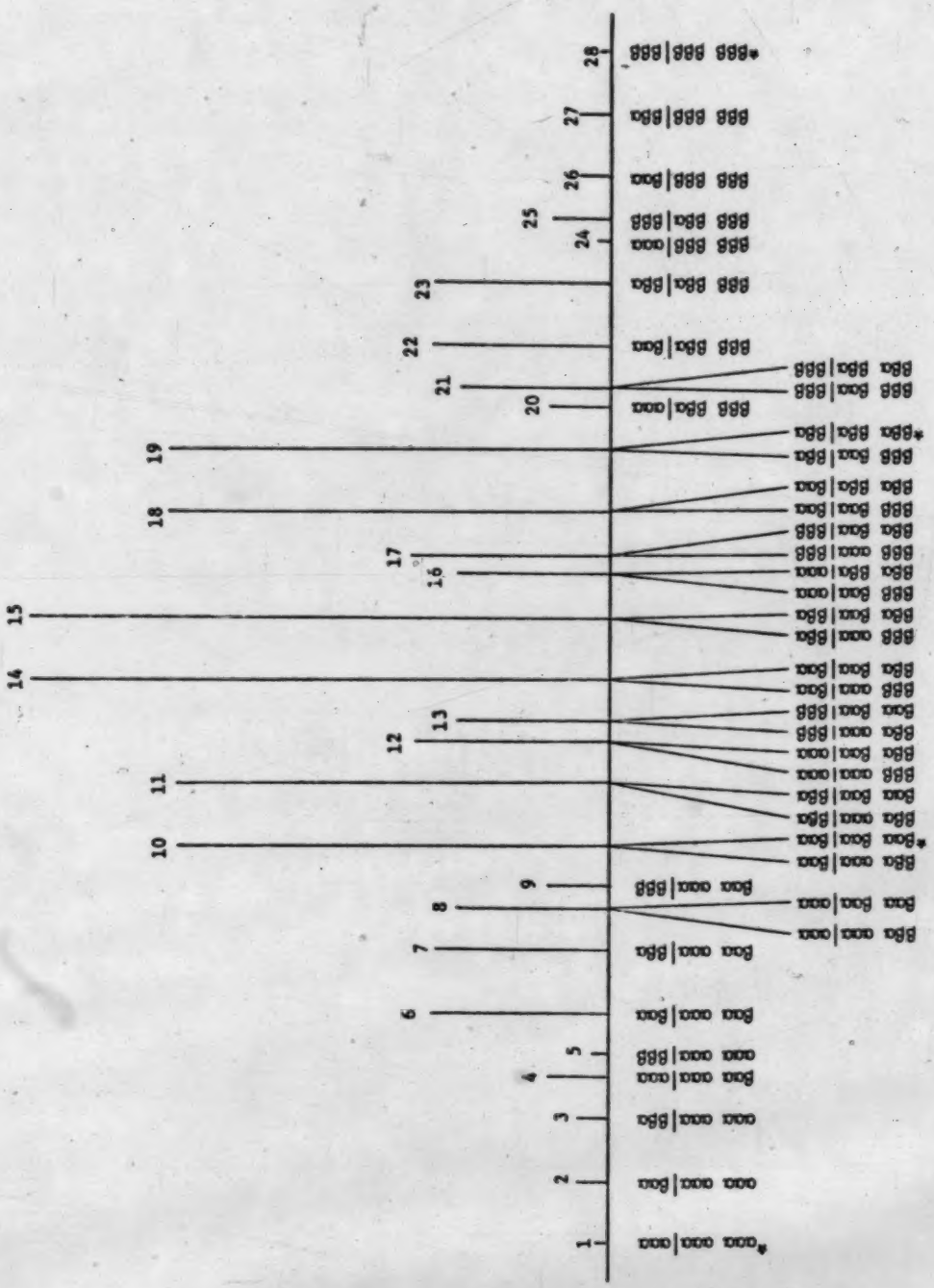

Figure 25 Spectral Assignments for the ^{31}P Half-spectrum of $(CF_3)_3P(F)Y$.

Figure 26 Experimental and calculated ($^{31}P - \{^{1}H\}$, 36.4 MHz) nmr spectra at particular temperatures and appropriate rates of exchange of magnetization for $(CF_3)_3P(F)NH(CH_3)$. The experimental spectra were obtained in a solution of $CFCl_3$, the calculated spectra were obtained using a K-matrix constructed for a pairwise (i.e., Berry, etc.) exchange mechanism. The frequency scale gives chemical shift values relative to P_4O_6 but was measured by heteronuclear lock techniques relative to ^{2}D of CD_2Cl_2 (in Hz).

$^{31}P - \{^{1}H\}$ (36.4 MHz) Half Spectra of

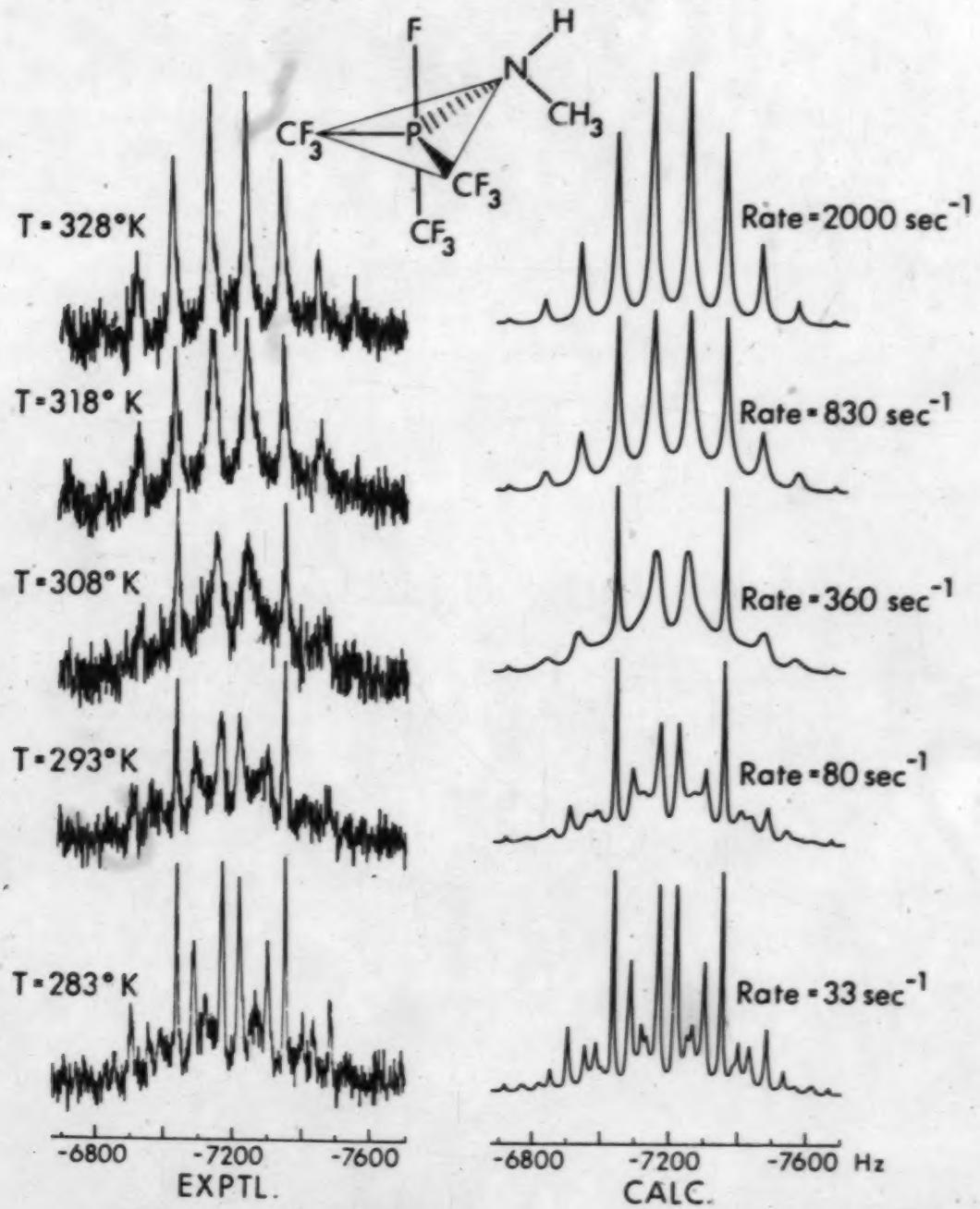

Figure 26

Figure 27 Experimental and calculated ($^{31}P - \{^{1}H\}$, 36.4 MHz) nmr spectra at particular temperatures and appropriate rates of exchange of magnetization for $(CF_3)_3P(F)N(CH_3)_2$. The experimental spectra were obtained in a solution of $CFCl_3$, the calculated spectra were obtained using a K-matrix constructed for a pairwise (i.e., Berry, etc.) exchange mechanism. The frequency scale gives chemical shift values relative to P_4O_6 but was measured by heteronuclear lock techniques relative to ^{2}D of CD_2Cl_2 (in Hz).

$^{31}P \sim \{^{1}H\}$ (36.4 MHz) Half Spectra of

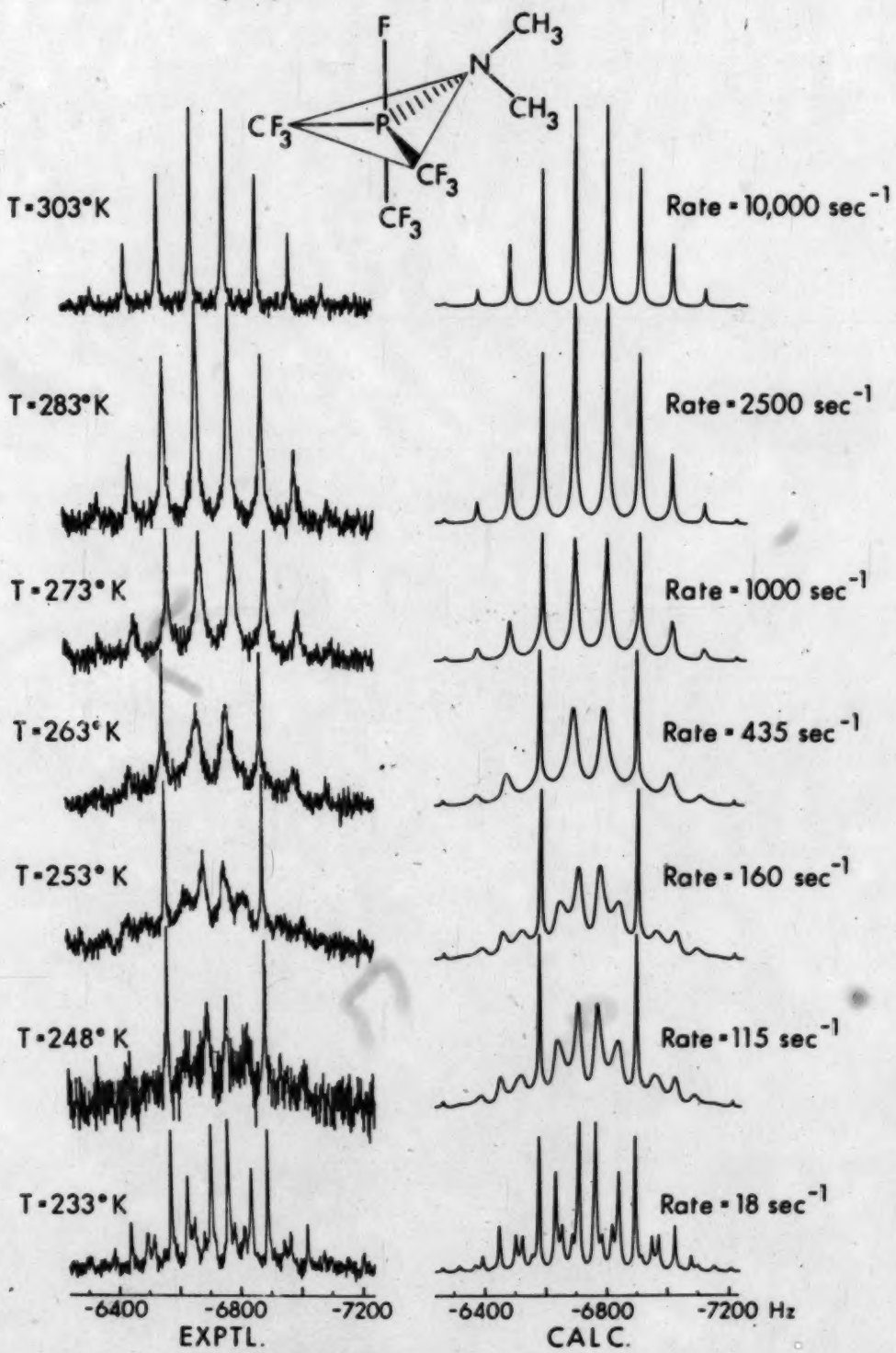

Figure 27

Figure 28 Experimental and calculated ($^{31}P - \{^{1}H\}$, 36.4 MHz) nmr spectra at particular temperatures and appropriate rates of exchange of magnetization for $(CF_3)_3P(F)NCH_3(CH_2C_6H_5)$. The experimental spectra were obtained in a solution of $CFCl_3/CF_2Cl_2$. The calculated spectra were obtained using a K-matrix constructed for a pairwise (i.e., Berry, etc.) exchange mechanism. The frequency scale gives chemical shift values relative to P_4O_6 but was measured by heteronuclear techniques relative to ^{2}D of CD_2Cl_2 (in Hz).

^{31}P (36.4 MHz) - $\{^1H\}$
HALF-SPECTRA OF

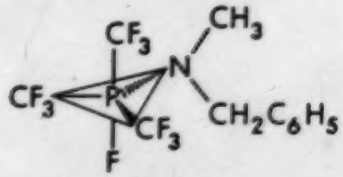

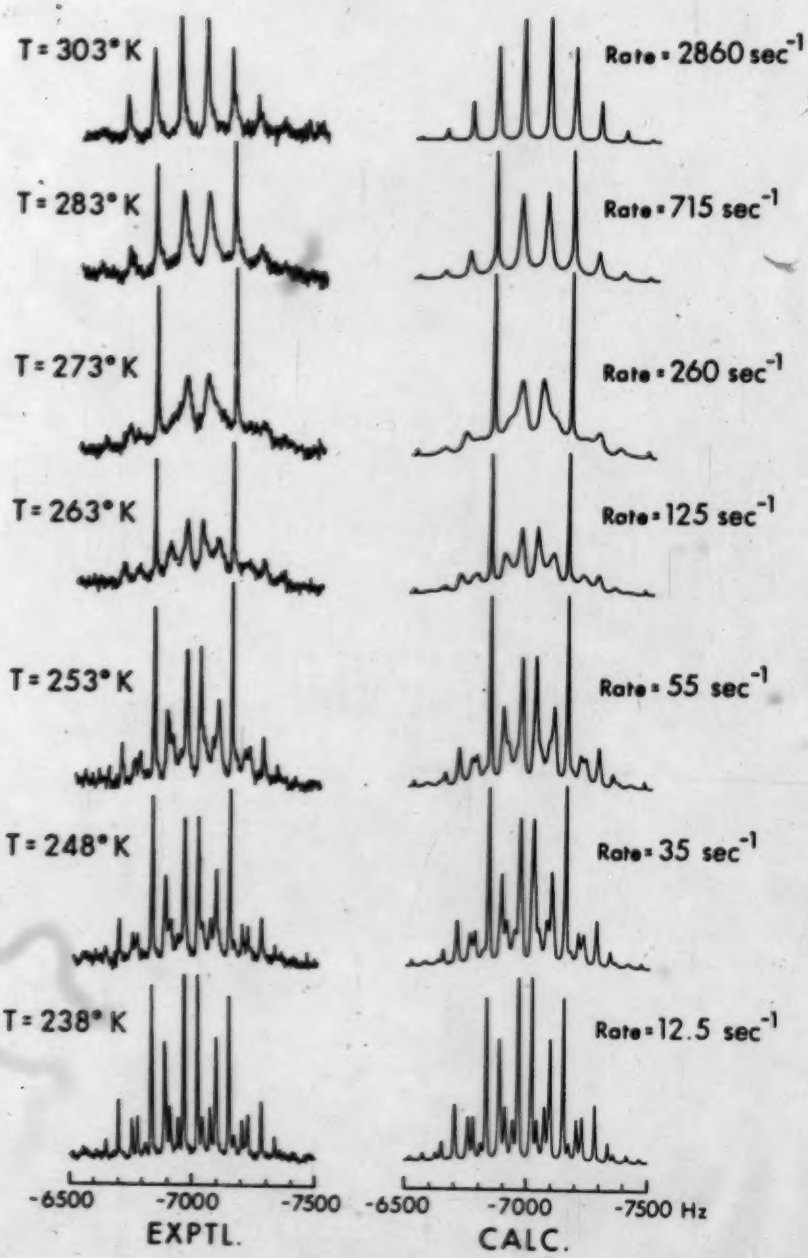

Figure 28

Figure 29 Experimental and calculated ($^{31}P - \{^{1}H\}$, 36.4 MHz) nmr spectra at particular temperatures and appropriate rates of exchange of magnetization for $(CF_3)_3P(F)OCH_3$. The experimental spectra were obtained in a solution of $CFCl_3$, the calculated spectra were obtained using a K-matrix constructed for a pairwise (i.e., Berry, etc.) exchange mechanism. The frequency scale gives chemical shift values relative to P_4O_6 but was measured by heteronuclear techniques relative to ^{2}D of CD_2Cl_2 (in Hz).

^{31}P - $\{^{1}H\}$ (36.4 MHz) Half Spectra of

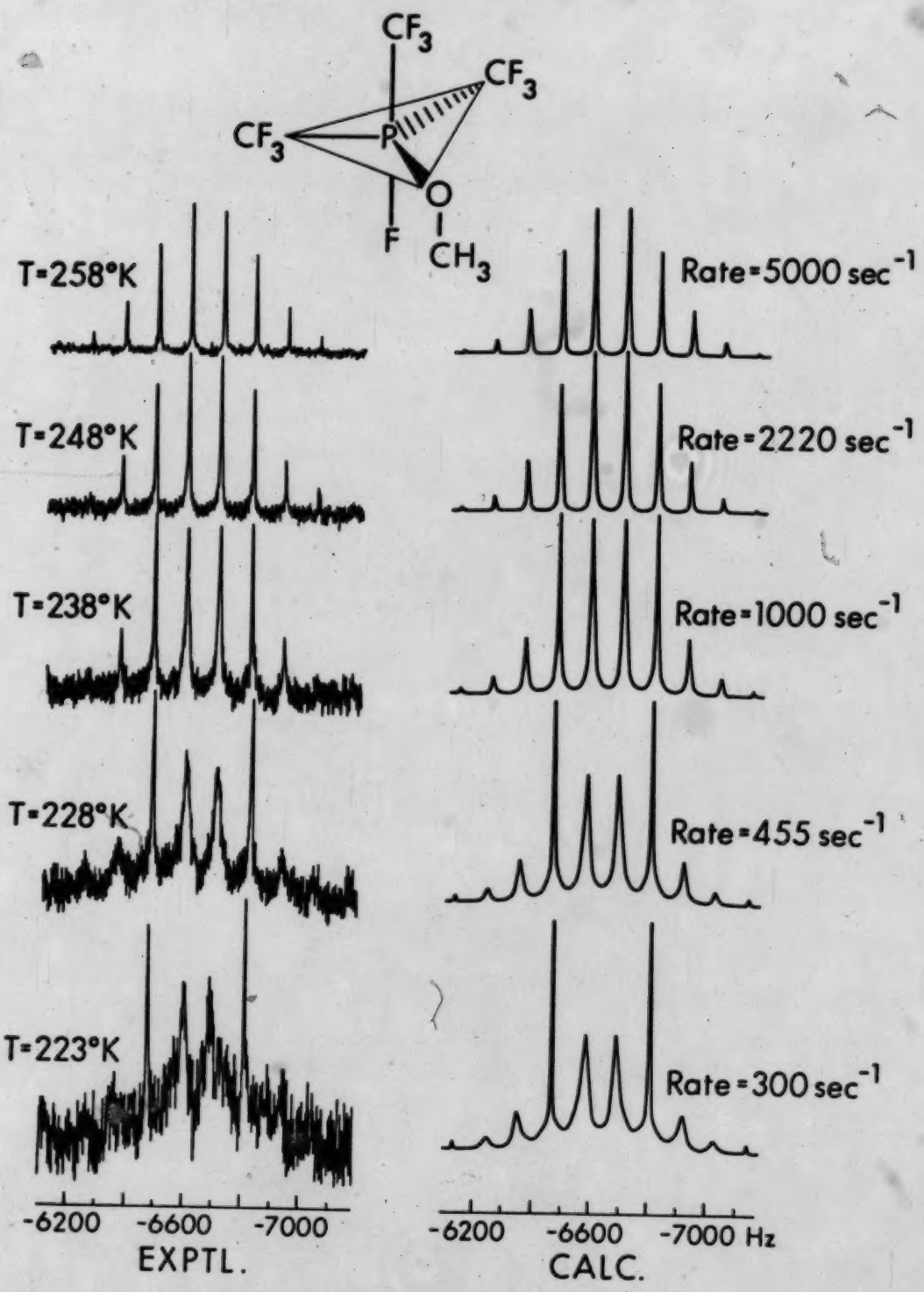

Figure 29

fluorine atoms belong to the axial CF_3 group. From the observed ^{31}P half-spectrum of $(CF_3)_3P(F)Y$ covered by the range of temperatures -35° to 30°, -40° to 30°, 0° to 55° and -15° to 50°, for $(CF_3)_3P(F)NCH_3(CH_2C_6H_5)$, $(CF_3)_3P(F)N(CH_3)_2$, $(CF_3)_3P(F)NH(CH_3)$ and $(CF_3)_3P(F)OCH_3$, respectively, there are four lines which are seen to be unaffected by exchange and remain sharp. These lines correspond to the spin states of ααα ααα|ααα, βαα βαα|βαα, ββα ββα|ββα and βββ βββ|βββ (Figure 26, 27, 28, and 29) which cannot suffer exchange. Permutational interchange process results in transfer of magnetization between transition 2 and 4, and the probability of exchanging of magnetization from transition 4 to transition 2 is one half of that from transition 2 to transition 4. Exchange of magnetization between transition 3 and 8, 5 and 12a, 8b and 6, 11b and 14b, 13b and 18a, 18b and 15b, 26 and 21a, 21b and 23, 27 and 25, can be interpreted similarly. Transition 11a and 16b, 17a and 24, exchange magnetization with equal probability. Transition states βαα ααα|ββα, ββα ααα|βαα and ββα βαα|ααα transfer the magnetization among themselves with equal probability with respect to the other two transition states. Transitions 9, 14a and 16a; 13a, 15a and 20; 17b, 19a and 22 can be interpreted similarly.

The temperature dependence of ^{13}C nmr spectra of $(CF_3)_3P(F)NCH_3(CH_2C_6H_5)$ was also examined from -20° to

65°, (Fig. 30). At 173°K the $^{13}C - \{^{19}F\}$ spectrum consists of a pair of doublets with a relative intensity ratio of 2:1 which can be considered as the limiting spectrum under conditions of slow exchange. The more intense doublet with the larger coupling constant ($^1J_{PC}$; 267 Hz) arises from two equivalent CF_3 groups and the doublet of lesser intensity with the smaller coupling constant ($^1J_{PC}$; 59 Hz) from the single axial CF_3 group since the $^1J_{PC}$ values appear to correlate linearly with $^2J_{PF}$ values.[65] At 338°K, the distinction between axial and equatorial environments is lost and the resultant average value of the coupling constant under rapid exchange conditions ($^1J_{PC}$; 198 Hz) is in good agreement with the weighted average of the above axial and equatorial $^1J_{PC}$ values. In the intermediate temperature range the three CF_3 groups are exchanging between axial and equatorial sites at intermediate rates which can be extracted from the line shape analysis. The calculated spectra included in Figure 30 were obtained using the computer program DNMR3,[38] using the following parameters (in Hz) to calculate the required eigenfunctions of the spin Hamiltonian: $\nu_{CF_3(eq)} - \nu_{CF_3(ax)} = 172$, $^1J_{PC}(eq) = 267$, $^1J_{PC}(ax) = 59$. Treating ^{13}C of the $(CF_3)_3P$ portion as an AABX spin system with A and B sites suffering mutual exchange:

$$AABX \rightleftharpoons ABAX \rightleftharpoons BAAX$$

Figure 30 Observed and calculated ($^{13}C - \{^{19}F\}$, 22.6 MHz) nmr spectra at particular temperatures and appropriate rates of exchange of magnetization for $(CF_3)_3P(F)NCH_3(CH_2C_6H_5)$. The observed spectra were obtained in either a solution of CD_2Cl_2 (low temperature range) or a solution of d_{14} methyl-cyclohexane (high temperature range). The calculated spectra were obtained using the DNMR3 program with exchanging spins treated in a manner equivalent to a pairwise (i.e., Berry, etc.) exchange mechanism as explained in the text. The frequency scales give chemical shift values from $(^{13}CH_3)_4Si$ in Hz.

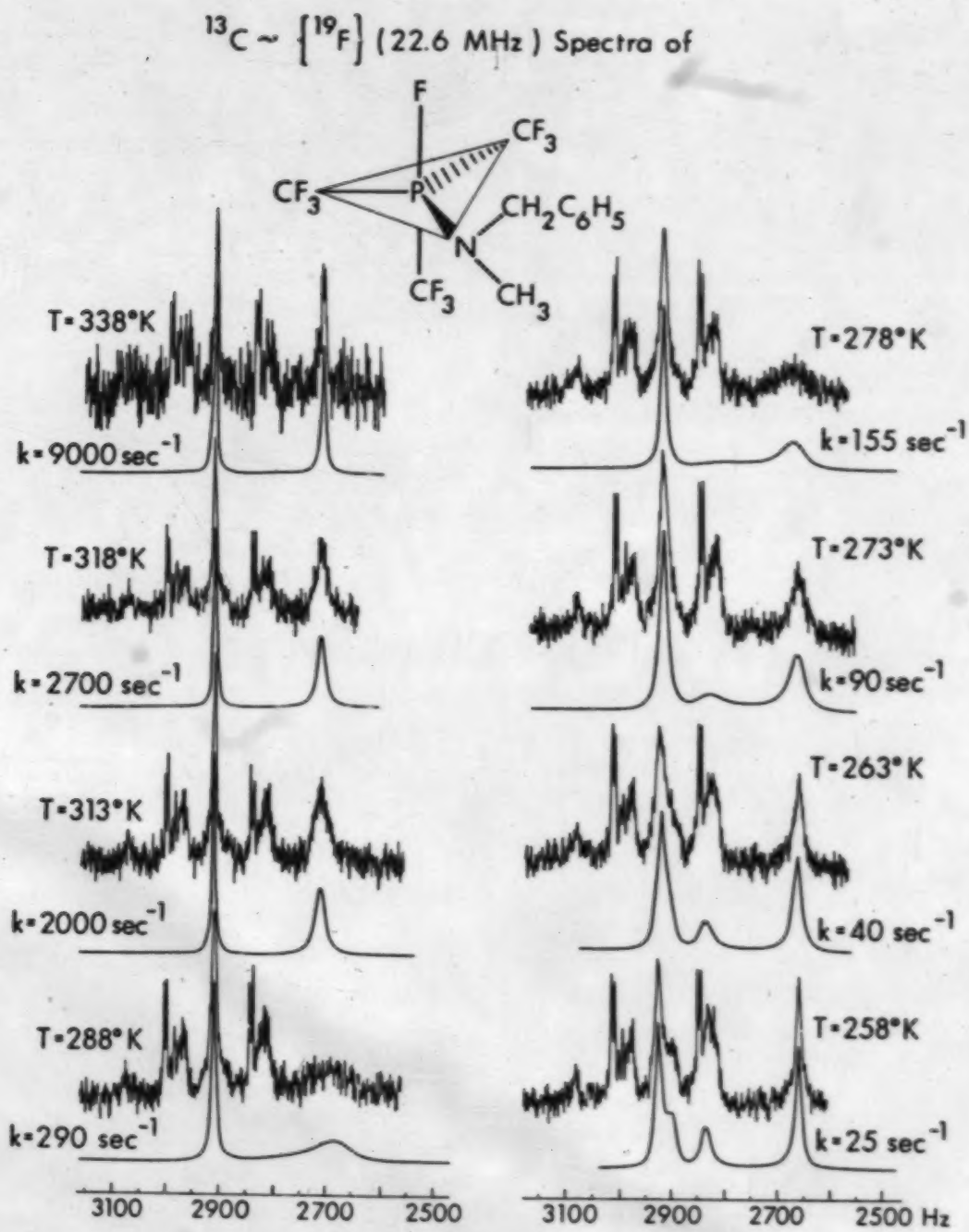
$^{13}C \sim \{^{19}F\}$ (22.6 MHz) Spectra of
F
CF_3
CF_3
P
$CH_2C_6H_5$
N
CF_3
CH_3
T=338°K
k=9000 sec^{-1}
T=318°K
k=2700 sec^{-1}
T=313°K
k=2000 sec^{-1}
T=288°K
k=290 sec^{-1}
T=278°K
k=155 sec^{-1}
T=273°K
k=90 sec^{-1}
T=263°K
k=40 sec^{-1}
T=258°K
k=25 sec^{-1}
3100
2900
2700
2500
3100
2900
2700
2500 Hz

Figure 30

is equivalent to the procedure employed for the K matrix analysis.

Exchange Barriers

A linear Arrhenius plot may be constructed from the rates of exchange (k) at different temperatures using equation 9 and least square fitting procedures:

$$\ln k = \frac{-E_a}{RT} + \ln A \qquad (9)$$

to provide the activation energy E_a from the slope and the frequency factor, A, from the intercept. An Arrhenius plot of course involves the tacit assumption that both E_a and A are temperature-independent, which can only be an approximation. Experience has shown this approximation to be a good one.[82] In general, it would mean taxing the accuracy of rate data beyond their limits to detect deviation from linearity with any degree of certainty. The enthalpies and entropies of activation are obtained by the substitution of $\Delta G^{\ddagger} = \Delta H^{\ddagger} - T\Delta S^{\ddagger}$ in the Eyring equation 10.

$$k = \left(\frac{\kappa T}{h}\right) \exp\left(-\Delta G^{\ddagger}/RT\right) \qquad (10)$$

which becomes;

$$k = \left(\frac{\kappa T}{h}\right) \exp\left(-\Delta H^{\ddagger}/RT\right) \exp\left(\Delta S^{\ddagger}/R\right) \qquad (11)$$

and, assuming $\Delta H^{\ddagger}$ and $\Delta S^{\ddagger}$ are temperature independent, by applying procedures to eq. 11. The linear plot of $\ln(k/T)$ *vs* $1/T$ gives a slope of $-\Delta H^{\ddagger}/R$ and the intercept is $\ln(\frac{K}{h}) + \frac{\Delta S^{\ddagger}}{R}$.

The linear Arrhenius plots for each compound, presented in Figure 31, gave the activation parameters (E_a, the Activation energy and A, the frequency factor). Fitting the same rate data to eqns 10 and 11 gave the Eyring activation parameters $\Delta H^{\ddagger}$(enthalpy), $\Delta S^{\ddagger}$ (entropy) and $\Delta G^{\ddagger}$ (free energy). All data are given in Table 13.

The values of $\Delta G^{\ddagger}$ are taken as the estimate of the barrier of positional interchange processes in these phosphoranes.[82] The $\Delta G^{\ddagger}$ value of $PF_4NCH_3(CH_2C_6H_5)$ of 8.3 ± 0.4 kcal/mole at 25° is in the same order as of $PF_4N(CH_3)_2$[29] (8.8 ± 0.2 kcal/mole at -85°) and $PF_4N(C_6H_5)_2$[83] (6.0 kcal/mole at unspecified temperature). Since the temperatures quoted are different, the comparison of the $\Delta G^{\ddagger}$ values of the above aminotetrafluorophosphoranes cannot be made precisely.

In the $(CF_3)_3P(F)NR_1R_2$ series (where R_1 = H, CH_3, R_2 = CH_3, $CH_2C_6H_5$), the highest barrier to intramolecular ligand exchange is found in $(CF_3)_3P(F)NH(CH_3)$ ($\Delta G^{\ddagger}$ = 14.5 ± 0.5 kcal/mole) presumably because intramolecular hydrogen bonding is also possible in this compound as suggested earlier.[84-86] Hydrogen bonding would hinder both the pairwise exchange and the rotation around the P-N bond, therefore increasing the $\Delta G^{\ddagger}$ value. The barrier to intramolecular ligand

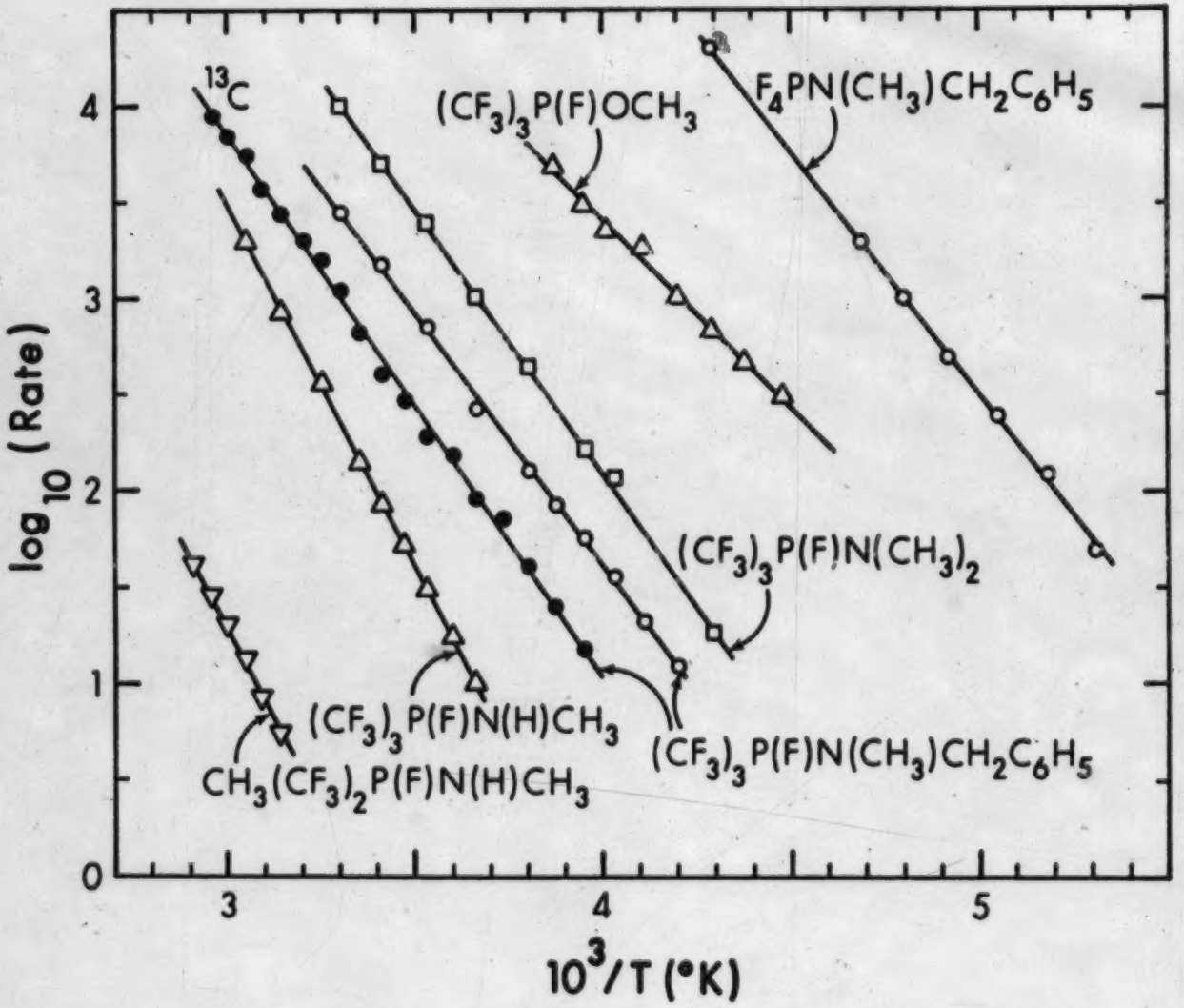

Figure 31 Arrhenius Plots for Phosphorane Exchange

TABLE 13

Activation Parameters of Some Phosphoranes

Compounds	E_a (kcal/mole)	A (sec^{-1})	$\Delta H^{\ddagger}$ (kcal/mole)	$\Delta S^{\ddagger}$ (e.u.)	$\Delta G^{\ddagger}_{298}$ (kcal/mole)
$(CF_3)_3P(F)NCH_3(CH_2C_6H_5)$	12.0 ± 0.2	0.12 (± 0.05) x 10^{13}	11.5 ± 0.2	-5.1 ± 0.8	13.0 ± 0.3
$(CF_3)_3P(F)NCH_3(CH_2C_6H_5)$[a]	12.9 ± 0.2	0.21 (± 0.05) x 10^{13}	12.3 ± 0.2	-4.1 ± 0.5	13.6 ± 0.2
$(CF_3)_3P(F)N(CH_3)_2$	12.6 ± 0.2	1.2 (± 0.5) x 10^{13}	12.1 ± 0.2	-0.4 ± 0.8	12.2 ± 0.3
$(CF_3)_3P(F)NH(CH_3)$	17.1 ± 0.3	48 (± 30) x 10^{13}	16.5 ± 0.3	6.6 ± 1.2	14.5 ± 0.5
$(CF_3)_3P(F)OCH_3$	9.1 ± 0.4	0.024 (± 0.018) x 10^{13}	8.6 ± 0.4	-8.0 ± 1.5	11.0 ± 0.6
$CH_3(CF_3)_2P(F)NH(CH_3)$	17.6 ± 1.0	0.64 (± 0.1) x 10^{13}	16.9 ± 1.0	-2.1 ± 3.1	17.5 ± 1.4
$PF_4NCH_3(CH_2C_6H_5)$	11.5 ± 0.2	130 (± 80) x 10^{13}	11.1 ± 0.2	9.3 ± 1.2	8.3 ± 0.4

[a] Obtained by DNMR3 method.

exchange in $(CF_3)_3P(F)NCH_3(CH_2C_6H_5)$ (II) of 13.0 ± 0.3 kcal/mole is higher than in $(CF_3)_3P(F)N(CH_3)_2$ (III) with $\Delta G^{\ddagger}$ of 12.2 ± 0.3 kcal/mole. The more bulky group on nitrogen in (II) tends to increase the ease of inversion at nitrogen but slows down the rotation around the P-N bond and presumably the latter effect overcomes the former resulting in a higher $\Delta G^{\ddagger}$ value for (II) relative to (III). For $(CF_3)_3P(F)NCH_3(CH_2C_6H_5)$, the activation parameters obtained from two different approaches (DNMR3 and EXCHSYS for ^{13}C and ^{31}P simulations respectively) are in agreement within experimental errors although the rates are substantially different at any given temperature, because the rates are in part dependent on the computational model. It was found that the rate of exchange of magnetization as determined from ^{31}P spectra, was independent of solvent and concentration for $(CF_3)_3P(F)$-$NCH_3(CH_2C_6H_5)$ since changing the solvent and reducing the concentration gave rates of exchange of magnetization in deuterated methyl cyclohexane (high temperature range solvent) which could be plotted on the same line in an Arrhenius plot as the ones obtained from the deuterated methylene chloride solution.

The barrier of the intramolecular averaging process in $CH_3(CF_3)_2P(F)NH(CH_3)$ with $\Delta G^{\ddagger}$ of 17.6 ± 1.4 kcal/mole is the highest among the phosphoranes studied in this work but the barrier is quite comparable to that of $(CF_3)_3$-$P(F)NH(CH_3)$. The effect of replacing one CF_3 group with

a CH_3 group in the equatorial position of the trigonal bipyramidal framework is apparently small relative to hydrogen bonding contributions which have a substantial effect. Structure of both methylamino compounds are nearly static at room temperature.

The $\Delta G^{\ddagger}$ value of $(CF_3)_3P(F)OCH_3$ of 11.0 ± 0.6 kcal/mole is smaller than those in $(CF_3)_3P(F)NR_1R_2$ series, this is probably due to the increased degree of multiple P-N bonding in the latter as suggested earlier.[4]

The large values of $\Delta S^{\ddagger}$ in $(CF_3)_3P(F)NH(CH_3)$, $(CF_3)_3P(F)OCH_3$, and $PF_4NCH_3(CH_2C_6H_5)$ are probably due to the lower accuracy of these measurements, since $\Delta S^{\ddagger}$ should be approximately zero for such an intramolecular process. The difficulties in obtaining good data for these compounds precludes extensive analysis of the $\Delta S^{\ddagger}$ terms.

CHAPTER 5

SUMMARY AND CONCLUSIONS

Nmr spectra of $(CF_3)_3P(F)NH(CH_3)$ (I), $(CF_3)_3P(F)$-$NCH_3(CH_2C_6H_5)$ (II), $CH_3(CF_3)_2P(F)NH(CH_3)$ (III) show a signal due to the fluorine with a large coupling to phosphorus strongly suggesting that the compounds are correctly formulated as five coordinate phosphoranes rather than phosphonium salts.

At ordinary temperatures, the CF_3 environments of (I) and (II) are equivalent. Axial and equatorial CF_3 environments were detected by low temperature ^{19}F, ^{31}P and ^{13}C (II) nmr spectroscopy. The CF_3 environments of (III) in a trigonal bipyramidal framework are distinguishable by ^{19}F and ^{31}P nmr at room temperature. Above -30° all four fluorines in $PF_4NCH_3(CH_2C_6H_5)$ (IV) are equivalent. At temperatures between -85° and -100°, ^{19}F and ^{31}P nmr spectra showed the presence of different axial and equatorial fluorine environments. At lower temperatures (> -100°), nonequivalent axial fluorines have been observed by ^{19}F and possibly ^{31}P nmr spectra.

The compounds (I), (II), (III), and (IV) possess ground state structures having either F and/or one CF_3 group in axial positions; CH_3, $NH(CH_3)$ or $N(CH_3)CH_2C_6H_5$ in the equatorial positions. The axial and equatorial CF_3 groups are characterized by a relatively small and

a relatively large value of $^2J_{PF}$ respectively.

A consistent interpretation of the nmr spectral behaviour is obtained for this and related[45, 53, 66-69] systems if the larger $^2J_{PF}$ values are associated with equatorial CF_3 and the smaller $^2J_{PF}$ values with axial CF_3 substitution. The relative numbers of CF_3 groups can be deduced from the relative intensity of the ^{19}F signal. The changes in the appearance of the spectra of all the phosphoranes studied on lowering the temperatures are due to

(i) a slowing down of the equilibrating permutational process and

(ii) the hindered rotation around the P-N bond which coupled with the inversion at nitrogen. Which in the present cases were not clearly distinguishable.

The temperature dependent study of the ^{31}P spectra of a series of compounds of the type $(CF_3)_3P(F)Y$ where $Y = NH(CH_3)$, $N(CH_3)_2$, $N(CH_3)CH_2C_6H_5$ and OCH_3; $CH_3(CF_3)_2P(F)NH(CH_3)$ and $PF_4NCH_3(CH_2C_6H_5)$ show the interchange of axial and equatorial fluorines in $PF_4NCH_3(CH_2C_6H_5)$, of axial and equatorial CF_3 groups in $(CF_3)_3P(F)Y$ and $CH_3(CF_3)_2P(F)NH(CH_3)$ which is consistent with a pairwise exchange mechanism such as Berry pseudorotation. The temperature dependence of the ^{13}C nmr spectra of $(CF_3)_3P(F)NCH_3(CH_2C_6H_5)$ was also examined and is consistent with the pairwise mechanism. The line shape

analysis of the ^{13}C and ^{31}P nmr obtained at different temperatures by means of existing computer programs (DNMR3 and EXCHSYS) yielded the activation parameters from the best straight line in the Arrhenius plots. By using the value of $\Delta G^{\ddagger}$ as the estimate of the barriers of positional interchange processes in these phosphoranes, the barriers to the averaging of CF_3 environments are in the order of $CH_3(CF_3)_2P(F)NH(CH_3)$ > $(CF_3)_3P(F)NH(CH_3)$ > $(CF_3)_3P(F)NCH_3(CH_2C_6H_5)$ > $(CF_3)_3P(F)N(CH_3)_2$ > $(CF_3)_3P(F)OCH_3$. The higher $\Delta G^{\ddagger}$ value of $(CF_3)_3P(F)N(CH_3)_2$ over $(CF_3)_3P(F)OCH_3$ is consistent with the result previously[53] predicted from the approximate coalescence temperatures. For $(CF_3)_3P(F)NCH_3(CH_2C_6H_5)$, the activation parameters obtained from two different approaches are in good agreement. The intramolecular averaging process in $PF_4NCH_3(CH_2C_6H_5)$ is assayed in terms of a PF_4 bending mode[30] probably coupled with a P-N rotation (and/or with nitrogen inversion) with an overall barrier of approximately 8 kcal/mole. The possible non-equivalent axial fluorines which were observed in both ^{19}F and ^{31}P nmr spectra at very low temperature (-100°) may be due to orientation of methyl and benzyl groups attached to nitrogen, relative to the axial FPF plane, thus the P-N bond rotation and/or nitrogen inversion may have ceased. Similar effects were observed in $(CF_3)_3P(F)-NCH_3(CH_2C_6H_5)$ at -120° in both ^{19}F and ^{31}P nmr spectra with

magnetic nonequivalencies developing in the axial CF_3 group. Unfortunately these latter effects were very small and not fully resolved due to freezing of the sample at very low temperatures and no definite conclusions could be reached.

REFERENCES

1. R. R. Holmes, Accounts Chem. Res., 5, 296 (1972).
2. E. L. Muetterties and R. A. Schunn, Quart. Revs., 245 (1966).
3. P. C. Van der Voorn and R. Drago, J. Amer. Chem. Soc., 88, 3255 (1966).
4. E. L. Muetterties, Accounts Chem. Res., 3, 266 (1970).
5. I. Ugi, D. Marguarding, H. Klusacek, P. Gillespie and F. Ramirez, Accounts Chem. Res., 4, 288 (1971).
6. J. B. Florey and L. C. Cusachs, J. Amer. Chem. Soc., 94, 3040 (1972).
7. R. Hoffmann, J. M. Howell and E. L. Muetterties, J. Amer. Chem. Soc., 94, 3047 (1972).
8. R. Schmutzler, Angew. Chem. Internat. Edit., 4, 496 (1965).
9. R. Schmutzler, "Halogen Chemistry," Vol II, V. Gutmann, Ed., Academic Press, New York, N.Y., 1967 (p 31ff).
10. K. W. Hansen and L. S. Bartell, Inorg. Chem., 4, 1775 (1965); *ibid*, 4, 1777 (1965).
11. R. J. Gillespie, J. Chem. Educ., 47, 18 (1970).
12. D. P. Craig, R. S. Nyholm, A. MacColl, L. E. Orgel and L. E. Sutton, J. Chem. Soc., 332 (1954).
13. A. Strich and A. Veillard, J. Amer. Chem. Soc., 95, 5574 (1973).
14. E. L. Muetterties, W. Mahler, and R. Schmutzler, Inorg. Chem., 2, 613 (1963).

15. I. Ugi, D. Marquarding, H. Klusacek, P. Gillespie, and F. Ramirez, Accounts. Chem. Res., 4, 288 (1971).

16. R. G. Cavell, D. D. Poulin, K. I. The, and A. J. Tomlinson, J.C.S. Chem. Comm., 19 (1974).

17. R. P. Wells, S. Ehrenson and R. W. Taft, *Progress in Physical Organic Chemistry*, Vol. 6, Interscience, New York, 1968.

18. J. W. Emsley, J. Feeney, and L. H. Sutcliffe, High Resolution Nuclear Magnetic Resonance Spectroscopy, Pergamon Press (1966).

19. E. Breitmaier, G. Jung, and W. Voelter, Angew. Chem. (Int. Ed.), 10, 673 (1971).

20. G. Binsch, Top. Stereochem., 3, 97 (1968).

21. E. L. Muetterties, J. Amer. Chem. Soc., 91, 1636 (1969).

22. J. C. Tebbe in "Organophosphorus Chemistry," Vol I, The Chemical Society, London, 1970, Chapter 11; Vol. II, 1971, Chapter 11; Vol. III, 1972, Chapter 11.

23. R. Schmutzler, Advances in Fluorine Chemistry, ed. M. Stacey, J. C. Tatlow and A. G. Sharpe, Pergamon, London (1965) Vol. 5, p 31.

24. A. Rauk, L. C. Allan, and K. Mislow, *ibid*, J. Amer. Chem. Soc., 94, 3035 (1972).

25. L. S. Bartell and V. Plato, *ibid*, 95, 3097 (1973).

26. W. G. Klemperer, J. Amer. Chem. Soc., 94, 8360, 6940 (1972); Inorg. Chem., 11, 2668 (1972); J. Chem. Phys., 56, 5478 (1972); E. L. Muetterties, J. Amer. Chem. Soc., 91, 4115 (1969).

27. B. F. Hoskins and F. D. Whillans, Coord. Chem. Rev., 9, 365 (1973); J. S. Wood, Progr. Inorg. Chem., 16, 227 (1972).

28. (a) P. Meakin, E. L. Muetterties, and J. P. Jesson, J. Amer. Chem. Soc., 94, 5271 (1972); (b) P. Meakin, E. L. Muetterties, F. N. Tebbe, and J. P. Jesson, *ibid*, 93, 4701 (1971).

29. M. Eisenhut, H. L. Mitchell, D. D. Traficante, R. J. Kaufman, J. M. Deutch, and G. M. Whitesides, J. Amer. Chem. Soc., 96, 5385 (1974).

30. R. S. Berry, J. Chem. Phys., 32, 933 (1960).

31. J. I. Kaplan, J. Chem. Phys., 28, 278 (1958); 29, 462 (1958).

32. S. Alexander, *ibid*, 37, 967, 974 (1962); 38, 1787 (1963); 40, 2741 (1964).

33. A. G. Redfield, IBM J. Res. Develop., 1, 19 (1957); Advan. Magn. Resonance, 1, 1 (1965).

34. R. A. Sack, Mol. Phys., 1, 163 (1958).

35. R. G. Gordon and R. P. McGinnis, J. Chem. Phys., 49, 2455 (1968).

36. G. Binsch, J. Amer. Chem. Soc., 91, 1304 (1969).

37. R. E. Schirmer, J. H. Noggle, and D. F. Gaines, *ibid*, 91, 6240 (1969).

38. DNMR3: A Computer Program for the Calculation of Complex Exchange-Broadened NMR Spectra Modified Version for Spin Systems Exhibiting Magnetic Equivalence or

Symmetry, D. A. Kleier and G. Binsch, Department of Chemistry and the Radiation Laboratory, University of Notre Dame, Notre Dame, Indiana.

39. D. F. Shriver, The Manipulation of Air Sensitive Compounds, McGraw-Hill, New York (1969).

40. R. E. Rondeau, J. Chem. Eng. Data, 10, 124 (1966).

41. F. W. Bennett, H. J. Emeléus and R. N. Haszeldine, J. Chem. Soc., 1565 (1953).

42. W. Mahler, Inorg. Chem., 2, 230 (1963).

43. K. J. Packer, J.C.S., 960 (1963); J. Grobe, Zeit. Anorg. Allg. Chem., 331, 63 (1964); J. F. Nixon, J.C.S., 777 (1965).

44. H. J. Emeléus, R. N. Haszeldine, and R. C. Paul, J. Chem. Soc., 563 (1955).

45. K. I. The and R. G. Cavell, Phosphoranes IV, in press.

46. A. A. Pinkerton and R. G. Cavell, Inorg. Chem., 10, 2720 (1971).

47. A. C. Chapman, J. Homer, D. J. Mowthorpe and K. T. Jones, Chem. Comm., 121 (1965), The chemical shift of 85% H_3PO_4 is +112 ppm *vs.* P_4O_6.

48. J. A Pople, W. G. Schneider, and H. J. Bernstein, "High-Resolution NMR," McGraw-Hill, New York (1959).

49. S. S. Chan and C. J. Willis, Can. J. Chem., 46, 1237 (1968); E. O. Bishop, P. R. Carey, J. F. Nixon and J. R. Swain, J. Chem. Soc., A, 1074 (1970).

50. R. G. Cavell, J. Chem. Soc., 1992 (1964).

51. T. A. Blazer, R. Schmutzler and I. K. Gregor, Z. Naturforsch, 24B, 1081 (1969).

52. R. G. Cavell and R. C. Dobbie, Inorg. Chem., 7, 101 (1968).

53. K. I. The and R. G. Cavell, Phosphoranes III, in press.

54. D. E. C. Corbridge, Topics in Phosphorus Chemistry, ed., by M. Grayson and E. J. Griffith, Wiley (New York) 1971, Vol. 6, p. 235.

55. D. H. Brown, G. W. Fraser, and D. W. A. Sharp, J. Chem. Soc., A, 171 (1966).

56. J. T. Braunholz, E. Ebsworth, F. Mann, and N. Sheppard, J. Chem. Soc., 2780 (1958).

57. M. A. Fleming, R. J. Wyrna, and R. C. Taylor, Spectrochim. Acta., 21, 1189 (1965).

58. W. S. Sheldrick, J.C.S. Dalton, 2301 (1973).

59. R. R. Holmes, Accounts of Chem. Research, 5, 296 (1972); R. R. Holmes, R. P. Carter, Jr., and G. E. Peterson, Inorg. Chem., 3, 1748 (1964); J. E. Griffiths, R. P. Carter, Jr., and R. R. Holmes, J. Chem. Phys., 41, 863 (1964); J. E. Griffiths, J. Chem. Phys., 49, 1307 (1968); *ibid*, 44, 2826 (1966); *ibid*, 41, 3510 (1964); J. E. Griffiths, and A. L. Beach, Inorg. Chem., 2, 613 (1963); A. J. Downs and R. Schmutzler, Spect. Acta., A 23, 681 (1967); *ibid*, 21, 1927 (1965).

60. The term phosphorane was reserved for a five coordinate compound of phosphorus which is formally a derivative of PH_5.

61. J. B. Stothers,"Carbon-13 NMR Spectroscopy," Academic Press, New York, N.Y., 1972, p. 197 and references therein.

62. F. J. Weigert and J. D. Roberts, Inorg. Chem., 12, 313 (1973).

63. G. A. Gray, J. Amer. Chem. Soc., 95, 7736 (1973).

64. H. J. Reich, M. Jautelat, M. T. Messe, F. J. Weigert and J. D. Roberts, J. Amer. Chem. Soc., 91 7445 (1969).

65. R. G. Cavell, K. I. The, N. Yap, and J. A. Gibson, unpublished work.

66. R. G. Cavell, D. D. Poulin, K. I. The, and A. J. Tomlinson, Chem. Comm., 19 (1974).

67. D. D. Poulin and R. G. Cavell, Inorg. Chem., 13, 2324 (1974), *erratum ibid*, 14, 2022 (1975).

68. D. D. Poulin and R. G. Cavell, Inorg. Chem., 13, 3012 (1974).

69. R. G. Cavell, R. D. Leary and A. J. Tomlinson, Inorg. Chem., 11, 2578 (1972).

70. (a) B. G. Pobedimskii, A. L. Buchachenko, and M. B. Neiman, Russ. J. Phys. Chem., 42, 748 (1968); (b) F. A. Neugebauer and S. Bamberger, Chem. Ber., 42, 2362 (1974).

71. S. C. Peake and R. Schmutzler, J. Chem. Soc. A, 1049 (1970).

72. M. A. Skol'skii, G. I. Drozd, M. A. Landau, and S. S. Dubov, J. Struct. Chem. (USSR), 10, 993 (1969) and references therein.

73. J. J. Harris and B. Rudner, J. Org. Chem., 33, 1392 (1968).

74. A. H. Cowley, R. W. Braun, J. W. Gilje, J. Amer. Chem. Soc., 97, 434 (1975).

75. E. L. Muetterties, P. Meakin, and R. Hoffmann, J. Amer. Chem. Soc., 94, 5674 (1972).

76. R. G. Cavell, A. J. Tomlinson, and R. D. Leary, Inorg. Chem., 11, 2577 (1972).

77. S. C. Peake and R. Schmutzler, Chem. Commun., 1662 (1968).

78. A. H. Cowley, M. J. S. Dewar, W. R. Jackson, and W. B. Jennings, J. Amer. Chem. Soc., 92, 5206 (1970).

79. Recent X-ray crystallographic studies have established that certain spirooxyphosphoranes and 1,3,2-dioxaphosphoranes possess approximately square pyramdial structures. See J. A. Howard, D. R. Russell, and S. Trippett, J. Chem. Commun., 856 (1973); and H. Wunderlich, D. Mootz, R. Schmutzler, and M. Wieber, Z. Naturforsch., 29b, 32 (1974); H. Wunderlich, Acta. Cryst., B30, 939 (1974).

80. For extensive compliations of nmr data see R. Luckenbach, "Dynamic Stereochemistry of Pentacoordinate Phosphorus and Related Elements," Georg. Thieme. Stuttgart, 1973; D. Hellwinkel, "Organo Phosphorus Compounds," Vol. 3, G. M. Kosolapoft and L. Maier, Ed., Wiley-Interscience, New York, N.Y., 1972, p. 185.

81. R. R. Holmes, J. Amer. Chem. Soc., 96, 4143 (1974).

82. Dynamic NMR Spectroscopy, ed. by L. M. Jackman and F. A. Cotton, Academic Press, New York, (1975).

83. F. N. Tebbe and E. L. Muetterties, Inorg. Chem., 7, 172 (1968).

84. A. H. Cowley and J. R. Schweiger, J.C.S. Chem. Comm., 560 (1972).

85. J. S. Harman and D. W. A. Sharp, Inorg. Chem., 10, 1538 (1971).

86. J. S. Harman and D. W. A. Sharp, J. Chem. Soc. A, 1138 (1970).

87. J. M. Lehn in "Conformational Analysis," G. Chiurdoglu, Ed., Academic Press, New York, N.Y., 1971, p. 129.

88. The program EXCHSYS is a shortened version of the program of the same name obtained from the Mass. Inst. of Technology and established at the University of Alberta by R. G. Cavell. The theory and stategy of the calculations are described in ref. 89 and 90.

89. J. K. Kreiger, J. M. Deutsch and G. M. Whitesides, Inorg. Chem., 12, 1535 (1973).

90. J. K. Kreiger Thesis, Mass. Inst. of Technology, Boston, Mass. (1971).

APPENDIX

The K matrix which describes the transfer of magnetization between the lines of the observed ^{31}P half-spectrum of $CH_3(CF_3)_2P(F)NH(CH_3)$ (16 x 16) and $(CF_3)_3PFNR_1R_2$ was constructed from the following facts:

i) there are four spin states in each of the CF_3 groups: ααα, ααβ, αββ, and βββ.

ii) the spin states are indistinguishable for a single CF_3 group, i.e., ααβ ≡ αβα ≡ βαα, therefore there is no exchange between these states.

iii) total spin states must be conserved during exchange of magnetization.

iv) the components of two degenerate CF_3 groups (i.e., two equatorial CF_3 groups) are degenerate set of groups, eg., ααα βββ consists of ααα βββ, βαα ββα, ββα βαα, and ββββ ααα.

v) the "indistinguishable" states which behave in an identical way with respect to transfer of magnetization can be combined for simplification.

The 16 x 16 matrix (Table 18) for $CH_3(CF_3)_2P(F)NH(CH_3)$ describes the exchange of magnetization of six fluorine spin states of two different CF_3 groups, axial and equatorial. Each of which consists of four spin states: ααα, ααβ, αββ, and βββ. The 16 x 16 matrix has identical

rows and columns, probabilities of exchange are all 0 or 1.0 and diagonals are 0 or -1.0.

The K matrix for the system of $(CF_3)_3P(F)Y$ (where $Y = NH(CH_3)$, $N(CH_3)_2$, $NCH_3(CH_2C_6H_5)$, and OCH_3) was constructed to describe the transfer of magnetization between nine fluorine spin states of three CF_3 groups, six of which belong to two degenerate CF_3 groups. Thus the slow exchange half spectra have 28 lines, a quartet of septets. All possible spin states from the six spin assembly combine with a set of indistinguishable spin states from axial CF_3 group to give rise to a 64 x 64 matrix (Table 19) e.g., the set of degenerate equatorial spin states of one particular M_I value for equatorial CF_3 groups (e.g., $M_I(eq) = 0$): ααα βββ|ααα, βαα ββα|ααα, ββα βαα|ααα and βββ ααα|ααα, all have a probability of exchange of 0.5 with spin states ααα ααα|βββ, βαα ααα|ββα, and ααα ββα|βαα, ααα βαα|ββα and ββα ααα|βαα and ααα ααα|βββ respectively, as a result of permutation of the axial CF_3 group with one equatorial CF_3 group which result in the transformation of magnetization from equatorial to axial environments without spin transitions within the CF_3 group. This 64 x 64 matrix has identical rows and columns, probabilities of exchange are all 0 or 0.5 and diagonals are 0, -0.5 or -1.0.

Because a 64 x 64 matrix cannot be taken into the program because of internal space limitation of the program, the matrix was reduced to dimensions of 40 x 40 case by

combining "indistinguishable" states, e.g., ββα βαα|ααα and βαα ββα|ααα and adjusting probabilities.

If a complete simulation including the two spin states of the single F is required for $CH_3(CF_3)_2P(F)NH(CH_3)$ and $(CF_3)_3P(F)Y$ cases then two submatrices of order 16 x 16 and 40 x 40 respectively are needed.

The computer program requires transition frequencies, peak width at half height and intensities of the lines. The transition frequencies can be obtained either from a stick diagram constructed using the values of coupling constants obtained from a stopped spectrum or from the measured frequencies obtained from the spectrum. Obtaining correct assignments in the latter case is more difficult especially when lines overlap and since it is essential that the spin state order be correct, the former approach is recommended. The intensities are calculable from stick diagrams. The transition frequencies and intensities are summarized in Table 14, 15, and 16. The peak width at half height (FWHM) is measued directly in Hz from the peak which remains sharp through the temperature range. In some cases the peak width at half height was increased with increasing temperature for better fitting. For $(CF_3)_3P(F)NCH_3(CH_2C_6H_5)$ a FWHM of 4.5 Hz was used for all spectra from -35° to 20°. At 30°, a value of 5.0 Hz was used. For $CH_3(CF_3)_2P(F)NH(CH_3)$, $(CF_3)_3P(F)N(CH_3)_2$ and $(CF_3)_3P(F)OCH_3$ FWHM values of 10.0, 6.0, and 4.0 Hz were

used throughout respectively. For $(CF_3)_3P(F)NH(CH_3)$, FWHM = 4.5 Hz at 5°, FWHM = 6.0 Hz between 10° and 20°, FWHM = 8.0 Hz at 25° and 35°, and FWHM = 10.0 Hz at 45° and 55°. For $PF_4NCH_3(CH_2C_6H_5)$, FWHM values of 4.5 and 6.0 Hz were used at temperatures between -90° and -60°, -50° and -40° respectively.

TABLE 14

Line Numbers, Spin States, Intensities and Frequencies used for Simulation of ^{31}P Spectra of $PF_4NCH_3(CH_2C_6H_5)$.

Line no.	Spin States (F) equatorial	axial	Frequencies	Intensities
1	αα	αα	3809.8	0.0625
2	αα	αβ	3024.9	0.125
4	αα	ββ	2240.6	0.0625
3	αβ	αα	2890.6	0.125
5	αβ	αβ	2105.7	0.250
7	αβ	ββ	1322.6	0.125
6	ββ	αα	1970.2	0.0625
8	ββ	αβ	1187.1	0.125
9	ββ	ββ	402.2	0.0625

TABLE 15

Line Numbers, Spin-states, Intensities and Frequencies used for Simulation of ^{31}P Spectra of $CH_3(CF_3)_2P(F)NH(CH_3)$

Line no.	Spin-States (CF_3) equatorial	axial	Frequencies	Intensities
1	ααα	ααα	40.0	0.0156
2	ααα	ααβ	704.6	0.0469
3	ααα	αββ	669.2	0.0469
4	ααα	βββ	633.8	0.0156
5	βαα	ααα	615.4	0.0469
6	βαα	ααβ	580.0	0.1406
7	βαα	αββ	544.6	0.1406
8	βαα	βββ	509.2	0.0469
9	ββα	ααα	490.8	0.0469
10	ββα	ααβ	455.4	0.1406
11	ββα	αββ	420.0	0.1406
12	ββα	βββ	384.6	0.0469
13	βββ	ααα	366.2	0.0156
14	βββ	ααβ	330.8	0.0469
15	βββ	αββ	295.4	0.0469
16	βββ	βββ	260.0	0.0156

Table 16

Line Numbers, Spin-states, Intensities and Frequencies used for Simulation of ^{31}P Spectra of $(CF_3)_3P(F)Y$

Line no.	Spin-States CF_3 equatorial	CF_3 axial	Intensities	Frequencies $(CF_3)_3P(F)NH(CH_3)$	$(CF_3)_3P(F)N(CH_3)_2$	$(CF_3)_3P(F)NCH_3(CH_2C_6H_5)$	$(CF_3)_3P(F)OCH_3$
1	ααα ααα	ααα	0.001953	1043.8	971.0	1010.7	1047.0
2	ααα ααα	βαα	0.005859	993.8	917.0	957.0	975.0
3	ααα ααα	ββα	0.005859	943.7	863.0	903.3	903.0
5	ααα ααα	βββ	0.001953	892.4	809.0	849.6	831.0
4	βαα ααα	ααα	0.01172	910.7	841.0	880.0	914.0
6	βαα ααα	βαα	0.03516	860.7	797.0	826.3	842.0
7	βαα ααα	ββα	0.03516	810.6	733.0	772.6	770.0
9	βαα ααα	βββ	0.01172	759.4	679.0	718.9	698.0
8a	ββα ααα	ααα	0.01172	777.7	711.0	749.5	791.0
10a	ββα ααα	βαα	0.03516	727.6	657.0	695.8	709.0
11a	ββα ααα	ββα	0.03516	678.8	603.0	643.3	637.0
13a	ββα ααα	βββ	0.01172	628.8	549.0	589.6	565.0
8b	βαα βαα	ααα	0.01757	777.7	711.0	749.5	781.0
10b	βαα βαα	βαα	0.05271	727.6	657.0	695.8	709.0

TABLE 16 (continued)

11b	βαα	βαα	ββα	0.05271	678.8	603.0	643.3	637.0
13b	βαα	βαα	βββ	0.01757	628.8	549.0	589.6	565.0
12a	βββ	ααα	ααα	0.00391	644.6	581.0	618.9	648.0
14a	βββ	ααα	βαα	0.01172	595.8	527.0	565.2	576.0
15a	βββ	ααα	ββα	0.01172	545.8	473.0	511.5	504.0
17a	βββ	ααα	βββ	0.00391	496.9	419.0	457.8	432.0
12b	ββα	βαα	ααα	0.03515	644.6	581.0	618.9	648.0
14b	ββα	βαα	βαα	0.10547	595.8	527.0	565.2	576.0
15b	ββα	βαα	ββα	0.10547	545.8	473.0	511.5	504.0
17b	ββα	βαα	βββ	0.03515	496.9	419.0	457.8	432.0
16a	βββ	βαα	ααα	0.01172	511.6	451.0	488.3	515.0
18a	βββ	βαα	βαα	0.03516	462.7	397.0	434.6	443.0
19a	βββ	βαα	ββα	0.03516	412.7	343.0	380.9	371.0
21a	βββ	βαα	βββ	0.01172	363.9	289.0	327.1	299.0
16b	ββα	ββα	ααα	0.01757	511.6	451.0	488.3	515.0
18b	ββα	ββα	βαα	0.05271	462.7	397.0	434.6	443.0
19b	ββα	ββα	ββα	0.05271	412.7	343.0	380.9	371.0
21b	ββα	ββα	βββ	0.01757	363.9	289.0	327.1	299.0
20	βββ	ββα	ααα	0.01172	378.5	321.0	357.6	382.0

TABLE 16 (continued)

22	βββ βα	βαα	0.03516	329.7	267.0	303.9	310.0
23	βββ βα	ββα	0.03516	280.9	213.0	250.2	238.0
25	βββ ββ	βββ	0.01172	230.8	159.0	196.5	166.0
24	βββ βββ	ααα	0.001953	245.5	191.0	227.0	249.0
26	βββ βββ	βαα	0.005859	196.6	137.0	173.3	177.0
27	βββ βββ	ββα	0.005859	147.8	83.0	119.6	105.0
28	βββ βββ	βββ	0.001953	97.8	28.0	65.9	33.0

TABLE 17

K-matrix Describing Transfer of Magnetization Between the Lines of the Observed ^{31}P Spectrum of $PF_4NCH_3(CH_2C_6H_5)$

eq	ax	αα αα	αα αβ	αα ββ	αβ αα	αβ αβ	αβ ββ	ββ αα	ββ αβ	ββ ββ	
αα	αα	0	0	0	0	0	0	0	0	0	*
αα	αβ	0	-1	0	1	0	0	0	0	0	
αα	ββ	0	0	-1	0	0	0	1	0	0	
αβ	αα	0	1	0	-1	0	0	0	0	0	
αβ	αβ	0	0	0	0	0	0	0	0	0	*
αβ	ββ	0	0	0	0	0	-1	0	1	0	
ββ	αα	0	0	1	0	0	0	-1	0	0	
ββ	αβ	0	0	0	0	0	1	0	-1	0	
ββ	ββ	0	0	0	0	0	0	0	0	0	*

* line which is unaffected by exchange

TABLE 18

K-matrix Describing Transfer of Magnetization Between the Lines of the Observed ^{31}P Spectrum of $CH_3(CF_3)_2P(F)NH(CH_3)$

(ax)	(eq)	(ax) \ (eq)	ααα	ααβ	αββ	βββ	βαα	βαβ	ββα	ββββ	βββα	βββα	ββββ	ββββ	ββββ	ββββ	ββββ	ββββ	
ααα	ααα		0	0	0	0	0	0	0	0	0	0	0	0	0	0	0	0	*
ααα	ααβ		0	-1	0	0	1	0	0	0	0	0	0	0	0	0	0	0	
ααα	αββ		0	0	-1	0	0	0	0	0	1	0	0	0	0	0	0	0	
ααα	βββ		0	0	0	-1	0	0	0	0	0	0	0	0	1	0	0	0	
βαα	ααα		0	1	0	0	-1	0	0	0	0	0	0	0	0	0	0	0	
βαα	ααβ		0	0	0	0	0	0	0	0	0	0	0	0	0	0	0	0	*
βαα	αββ		0	0	0	0	0	0	-1	0	0	1	0	0	0	0	0	0	
βαα	βββ		0	0	0	0	0	0	0	-1	0	0	0	0	0	1	0	0	
ββα	ααα		0	0	1	0	0	0	0	0	-1	0	0	0	0	0	0	0	
ββα	ααβ		0	0	0	0	0	0	1	0	0	-1	0	0	0	0	0	0	
ββα	αββ		0	0	0	0	0	0	0	0	0	0	0	0	0	0	0	0	*
ββα	βββ		0	0	0	0	0	0	0	0	0	0	0	-1	0	0	1	0	
βββ	ααα		0	0	0	1	0	0	0	0	0	0	0	0	-1	0	0	0	
βββ	ααβ		0	0	0	0	0	0	0	1	0	0	0	0	0	-1	0	0	
βββ	αββ		0	0	0	0	0	0	0	0	0	0	0	1	0	0	-1	0	
βββ	βββ		0	0	0	0	0	0	0	0	0	0	0	0	0	0	0	0	*

* unchanged by exchange

TABLE 19

64 x 64 matrix for $(CF_3)_3P$ system (2 equatorial, 1 axial)

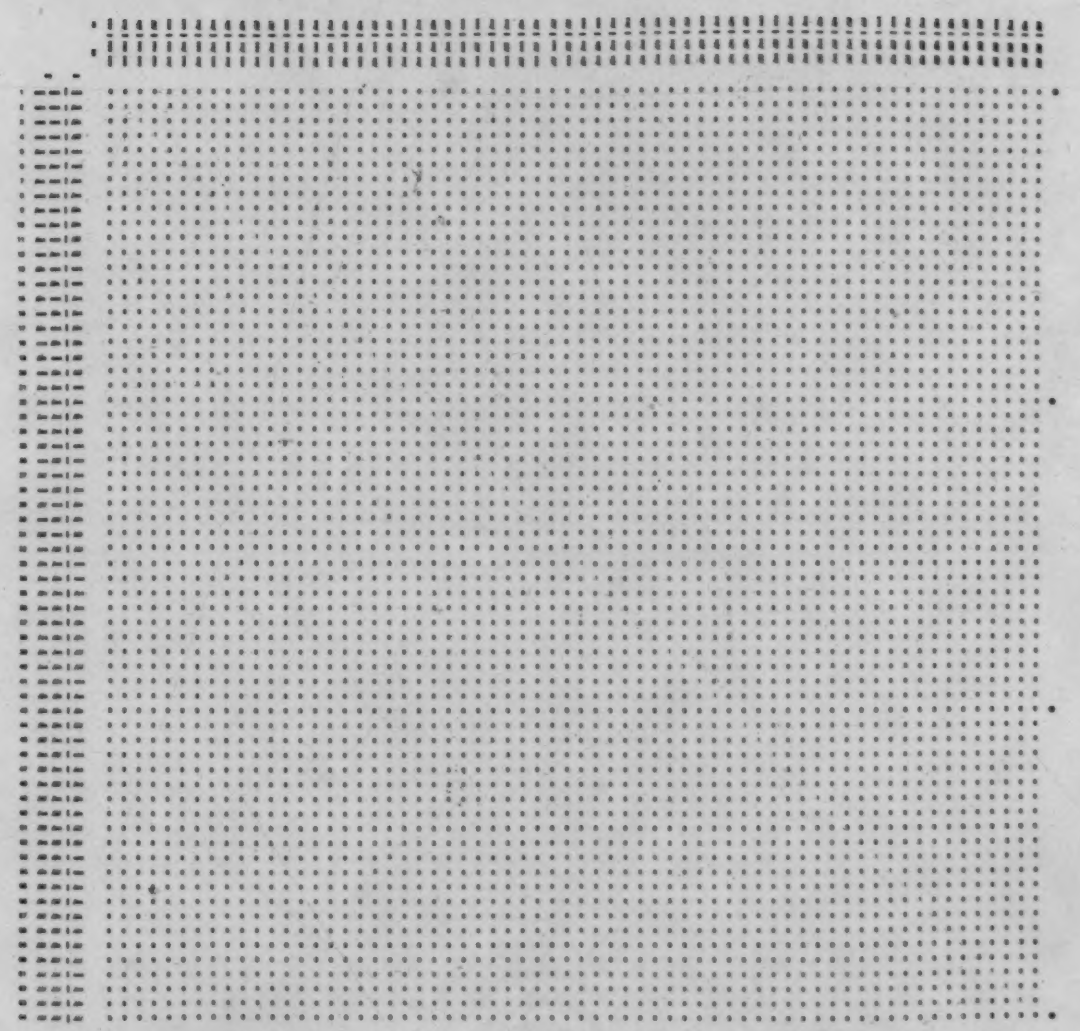

* Unchanged by Exchange

TABLE 20
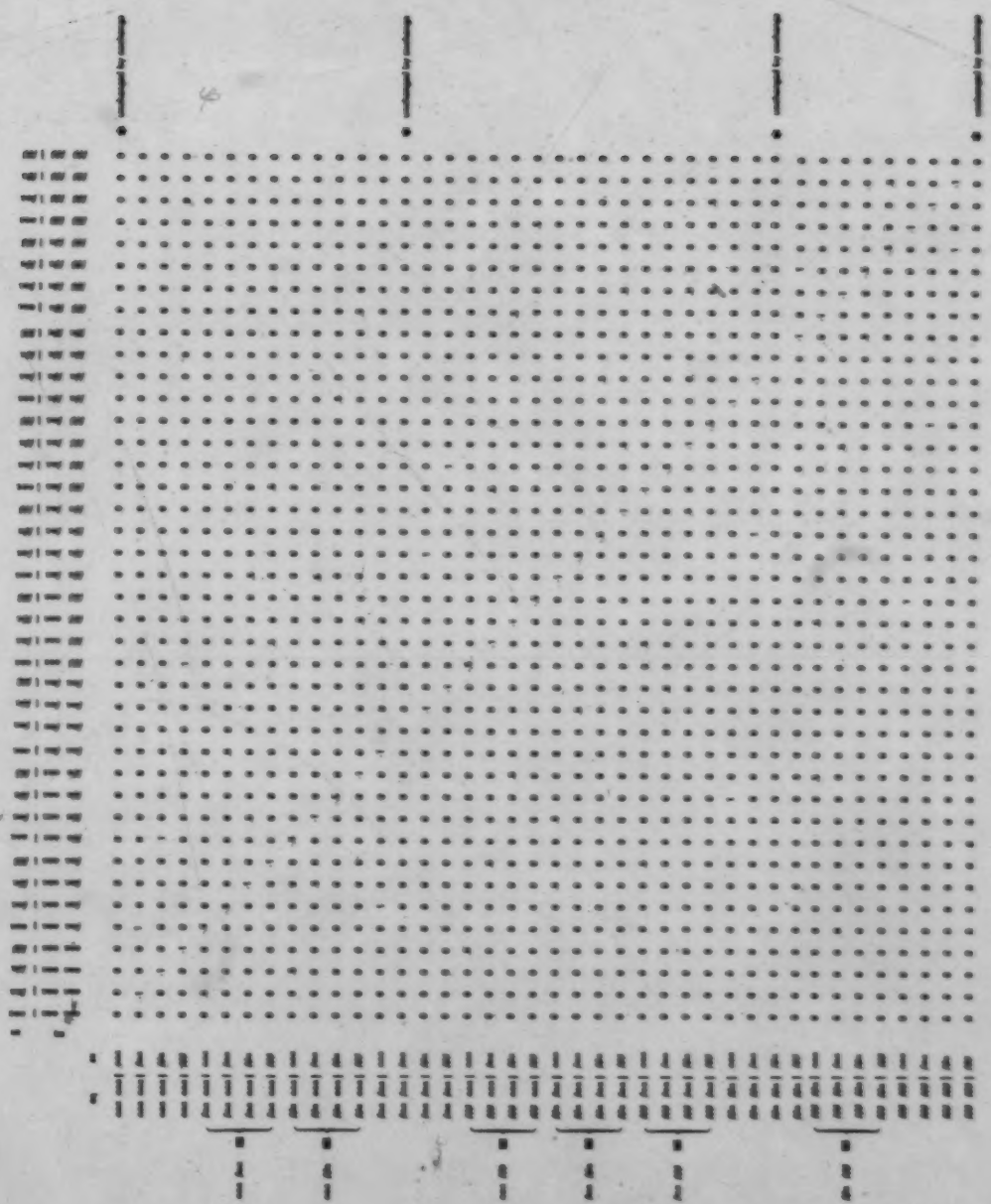
40 x 40 Matrix for $(CF_3)_3P$ systems (2 equatorial, 1 axial)